

AD A110671

15

LEVEL II

**RADC-TR-81-313**

Final Technical Report

November 1981



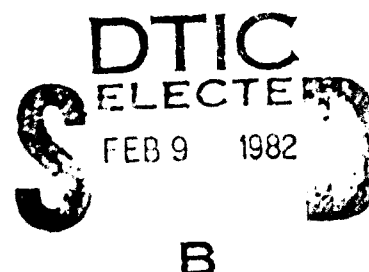
# **VLF/LF LONG WAVE PROPAGATION STUDY**

**Megapulse, Incorporated**

**Dr. Peter Ver Planck**

**Royce C. Kahler**

**James B. Donohoe**



APPROVED FOR PUBLIC RELEASE; DISTRIBUTION UNLIMITED

DTIC FILE COPY

**ROME AIR DEVELOPMENT CENTER  
Air Force Systems Command  
Griffiss Air Force Base, New York 13441**

82 02 08 241

This report has been reviewed by the RADC Public Affairs Office (PA) and is releasable to the National Technical Information Service (NTIS). At NTIS it will be releasable to the general public, including foreign nations.

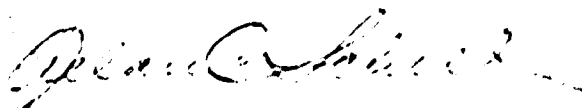
RADC-TR-81-313 has been reviewed and is approved for publication.

APPROVED:



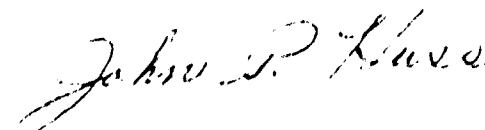
JOHN E. RASMUSSEN, Acting Chief  
Propagation Branch  
Electromagnetic Sciences Division

APPROVED:



ALLAN C. SCHELL  
Chief, Electromagnetic Sciences Division

FOR THE COMMANDER:



JOHN P. HUSS  
Acting Chief, Plans Office

If your address has changed or if you wish to be removed from the RADC mailing list, or if the addressee is no longer employed by your organization, please notify RADC (EEPL) Hanscom AFB MA 01731. This will assist us in maintaining a current mailing list.

Do not return copies of this report unless contractual obligations or notices on a specific document requires that it be returned.

UNCLASSIFIED

SECURITY CLASSIFICATION OF THIS PAGE (When Data Entered)

REPORT DOCUMENTATION PAGE		READ INSTRUCTIONS BEFORE COMPLETING FORM
1. REPORT NUMBER RADC-TR-81-313	2. GOVT ACCESSION NO. AD A110	3. RECIPIENT'S CATALOG NUMBER 671
4. TITLE (and Subtitle) VLF/LF LONG WAVE PROPAGATION STUDY		5. TYPE OF REPORT & PERIOD COVERED Final Technical Report
		6. PERFORMING ORG. REPORT NUMBER N/A
7. AUTHOR(s) Dr. Peter Ver Planck Royce C. Kahler James B. Donohoe		8. CONTRACT OR GRANT NUMBER(s) F19628-77-C-0233
9. PERFORMING ORGANIZATION NAME AND ADDRESS Megapulse, Incorporated 8 Preston Court Bedford MA 01730		10. PROGRAM ELEMENT, PROJECT, TASK AREA & WORK UNIT NUMBERS 62702F 46001631
11. CONTROLLING OFFICE NAME AND ADDRESS Deputy for Electronic Technology (RADC/EEPL) Hanscom AFB MA 01731		12. REPORT DATE November 1981
		13. NUMBER OF PAGES 44
14. MONITORING AGENCY NAME & ADDRESS (if different from Controlling Office) Same		15. SECURITY CLASS. (of this report) UNCLASSIFIED
		15a. DECLASSIFICATION/DOWNGRADING SCHEDULE N/A
16. DISTRIBUTION STATEMENT (of this Report) Approved for public release; distribution unlimited		
17. DISTRIBUTION STATEMENT (of the abstract entered in Block 20, if different from Report) Same		
18. SUPPLEMENTARY NOTES RADC Project Engineer: John E. Rasmussen (EEPL)		
19. KEY WORDS (Continue on reverse side if necessary and identify by block number) VLF/LF Transverse Electric/Magnetic Polarization Survivable Propagation Powerline Antenna Rocket Probes Ionosounding Earth-Ionospheric Waveguide C-Layer		
20. ABSTRACT (Continue on reverse side if necessary and identify by block number) A program of ARCAS rocket measurements provided field strength data from 0 to 75 km altitude, in both Transverse Magnetic (TM) and Transverse Electric (TE) polarizations. Sky wave parameters related to survivable ground wave communications were measured at a frequency of 100 kHz, and a method of communicating with short (ground wave) pulses was demonstrated on a 230 km propagation path. Measurements were made in New York state, and in Brazil, to further define the nature of pulse reflections from ionospheric heights		

DD FORM 1 JAN 73 1473 EDITION OF 1 NOV 65 IS OBSOLETE

UNCLASSIFIED

SECURITY CLASSIFICATION OF THIS PAGE (When Data Entered)

AIR FORCE 8 December 1981-25

408 111

UNCLASSIFIED

SECURITY CLASSIFICATION OF THIS PAGE(When Data Entered)

below the classical D-region. Instrumentation was developed to detect small changes in 100 kHz ground wave propagation velocity which might correlate with tropospheric conditions. Preliminary mechanical considerations indicate that it might be possible to deploy long center-fed dipole antennas from an earth satellite. The program of high-resolution ionosounding with TM pulses in Greenland was augmented by transmitting TE pulses from an unused powerline at Thule Air Base. It was demonstrated that the effects of ionospheric disturbances can now be observed simultaneously with both polarizations. Input resistances and reactances of the powerline antenna were measured as functions of frequency in preparation for a follow-on program of long range propagation tests.

UNCLASSIFIED

SECURITY CLASSIFICATION OF THIS PAGE(When Data Entered)

## TABLE OF CONTENTS

### GENERAL INTRODUCTION

#### SECTION A - FIELD PROFILE MEASUREMENTS WITH ROCKETS AND BALLOONS

<u>Subsection</u>		<u>Page</u>
A.1	Introduction	5
A.2	Rocket Measurements	10
A.3	Dartsonde Packages	24
	References	30

#### SECTION B - SURVIVABLE GROUND WAVE COMMUNICATIONS

B.1	Introduction	31
B.2	Description of the CW Measurements	32
B.3	Reduction of CW Data	40
B.4	CW Field Measurement	40
B.5	Demonstration of Pulse Position Modulation Communication	47
B.6	Conclusions	50
	References	51

#### SECTION C - C-LAYER IONOSOUNDING WITH THE FORESTPORT TOWER

C.1	Introduction	52
C.2	Instrumentation	53

## TABLE OF CONTENTS (Continued)

<u>Subsection</u>		<u>Page</u>
C.3	Data and Conclusions	56
	References	63
SECTION D - PHASE STABILITY OF GROUND WAVE PROPAGATED LORAN-C PULSES		
D.1	Introduction	64
D.2	Experiment Approach	69
D.3	Conclusions	78
	References	79
SECTION E - SPACE ANTENNA STUDY		
		80
	References	88
SECTION F - TRANSVERSE ELECTRIC (TE) VLF IONOSOUNDING BETWEEN THULE AIR BASE AND QANAQ, GREENLAND		
F.1	Introduction	89
F.2	Installation	91
F.3	Verification Tests	94
F.4	Calibration Experiment	96
F.5	Waveform Improvement	103
	References	107

# TABLE OF CONTENTS (Continued)

<u>Subsection</u>		<u>Page</u>
SECTION G - C-LAYER STUDIES IN BRAZIL		
G.1	Introduction	108
G.2	Description of Experiment	108
G.3	Data and Conclusions	118
	References	122
SECTION H - POSSIBILITIES FOR CONTINUOUS WAVE OPERATION OF THE 120-METER (400-FOOT) TOWER AT THULE AFB		
H.1	Introduction	123
H.2	120-Meter (400-Foot) Tower	123
H.3	The Powerline Antenna	126



✓	
Dist	
Special	
A	

## LIST OF ILLUSTRATIONS

### SECTION A - FIELD PROFILE MEASUREMENTS WITH ROCKETS AND BALLOONS

<u>Figure No.</u>		<u>Page</u>
A-1	Idealized Wave Patterns with Transverse Magnetic Polarization	7
A-2	Idealized Wave Patterns with Transverse Electric Polarization	7
A-3	TM Profile Observed with Rocket Package #1, 29 October 1980	14
A-4	TE Profile Observed with Rocket Package #1, 29 October 1980	15
A-5	TE Profile Observed with Rocket Package #4, 29 October 1980	16
A-6	Rocket, Showing Telemetry Slot Antenna	17
A-7	Rocket Launch Tube, Showing Fiberglass Section	19
A-8	System Flow Diagram, Super ARCAS TE/TM Rocket Launch	21
A-9	Thermal Package for Dartsonde Receivers	26
A-10	400 MHZ Cutdown System	28

### SECTION B - SURVIVABLE GROUND WAVE COMMUNICATIONS

B-1	Block Diagram, Loran Receiver System	34
B-2	Outside of Loran Receiver Trailer	35
B-3	Inside of Loran Receiver Trailer	36
B-4	Loran Signals Received at HAFB from Seneca on 29 December 1980	38
	(a) Ground Wave with No Sky Wave	
	(b) Ground Wave with Night Time Sky Wave	
	(c) Residual Night Time Sky Wave	



# LIST OF ILLUSTRATIONS (Continued)

<u>Figure No.</u>		<u>Page</u>
B-5	Plot Showing Rapid Transition of the Ionosphere at Dawn	42
B-6	Averaged Loran Sky Wave Ground Wave Ratios Between Levels, Seneca to HAFB	43
B-7	Averaged Loran Sky Wave Ground Wave Ratios Above Levels, Seneca to HAFB	44
B-8	Averaged Loran Sky Wave Ground Wave Ratios Between Levels, Seneca to Pittsfield	45
B-9	Averaged Loran Sky Wave Ground Wave Ratios Above Levels, Seneca to Pittsfield	46

## SECTION C - C-LAYER IONOSOUNDING WITH THE FORESTPORT TOWER

C-1	Transmitter Trailer at Base of 1200' Tower	55
C-2	Receiving and Recording System	57
C-3	Trailer Containing Receiving System	58
C-4	Data Samples at 160 km and 200 km from Transmitter	59
C-5	Data Samples at 220, 245 and 260 km from Transmitter	60
C-6	Data Samples Showing Two Types of Daytime Ionospheric Reflection	62

## SECTION D - PHASE STABILITY OF GROUND WAVE PROPAGATED LORAN-C PULSES

D-1	Loran Pulse Showing Reference Zero Crossing - D	66
D-2	Variation of Secondary Factor vs. Range for Different Ground Conductivities	68
D-3	Plot of Surface N and Alpha for a Week in Mid-September 1979 Between Seneca NY and HAFB	70

## LIST OF ILLUSTRATIONS (Continued)

<u>Figure No.</u>		<u>Page</u>
D-4	Plot of Time of Arrival for a Week in Mid-September Between Seneca NY and HAFB	71
D-5	Time of Arrival with Slope Removed	74
D-6	Block Diagram - Loran Receiver Base Station	76

### SECTION E - SPACE ANTENNA STUDY

E-1	Monopole Antenna "Suspended" from an Earth Satellite	81
E-2	Acceleration Toward Earth as a Function of S	84
E-3	Satellite with Center-Fed Dipole Antenna	85
E-4	Potential Function	86

### SECTION F - TRANSVERSE ELECTRIC (TE) VLF IONOSOUNDING BETWEEN THULE AIR BASE AND QANAQ, GREENLAND

F-1	AVIATION WEEK Item on Powerline Antenna	92
F-2	Transmitter Shelter and Powerline Antenna	93
F-3	TE Receiving Equipment at Qanaq	100
F-4	PCA Effects on TE Reflectivity	101
F-5	Comparison of TE and TM Data from a PCA	102

### SECTION G - C-LAYER STUDIES IN BRAZIL

G-1	Block Diagram - Portable Ionosounder Receiver System	110
-----	--	-----

## LIST OF ILLUSTRATIONS (Continued)

<u>Figure No.</u>		<u>Page</u>
G-2	Portable Ionosounder Receiver System	111
G-3	Antennas for Portable Ionosounder Receiver	112
G-4	Receiver Unit	113
G-5	Map - Transmitter and Receiver Sites	114
G-6	Building Provided by the Brazilian Air Force for an Ionosounder Receiver Site	116
G-7	Trailer and Van Provided by the Brazilian Air Force for Transporting the Ionosounder Receivers	117
G-8	3-D Plot of Received Ionosounder Signals at Camboriu for Four Days	119
G-9	3-D Plot for 28/29 May 1980 at Five Sites Showing Possible Solar Flare Disturbances	120

### SECTION H - POSSIBILITIES FOR CONTINUOUS WAVE OPERATION OF THE 120-METER (400-FOOT) TOWER AT THULE AFB

H-1	Impedance Between Ground and J-Site Side of Powerline Antenna	127
H-2	Impedance Between Ground and Thule Side of Powerline Antenna	128

LIST OF TABLES

SECTION A - FIELD PROFILE MEASUREMENTS  
WITH ROCKETS AND BALLOONS

<u>Table No.</u>		<u>Page</u>
A-1	TE Receiver Channel Measurements Obtained During Second Launch, July 1979	22

SECTION B - SURVIVABLE GROUND WAVE  
COMMUNICATIONS

B-1	Character and Space Assignment	49
-----	--------------------------------	----

## GENERAL INTRODUCTION

Under Air Force Contract Number F19628-77-C-0233, Megapulse, Incorporated significantly advanced the state of the art in the generation, propagation, and reception of Low Frequency (LF) and Very Low Frequency (VLF) radio waves. The VLF band extends from 3 kHz to 30 kHz and from wave lengths of 100 km to 10 km, while the LF band covers the interval 30 kHz to 300 kHz, or 10 km to 1 km in wave length. Together the two bands cover only about  $10^{-5}$  of the radio spectrum up to millimeter waves (30 GHz). However this small part of the spectrum has a military importance far greater than might be supposed on the basis of bandwidth alone. Some of the reasons for this are outlined below.

Frequencies above about 30 MHz propagate primarily on line-of-sight paths so that ground/ground and aircraft/ground links are confined to short distances because of earth curvature. While earth satellites can provide global, or near global, coverage at frequencies above 30 MHz under benign conditions, the possible vulnerability of satellites to enemy action must be a factor in military considerations. Frequencies in the High Frequency (HF) band (3 MHz to 30 MHz) can be reflected back to Earth by the ionosphere, and, under favorable conditions, can give essentially around-the-world coverage. However there are problems in choosing the best frequency for a given path at a given time. Since HF waves reflect relatively high in the ionosphere, they must pass

through the lower ionosphere (D region) twice in order to reflect once. Under certain naturally occurring ionospheric disturbances (such as Polar Cap Absorption events) and under man-made conditions of excess ionization, the D region absorption may be severe enough to prohibit HF communications on certain links. On the other hand, LF and VLF waves which can reflect from far fewer electrons per cubic centimeter, are typically reflected quite well from the same D region that absorbs the HF waves. This property of long waves is militarily attractive for long range, essential, communications with minimal frequency bandwidth requirements. The Megapulse work described in Sections A, B, C, F, and G all relate to specific aspects of this application.

The D region is perhaps the least understood part of the ionosphere, and the physical and chemical processes which determine its structure are only partially known. Direct rocket measurements of such quantities as free electron density and electron-neutral collision frequencies have a rather limited confidence factor, one reason being that the introduction of invasive probes may alter the parameters being measured in the local vicinity of the hardware. Measurements of electron densities less than 10 per cubic centimeter are considered especially questionable. The noninvasive technique of observing the reflection properties of LF and VLF waves in the form of short pulses provides D region information in a less disturbing and more continuous way than is

possible with direct rocket probes. Recent studies of the C layer are a case in point. Megapulse's work relating to this diagnostic area are described in Sections C and G.

Another feature of long waves is their ability to propagate over the ground around the curve of the Earth (ground wave) with much lower loss than with higher frequencies. At 100 kHz, for example, ground wave propagation has been detected out to at least 2000 km over seawater. Section B describes measurements and exploratory demonstrations leading to a possible ground wave communication link.

The ground wave is a very stable propagation mode and provides the basis of a very accurate radio navigation system (LORAN-C) which has a repetition accuracy in the order of 100 feet or better depending on geometric factors, and which does not depend on earth satellites. The precision is probably limited by variations in the refractive index of the air and it is believed that these variations are now measurable with modern equipment. It is therefore possible that LF propagation measurements may prove to be capable of providing refractive-index information over large regions of the Earth. Section D describes progress toward a system sensitive and reliable enough to study refractive-index variations.

Whereas LF and VLF waves can be received with modest, even pocket-sized antennas, the antennas required to generate or excite the waves tend to be very large. This asymmetric situation arises

from the presence of a natural, nonthermal, background noise due principally to radiation from world-wide lightning discharges. Typically the excitation of a competitive man-made signal requires both antenna efficiency and large input power, and efficiency typically means large antenna structures such as tall, base-insulated towers, long wires trailed behind aircraft, or, as discussed in Section F, long horizontal wires near the ground. Another possibility representing a challenging prospect for the future is to deploy dipole conductors in the ionosphere, see Section E. Theoretically, the presence of free electrons increases the phase velocity of radio waves to values much larger than the velocity in free space. This corresponds to a shortened wave length, which is equivalent to increasing the electrical length of the conductor, which at least under more conventional circumstances would tend to improve the efficiency of the antenna. The theory of dipole antennas in the ionosphere is very complex, especially when the anisotropies due to the geomagnetic field are considered.

The Megapulse contributions made under this contract have been closely coordinated with the RADC/EEPL program, to ensure compatibility with equipment, data recording, data recovery and processing, test range arrangements, international agreements, etc. The Megapulse work, and its tie-in with the overall objectives of the program, are described in more detail in the following pages.



## SECTION A

### FIELD PROFILE MEASUREMENTS WITH ROCKETS AND BALLOONS

#### A.1 Introduction

The objectives of this work were to provide direct engineering demonstrations of the Low Frequency wave field distributions between the Earth and the ionosphere, and to provide a basis for relating field amplitudes to the current moments and orientations of the transmitting antennas. The field distributions above the Earth's surface are of particular interest for Air Force applications and attempts to deduce the distributions indirectly from measurements on the Earth's surface would be difficult enough for fields in the Transverse Magnetic (TM) polarization, and largely out of the question for fields in the Transverse Electric (TE) polarization. Accordingly, the approach followed that of RADC/EEPL which had already been developing balloon and small rocket technologies capable of making in situ field measurements over substantial portions of the distance across the "wave guide" formed by the Earth and the ionosphere. In the daytime this distance is in the order of 70 km (230 thousand feet). The direct probe approach is specially attractive now that the United States Air Force and Navy have developed airborne transmitters which can provide signal sources at aircraft altitudes.

Figure A-1 illustrates a vertical dipole transmitting antenna in a wave guide which is shown as flat, although of course in reality both the Earth and the ionosphere are curved. The verti-

cal antenna excites fields in the TM polarization with the magnetic field H transverse to the plane of the illustration. The electric vector E is approximately vertical, and the wave power flow is in the outward direction S. Sensing of the magnetic field is with a loop antenna mounted in the rocket with its axis perpendicular to the rocket axis. In flight, the rocket spins for mechanical stabilization purposes and therefore the signal picked up by the antenna has a sinusoidal amplitude modulation. This causes no interpretational problems, and the presence of the modulation in the data output is actually reassuring as to the correct functioning of the payload telemetry recording playback system.

Far away from the transmitter, propagation theory (Wait, 1962; Galejs, 1972; Kelly, 1970; Pappert, 1970) suggests that the wave pattern should resemble (1) in Figure A-1. This has its strongest field at the ground and essentially no field at the ionosphere. In a uniform wave guide this pattern would continue to propagate with little change in shape but with gradually diminishing amplitude due to power losses in the Earth and the ionosphere. Somewhat nearer the transmitter, contributions from pattern (2) would be expected to show up. This pattern has a maximum at the ground and another around  $2/3$  of the way across the guide: it is more complex than pattern (1), attenuates more rapidly with distance, and has a lower phase velocity. A composite pattern consisting of a mixture of patterns (1) and (2) will therefore

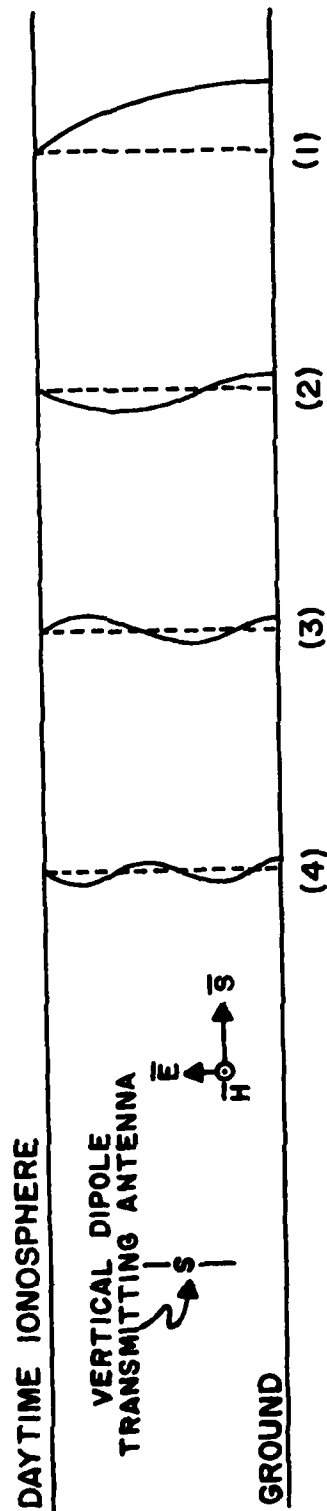


Figure A-1. Idealized Wave Patterns with Transverse Magnetic Polarization.

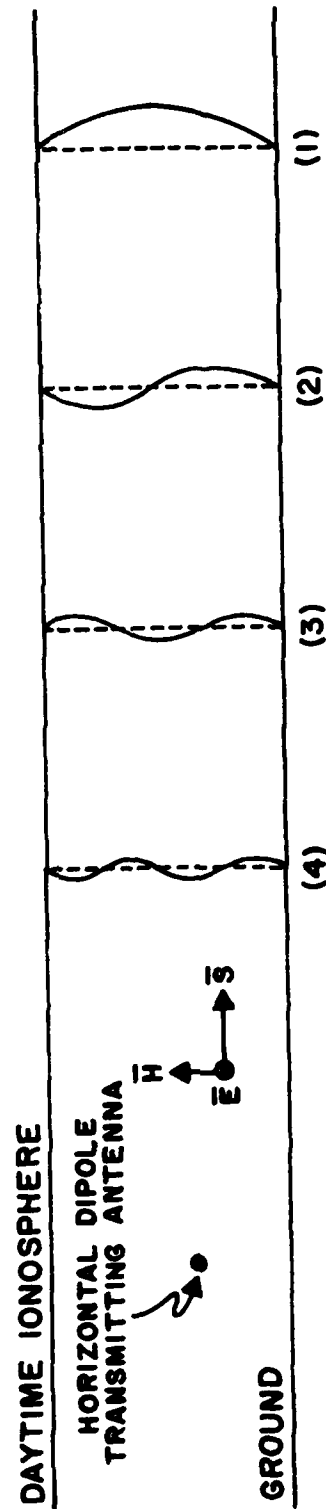


Figure A-2. Idealized Wave Patterns with Transverse Electric Polarization.

vary with distance even though the shape of its components don't. Still closer to the transmitter the higher mode patterns, (3), (4) and so on, become more evident.

Figure A-2 illustrates a section of the wave guide in a direction broadside to an elevated horizontal dipole transmitter. Here the wave polarization is TE: the electrical field is transverse to the plane of the illustration, while the magnetic field is approximately vertical. The rocket borne sensor for the magnetic field of the TE wave is a loop antenna with its axis congruent with the rocket axis, which is roughly vertical throughout the flight. Ideally the rotation of the rocket produces little or no modulation in the signal picked up. Far from the transmitter the TE field pattern is expected to resemble that shown in (1) of Figure A-2. This field has nulls, or low values, at the ground and at the ionosphere, with a maximum value about half way between. In a way similar to that discussed above for the TM modes, the higher order TE patterns, (2), (3), etc., become more important nearer the transmitter.

All the TE patterns have nulls, or low values, near the Earth's surface, which is consistent with the electromagnetic boundary conditions at the surface of a good conductor. Except for residual fields due to the earth resistivity not being exactly zero, an elevated platform is required to observe the TE fields. Similarly reciprocity arguments show that the horizontal dipole antenna must be at a high altitude to excite the TE waves effici-

ently. The airborne trailing wire transmitters can play an essential role in this regard. However, since the trailing wire has both vertical and horizontal components, it will excite both TM and TE waves simultaneously. The antenna arrangements on the probe rockets allow the two polarizations to be sorted out.

In Figures A-1 and A-2, it has been tacitly assumed that the ionosphere is of the 'E-layer' type which provides a simplification over the typical nighttime ionosphere which is at a higher altitude where the electron mean free path is large enough to allow an appreciable interaction with the geomagnetic field. This can cause an incident TM wave to partially convert to TE, and vice versa. This introduces the complicating features of mode coupling. Under normal daytime conditions this coupling is small, and it is almost certain to be even smaller under disturbed ionospheric conditions. Since the need for LF/VLF communication links is most critical under disturbed conditions when certain other links may fail, it seemed appropriate to begin the study of field profiles under low coupling conditions on the propagation paths. Accordingly, all the profile measurements under this contract took place during daylight hours.

A factor almost equal in importance to signal field strength is the background noise level, because it is the signal-to-noise ratio that determines the usefulness of a communication link. In the LF/VLF bands the background noise comes mainly from lightning discharges. It might be supposed that the noise profiles in the

ently. The airborne trailing wire transmitters can play an essential role in this regard. However, since the trailing wire has both vertical and horizontal components, it will excite both TM and TE waves simultaneously. The antenna arrangements on the probe rockets allow the two polarizations to be sorted out.

In Figures A-1 and A-2, it has been tacitly assumed that the ionosphere is of the 'daytime' type which provides a simplification over the typical nighttime ionosphere which is at a higher altitude where the electron mean free path is large enough to allow an appreciable interaction with the geomagnetic field. This can cause an incident TM wave to partially convert to TE, and vice versa. This introduces the complicating features of mode coupling. Under normal daytime conditions this coupling is small, and it is almost certain to be even smaller under disturbed ionospheric conditions. Since the need for LF/VLF communication links is most critical under disturbed conditions when certain other links may fail, it seemed appropriate to begin the study of field profiles under low coupling conditions on the propagation paths. Accordingly, all the profile measurements under this contract took place during daylight hours.

A factor almost equal in importance to signal field strength is the background noise level, because it is the signal-to-noise ratio that determines the usefulness of a communication link. In the LF/VLF bands the background noise comes mainly from lightning discharges. It might be supposed that the noise profiles in the

TE and TM polarizations might be somewhat similar to the corresponding signal profiles, but considerably 'smeared' due to the different propagation distances to the sources, and their different altitudes.

#### A.2 Rocket Measurements

U.S. Navy "TACAMO" aircraft provided TE and TM signals which were received on ARCAS rockets launched from Wallops Island, Virginia. The propagation paths were from East to West over sea water. The aircraft flew back and forth on lines perpendicular to the propagation path in order to have the trailing wire antenna in the broadside orientation required for best TE reception on the rockets. At the end of the straight line runs the aircraft turned around and the antenna orientation changed. To avoid taking data during these times, the aircraft transmitted warning signals.

With experimental programs involving rockets and aircraft, there are ample opportunities for things to go wrong, and our program was no exception in this regard.

During the term of this contract, there were fifteen scheduled rocket launches; of these only six launches actually took place. The following is a summary of the six rocket launches which took place over a three-year period.

#### November 1978

Two launches were scheduled for the month of November. One launch was scheduled and performed on the 13th of the month, the second launch was to have been on the 17th, but was cancelled due

to equipment difficulties with the trailing wire aircraft. The cancelled launch was rescheduled for the 20th, but was again cancelled at the last minute by the Navy due to equipment problems with the trailing wire aircraft.

The Transverse Magnetic (TM) profile data was of good quality on the launch that took place. Unfortunately, the Transverse Electric (TE) profile data was of poor quality. The gain setting on the TE channel was set too high. This high gain setting caused an overload condition to occur in the voltage controlled oscillator.

#### March 1979

Three launches were scheduled for the field trip which occurred on 21 through 23 March. The first two launches were scheduled for the 21st and the third for the 23rd.

The first launch took place on the 21st of March. The TM profile data was of good quality, but the TE profile data was of poor quality. Our post-flight analysis revealed that the voltage controlled sub-carrier oscillator failed at liftoff.

The second launch, which was also to have taken place on the 21st, was cancelled when the NASA surveillance aircraft experienced a radar failure. The range safety personnel were uncertain of shipping activity in the impact area, so the launch was cancelled. The third launch, scheduled for the 23rd of March, was cancelled by the Navy.



#### July 1979

Two rocket launches were scheduled for the 22nd of July. The first launch was on the northbound broadside leg of the trailing wire aircraft flight. The second launch was scheduled twenty minutes after the first, on the southbound broadside leg of the trailing wire aircraft flight.

The TM/TE profile data received from both launches was of first-rate quality. The TE data obtained from these flights was the first time good quality amplitude versus signal strength data was obtained using a rocket-borne VLF receiver.

#### March 1980

Both launches scheduled for this month were cancelled due to a severe storm in the transmitter source deployment area.

#### May 1980

Both launches scheduled for this month were cancelled by the Navy, due to operational schedule conflicts.

#### July 1980

Both launches scheduled for this month were cancelled by the Navy, for unspecified reasons.

#### October 1980

Four launches were scheduled for the month of October, two on the 28th and two more on the 29th. The launches which were scheduled for the 28th were cancelled by both the Wallops Island range personnel and by the Navy. The range personnel cancelled due to high water at the launch facilities. The high water was due to a Northeast storm on the 26th and 27th. The Navy cancelled due to equipment difficulties.

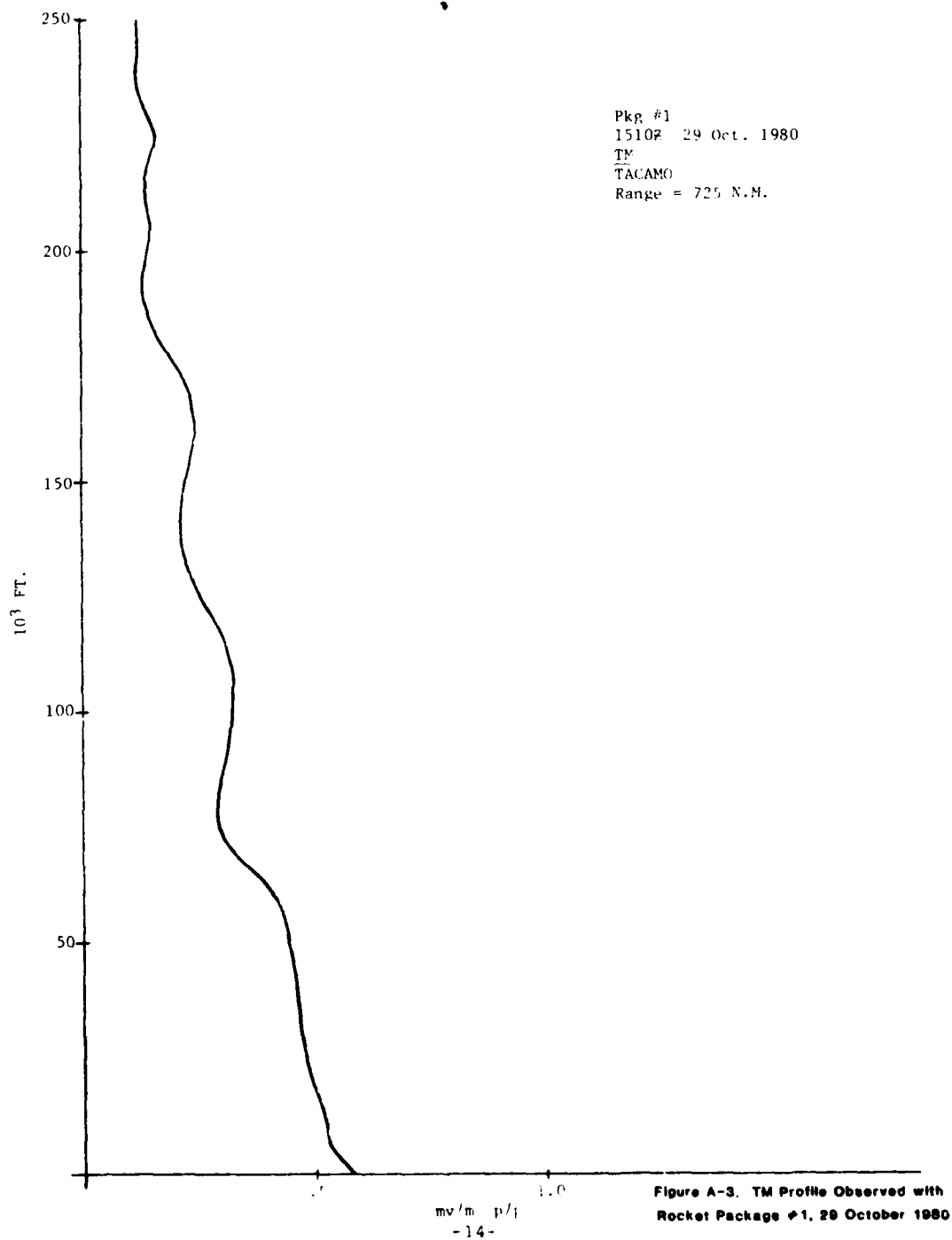
The two launches scheduled for the 29th did take place and the data received during both of these flights was of excellent quality. The plots of field strength as a function of altitude for the TM and TE profiles from the trailing wire aircraft have been completed by the project's principal researcher, Mr. Robert Harrison. These plots are presented in Figures A-3, A-4 and A-5. The profile shapes are very similar to those expected for the lowest order modes (refer to Figures A-1 and A-2).

Early in the support program, Megapulse and Air Force personnel embarked on an extensive effort aimed at upgrading the rocket VLF payload package.

The first effort was directed at the redesign of the telemetry antenna used in the payload package. The antenna which had been used in the past was a four element,  $1/4$  wave turnstile antenna. This type of antenna had two major disadvantages. These were:

- 1) The antenna elements protruded from the skin of the payload package a distance of 4.5 cm. This created drag and hence limited achievable maximum altitude.
- 2) These protruding elements could easily be broken off as the rocket left the launching tube at liftoff.

A five element slot antenna system was developed, under Air Force contract, by the University of New Mexico. This antenna allowed us to replace the four element,  $1/4$  wave turnstile antenna. By using the new slot antenna (see Figure A-6, arrow marker) we



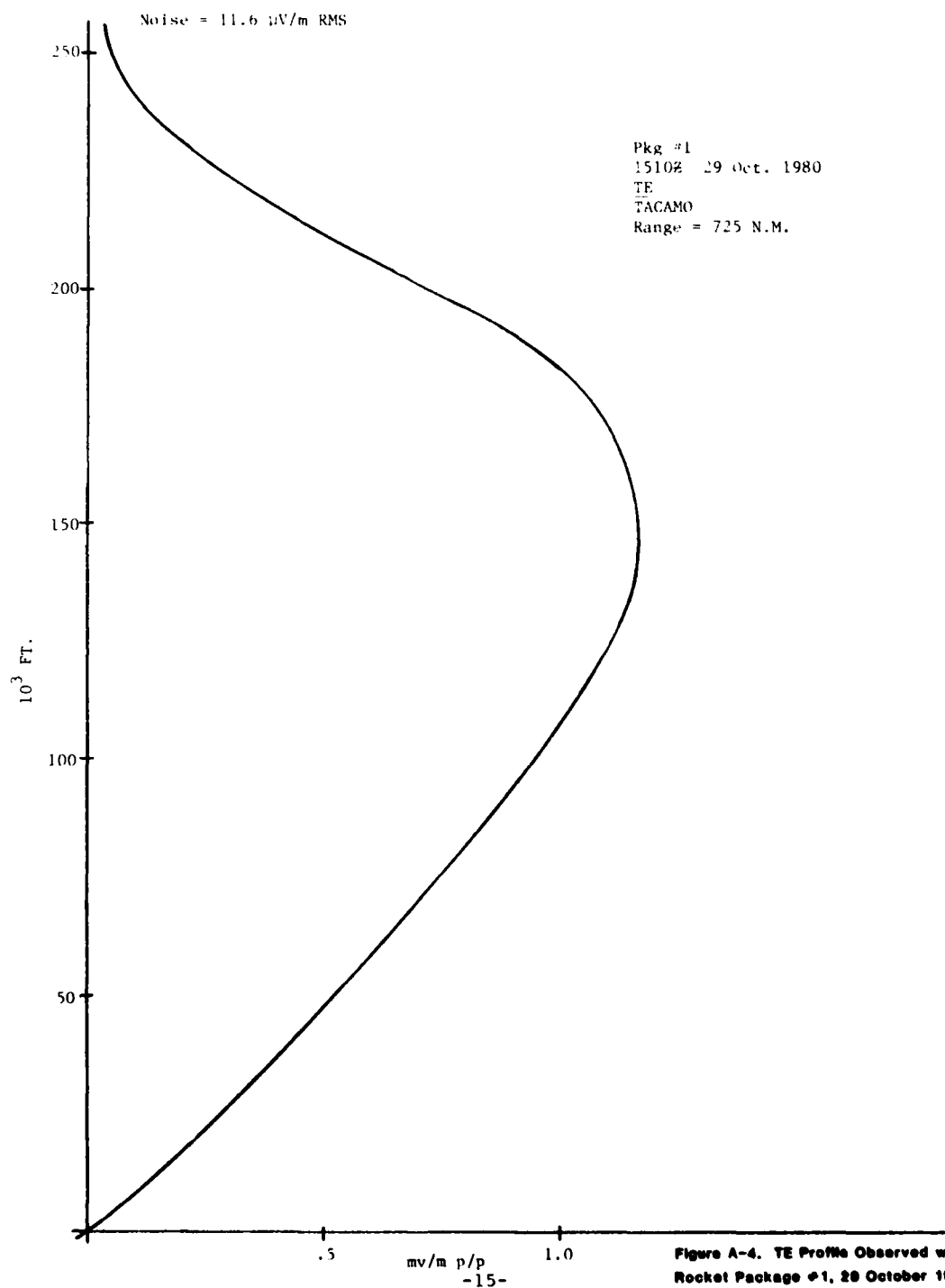
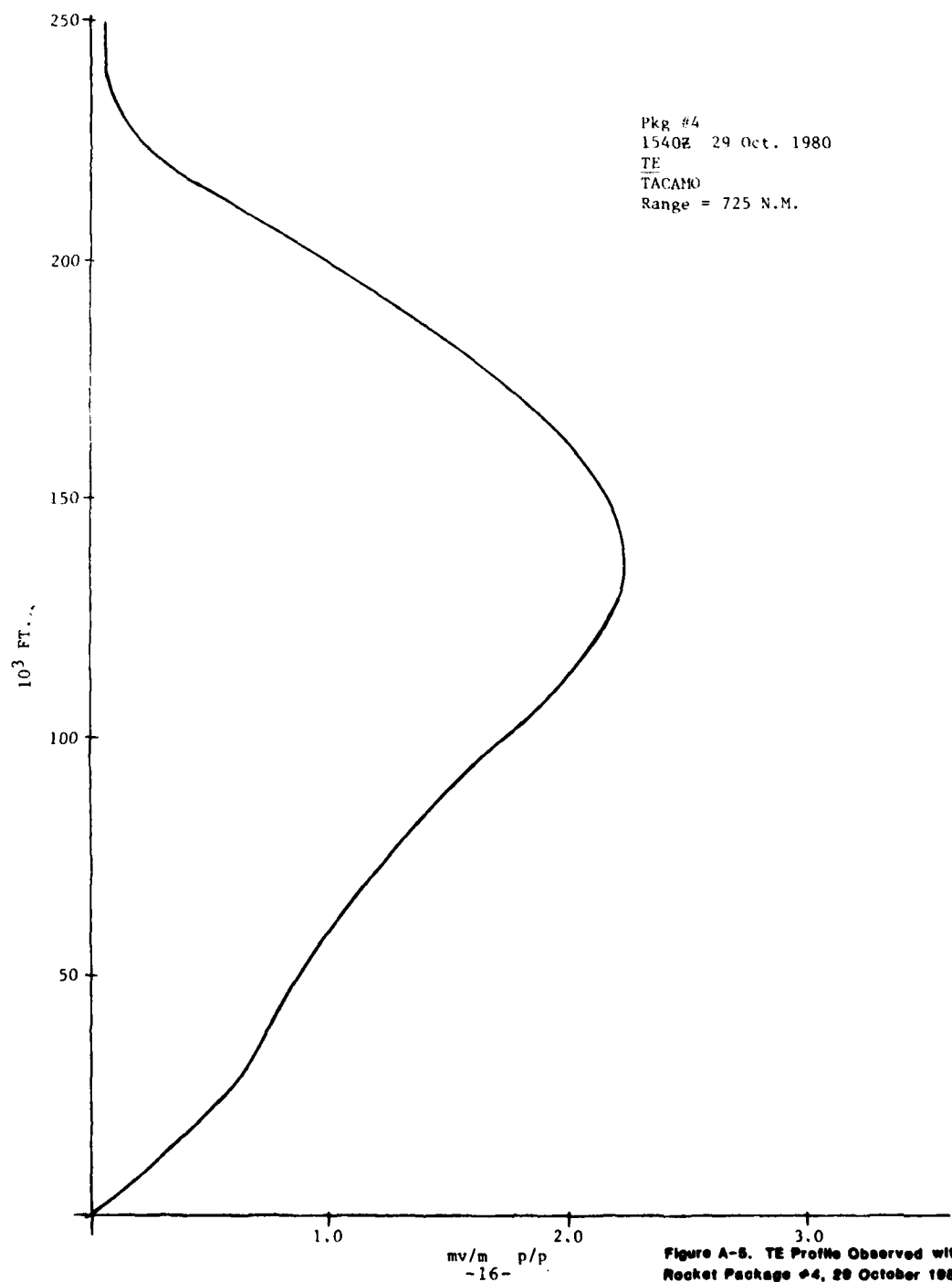


Figure A-4. TE Profile Observed with Rocket Package #1, 29 October 1980.





**Figure A-6. Rocket, Showing Telemetry Slot Antenna.**

were also able to replace the RCA 1680 MHz on-board (telemetry) transmitter with an 2251.5 MHz S-Band transmitter. This gave us twice the transmitter power and also enabled us to use the S-Band tracking system at Wallops Island.

The second step taken in the improvement of the payload package was the acquisition of a new type organic Lithium primary battery. This battery increased our power pack capacity from 600 MAH to 1100 MAH, while also giving us a slight decrease in payload weight. This new battery gave us a minimum on-air time of one hour, and by adding a second battery in parallel, we can effectively double our on-air time. With this improvement in battery life we now have a VLF payload which can remain in the launch tube, ready to be fired, if a long countdown hold takes place.

Because of the above additions, a repackaging effort of the VLF Receiver/Signal Processing section of the payload resulted in the elimination of the sun-aspect sensor and the baro switch. Both of these items can be classified as ancillary components which are nice to have but are not necessary for mission success.

First, the barometric switch was used to provide a "back-up" system turn on, and for giving a reference trajectory mark at 70 K. FT. on the ascent and another during the descent at 57 K. FT. Good radar tracking by the Wallops Island personnel, plus a good package system design which provided long-life batteries and continuous pre-launch monitoring, rendered this device unnecessary. See Figure A-7 (arrow) and note the fiberglass section in the launch tube, which enables us to monitor the S band signals from the payload prior to launch.

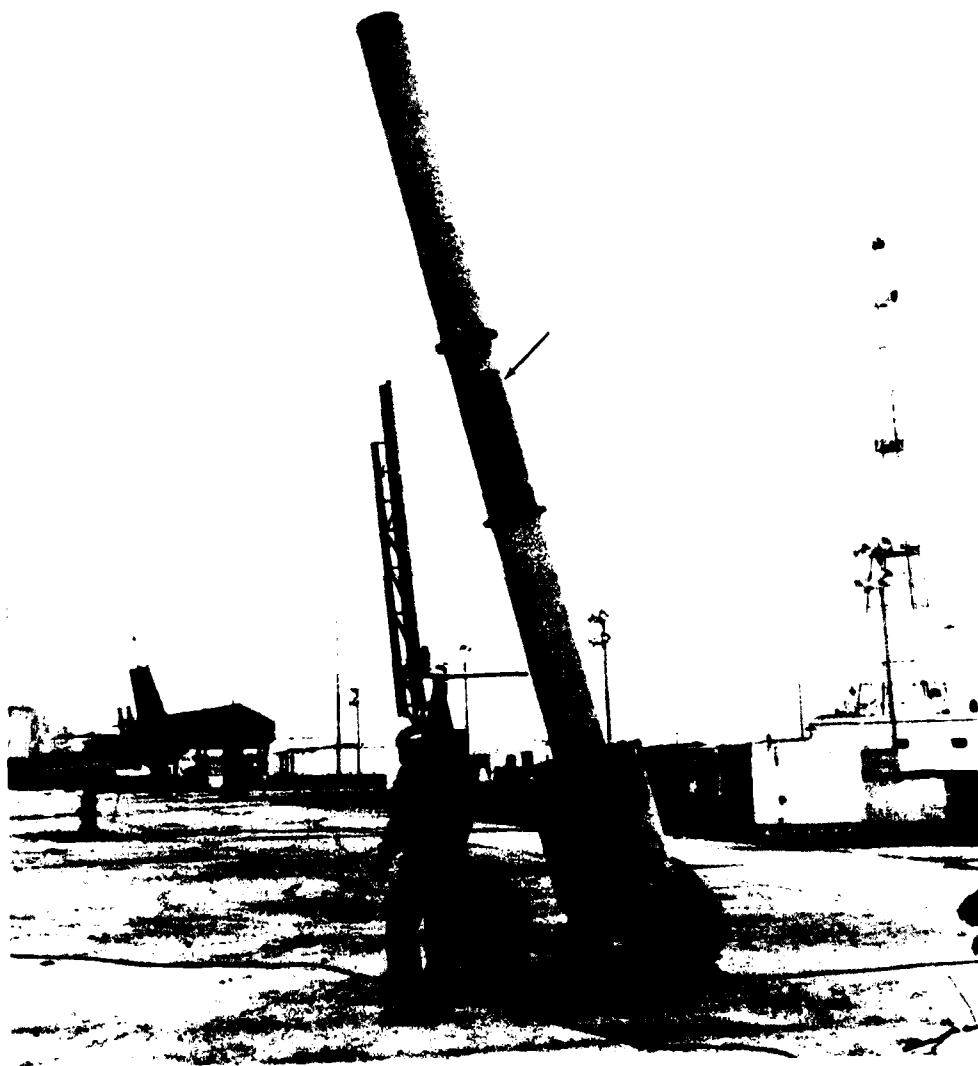


**Figure A-7. Rocket Launch Tube, Showing Fiberglass Section.**



The aspect sensor is a solar detector which produced attitude information from its position relative to the sun. We found that by carefully monitoring the spin component on the TE VLF channel, we could accurately determine the degree in which the payload was deviating from the vertical.

One of the more important innovations in our payload development program has been the inclusion of a shake and shock test (0 to 2000 Hz for 30 seconds and 50 g) on every payload package prior to launching. This was incorporated into our program after an in-flight failure during the March 1979 field trip. Since the inclusion of this test in our program, we have had no in-flight component failures.

Figure A-8 is a system flow diagram showing the system for payload development through component procurement, final assembly, test, and rocket launches. The salient point one derives from looking at this flow diagram is that many different groups and sources must make their individual contributions to the final payload package.

As reported in our July 1979 launch report, an increase in background noise was noted during the time the rocket motor was firing. This noise was found to be broad-banded in nature and is relatively flat across the VLF band. As seen in Table A-1, the relative amplitude of the rocket-induced noise increases with increasing altitude. Since this noise may impose a fundamental limit on the weakest signal that can be measured during the thrust portion of a rocket flight, it is of interest to speculate briefly on a possible origin of this noise.

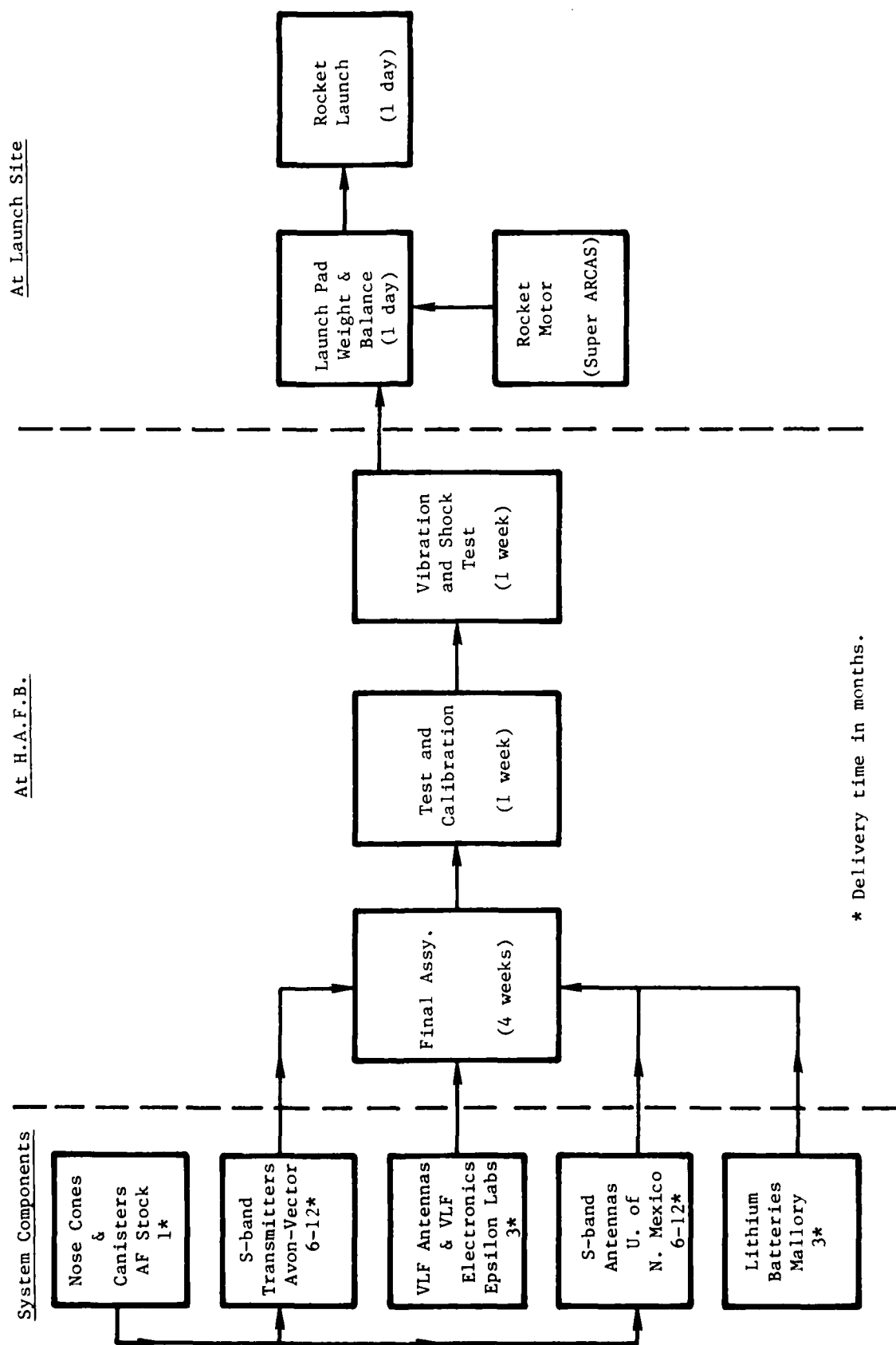


Figure A-8. Super ARCAS TE/TM Rocket Launch, System Flow Diagram.

TABLE A-1.

TE RECEIVER CHANNEL MEASUREMENTS  
OBTAINED DURING  
SECOND LAUNCH, JULY 1979

Relative Increase in VLF Noise in dB	Time Into Launch in Seconds	Altitude in km	Atmospheric Pressure in mm Hg
+2	T +10	1.5	630.7
+ 5 to + 7	T +20	5.6	377.2
+20 to +23	T +30	11.4	156.0
+20 to +23	T +36	16.0	81.0
0	T +50	29.4	10.8

NOTE: Rocket motor turns off sometime after  
T +32 seconds. Therefore by T +50 seconds  
there is no ionized trail remaining.

Suppose that the mobility of the negative ions in the combustion chamber of the rocket is greater than the mobility of the positive ions, both of which are created by the combustion process. There would then be more negative ions giving up their charge to the chamber walls than positive ones. The hot gas expelled through the exhaust orifice, and forming the plume, would then carry an excess of positive charge, while an equal but opposite (negative) charge would appear on the outer surface of the rocket body. The rocket has only a small electrical capacitance, and this charging process would soon give it a very high negative potential with respect to its surroundings except that when a certain potential is reached, corona discharge into the air will begin. Eventually the system reaches an equilibrium condition in which the negative corona current equals the current of positive charges being carried off by the exhaust plume.

The corona current tends to flow from sharp points where the electric field is large due to the concentration of field lines. Such points may be found at the rocket tip, around the stabilizing fins, telemetry stubs, or even at small burrs on the rocket body. Under laboratory simulation conditions, the corona is typically not a steady current, but consists of a series of individual charge-bursts. These occur when the air in the immediate vicinity of the point suddenly ionizes, and then more suddenly de-ionizes -- a process which repeats rapidly. The ionization phase occurs very rapidly, and consequently the corona currents have

spectral components extending well up into the high radio frequencies. The coupling of these currents to the on-board receiving antenna or its associated circuitry would inject radio noise into the receiver.

In a manner reminiscent of Paschen's Law, there is a particular air density at which corona occurs most readily (least voltage). Using data from published curves (Loeb, 1974) it appears this density is about 1/760th of the air density at the Earth's surface. Inspection of model atmospheres (Valley, 1965) indicates this density ( $1.6 \text{ gm}^{-3}$ ) occurs at an altitude around 45 km. In the case described in Table A-1, the rocket motor cut off at around 15 km, so that in a loose qualitative sense, coronal conditions were becoming increasingly favorable throughout the burn portion of the flight. This may relate to the observation that the noise increased up to around the altitude of burn-out.

Corona noise on aircraft (often called "precipitation noise" because the charge accumulates in passing through clouds of water or ice particles) can be reduced by attaching discharge wicks of resistive material which allows the electrical charge to drain off more smoothly into the air. It might be interesting to look into the adaptability of this technique to rockets.

### A.3 Dartsonde Packages

The balloon-dartsonde concept had already been developed by RADC/EEPL. Briefly, a meteorological type balloon is used to carry a torpedo shaped electronics package ("dart") to an altitude around fifty thousand feet (15 km). The package is then released

by a baro switch or by radio control, allowing it to fall. The aerodynamic shape of the package (which has tail fins and a concentration of mass in its rounded nose) causes it to fall with its axis nearly vertical. Like the rocket payloads, the dart has separate TE and TM loop antennas, and like the rockets, there is a slow spin about the vertical axis (imparted by the tail fins). The dartsonde is less expensive than a rocket probe; it does not have to withstand the g-forces of launching, and does not require the full services of a rocket launching range. On the other hand, its altitude is much less, and it takes much longer to reach it.

On this contract, a number of significant improvements were made on the dart design. The following paragraphs describe the various problem areas and the steps taken to remedy them.

Drift in the on-board frequency of the sub-carrier VCOs was experienced due to extremely low temperatures ( $-60$  to  $-70^{\circ}\text{C}$ ). This created a change in value of key components.

The on-board receiver package was modified (see Figure A-9) from a configuration which used a flat disk PC board to one which was folded in a box fashion. The next step was the encasement of this PC board in a high density foam package with a minimum of one inch of foam on all sides. This foam/PC board package was then covered with aluminum foil and the circuit was subjected to test in an environmental chamber through one long cycle of very low temperatures ( $-70^{\circ}\text{C}$  for 2 hours).

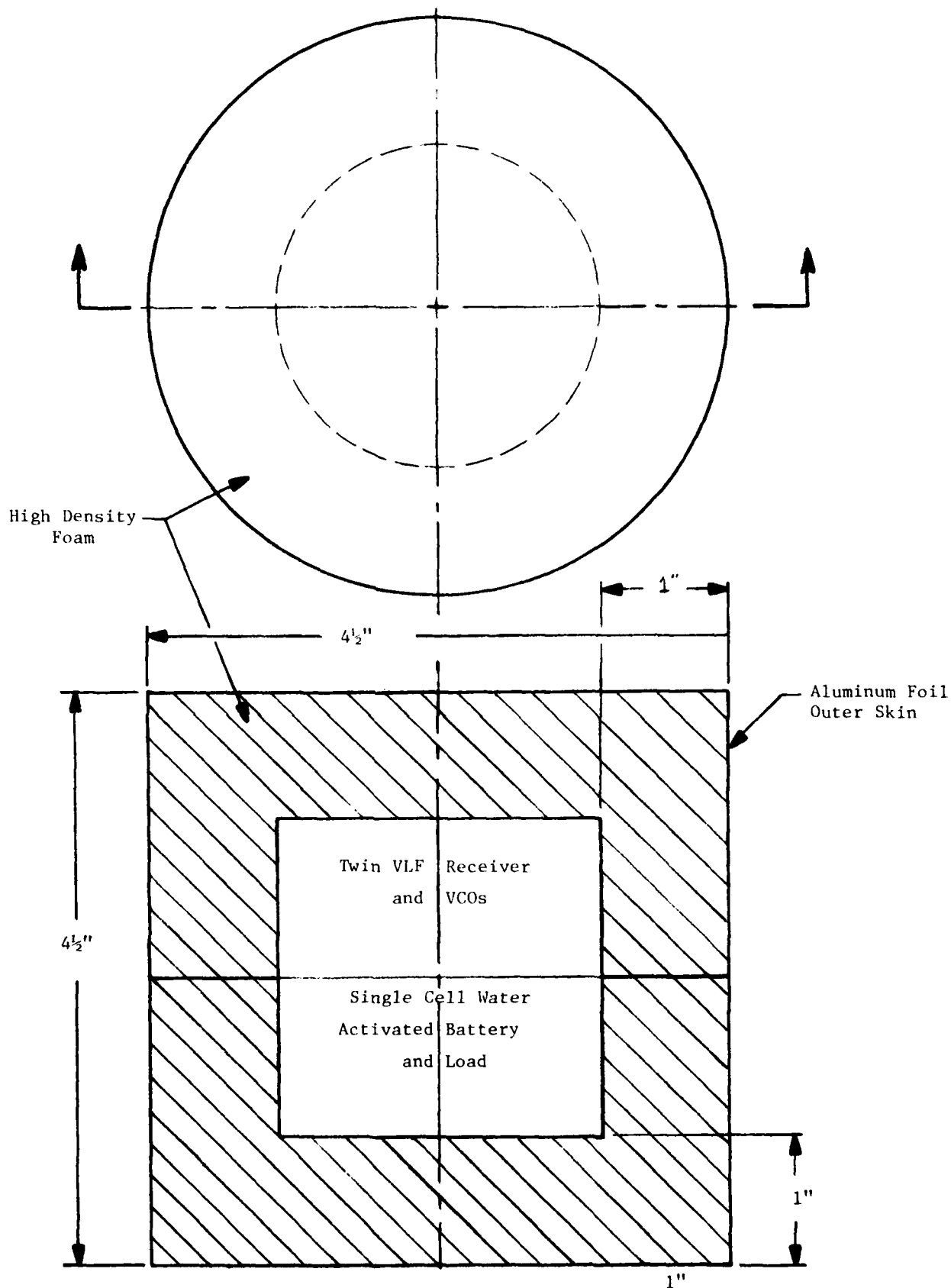


Figure A-9. Thermal Package for Dartsonde Receivers.

While the receiver worked well through most of the above testing, it was found that a slight VCO frequency shift did take place towards the end of the two-hour test period. To remedy this slight shift, an internal heat source was provided for the package. This was accomplished by the inclusion of a small water-activated battery cell inside the foam package. These cells exotherm during operation, and with the cells' loads adjusted for a two-hour operational life, this battery maintained an internal package temperature between  $+35^{\circ}\text{C}$  and  $+25^{\circ}\text{C}$  during the two hour environmental test.

It became apparent that a device was needed to separate the dartsonde package from its lifting balloon on command from the ground. (This is true for a dart which is being used for TM/TE profiles, but is not necessary for darts which are being used for spheric measurements.) Figure A-10 is a block diagram of the separating system which was designed for this program. The ground equipment consists of a 400 MHz RF source, a linear power amplifier and a high gain antenna. The on-board equipment consists of a monitor super regenerative receiver, tone decoder and solid-state relay which fires the separation squib.

A highly desirable improvement would be a mechanism for holding the dartsonde package vertical during the ascent portion of the balloon flight. This would multiply the data collection by at least a factor of ten and would render the cut-down signal unnecessary. It might be thought that the use of some sort of a gimble



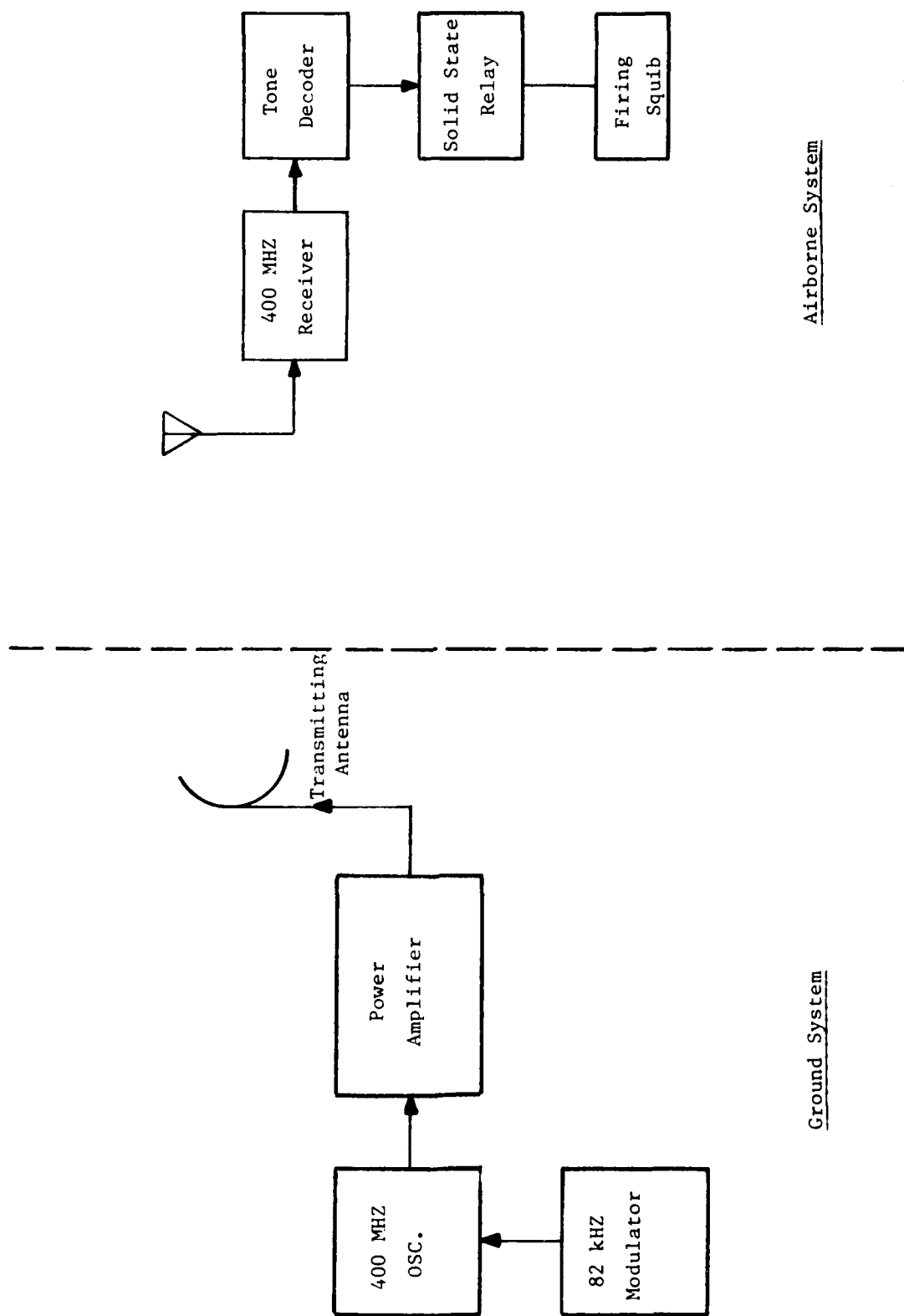


Figure A-10. 400 MHz Outdown System.

system would provide the solution to this problem. However since the gimble would respond to both the acceleration of gravity, and the acceleration due to motion of the package, it probably would not be very effective. A mock-up test made in the laboratory tended to confirm this conclusion.

As a result of the priority given to the rocket, and other work under this contract, field experiments with dartsondes were somewhat curtailed. The principal field exercise was the measurement at Swan Island, Honduras of atmospheric noise in the TE and TM polarizations. This work has been reported separately (Donohoe, 1978) and will not be repeated here. The principal conclusion was that with the noise fields existing at the times of the flights, no marked difference between noise amplitudes in the two polarizations was noted.

#### REFERENCES, SECTION A

- Donohoe, J.B.; Launch Report, Swan Island, Megapulse, Incorporated, Bedford, MA; 1978.
- Galejs, J.; Terrestrial Propagation of Long Electromagnetic Waves, Pergamon Press; 1972.
- Kelly, F.; VLF Field Strength Variations from An Airborne Trailing Wire Antenna, Radio Science, Vol. 5, No. 5, Pages 587-791; May 1970.
- Loeb, L.B.; Fundamental Processes of Electrical Discharges in Gases, J. Wiley & Sons, New York, Page 508; December 1947.
- Pappert, R.H.; The Effects of Elevation and Ground Conductivity on Horizontal Dipole Excitation of the Earth Ionosphere Wave Guide, Radio Science, Vol. 5; 1970.
- Valley, S.; Handbook of Geophysics and Space Environments, United States Air Force Publication, Table 2.4; 1965.
- Wait, J.R.; Electromagnetic Waves in Stratified Media, MacMillan, New York; 1962.

SECTION B  
SURVIVABLE GROUND WAVE COMMUNICATIONS

B.1 Introduction

The possibility that a signal fade might occur in an essential communication link of national, or military, importance is a matter of great concern. The possibility of a fade in a LF/VLF link comes about because the received signal is a composite of waves arriving at the receiver with different amplitudes and phases. The vectorial addition of such waves might just happen to give a low value, especially under violently disturbed ionospheric conditions. A simple way of avoiding this difficulty is to keep the propagation paths so short that the ground wave will always be larger than any possible combination of skywaves. Another, more sophisticated, way is to transmit pulses with short rise times and by some gating or switching technique at the receiver, eliminate the sky waves on the basis of their later arrival times. Of the two methods, the second is more likely to give the longer communication distance.

The time interval between the first arrival of the ground wave, and the first arrival of the sky wave is given approximately by:

$$\Delta t = \frac{2}{c} \sqrt{h^2 + 2a(a+h)(1-\cos\theta)} - s/c$$

where:

a = the radius of the Earth,

c = the velocity of radio waves,

h = the ionospheric reflection height,

s = the great circle propagation distance; and,

$= s/(2 a)$ .

If a minimum height h can be specified, this formula gives an estimate of the time in which the gating function must operate, and in which the information must be contained. As an example, for h = 30 km, s = 480 km (or 300 miles), c =  $3 \times 10^5$  km/sec, and a = 6400 km, the formula gives  $\Delta t = 16$  microseconds. This time window would be filled by just one cycle of a 62.5 kHz wave, but it might not be necessary to have a full cycle in order to communicate.

The work described in the following paragraphs was divided into two efforts: (a) to measure the CW sky wave/ground wave amplitude at two distances from a 100 kHz transmitter under normal diurnal conditions, and (b) a demonstration of communication with ground wave pulses at 33 kHz.

## B.2 Description of the CW Measurements

The relative strengths of the CW sky wave and ground wave were inferred from measurements of 100 kHz pulses from a LORAN-C transmitter at Seneca, New York. The measurements were made at Hanscom Air Force Base, Massachusetts and at Pittsfield, Massachusetts, the propagation path lengths being 456 km and 295 km re-

spectively. Data was recorded for three twenty-four hour periods at both Hanscom and Pittsfield. The same transportable receiving equipment was used at the two sites.

The receiving system was comprised of the items shown in the block diagram (see Figure B-1), which were housed in a camping trailer (see Figure B-2) that was modified by Megapulse specifically for Loran studies under this contract. The equipment is configured as shown in Figure B-3. The rack is shock mounted for traveling. Also, brackets and shroud lines are installed for traveling to prevent sway and tilt.

The receiving loop antenna is a Stoddard, Model Number AT-206/URM. The loop antenna was mounted on the Pre-Amp housing.

The Pre-Amp was designed and built by Megapulse, Incorporated and is broadly tuned around 100 kHz. The Waveform Recorder is a Biomation Model 805. It converts an analog input signal into an internally stored digital signal of 2048 eight-bit bytes. Operation is initiated by the receipt of a trigger from the Pulse Rate Generator. An analog to digital conversion is performed at the sample rate of 200 nanoseconds, this interval is also generated by the Pulse Rate Generator. After completion of a Loran pulse recording the digitized signal is transferred to the Signal Averager.

The Signal Averager is a Nicolet Model 1074. It is a general purpose data logging device. It has a total memory of 4096 eighteen-bit bytes. The memory can be divided in half and each half can be operated on separately or together.

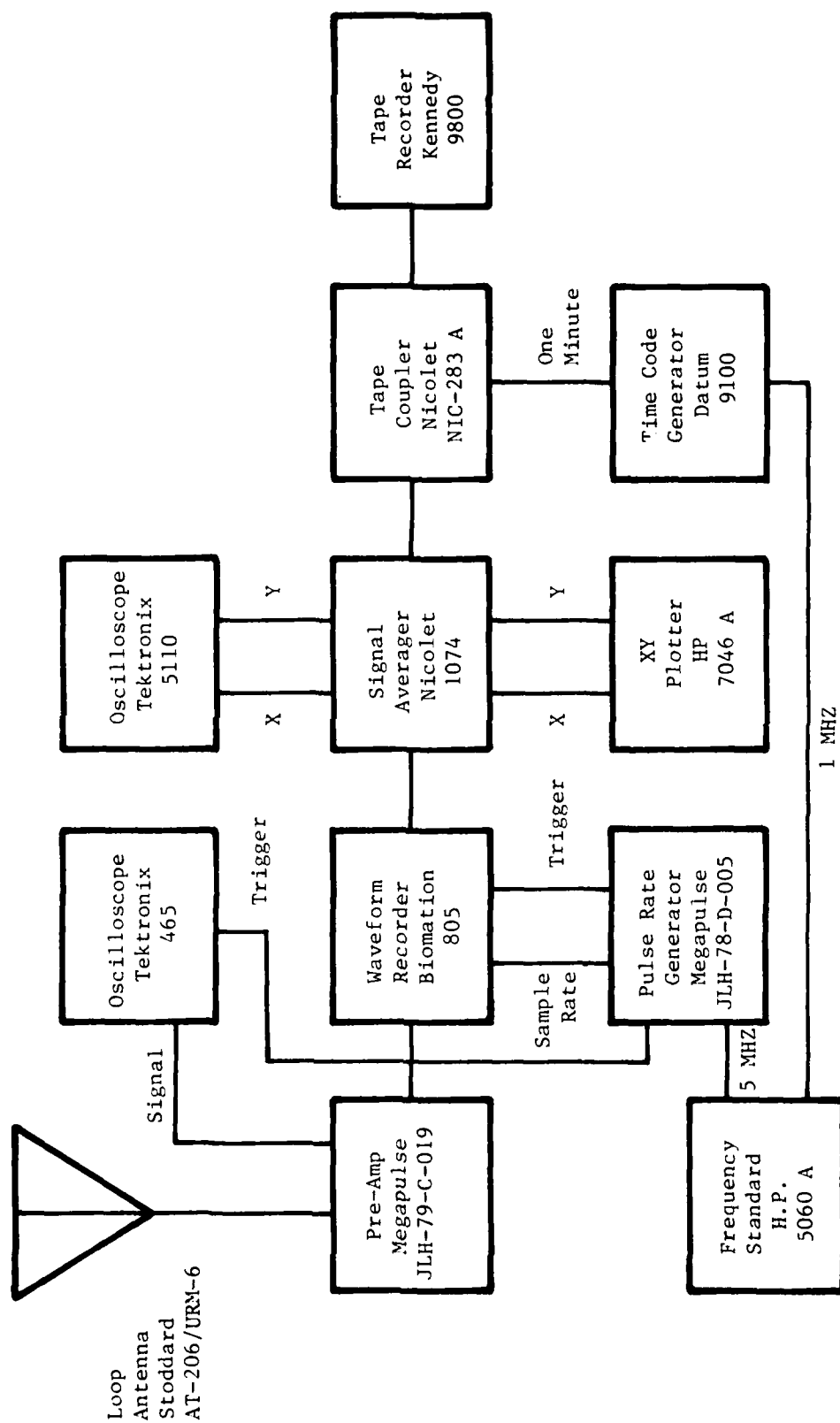


Figure B-1. Block Diagram, Loran Receiver System.

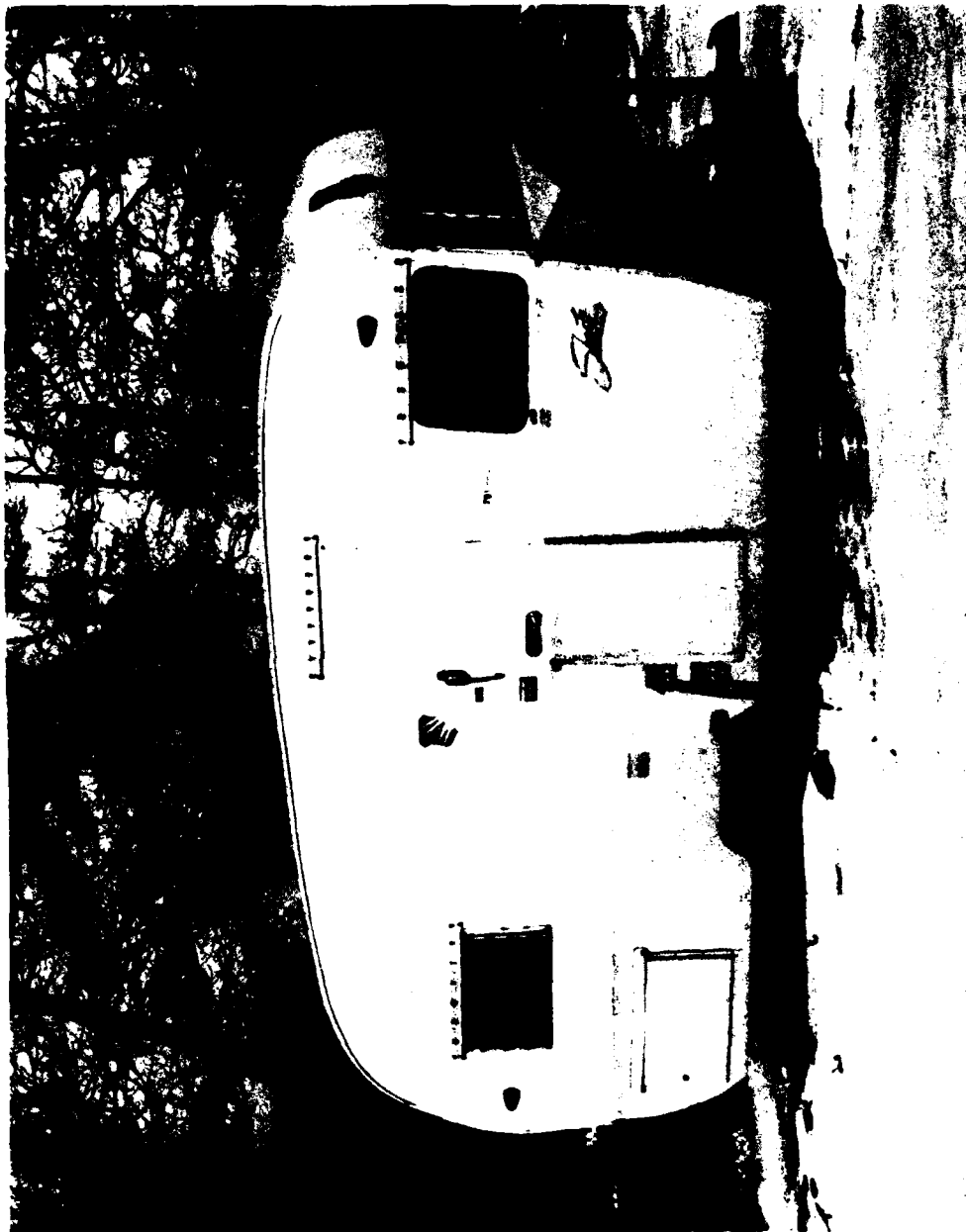


Figure B-2. Loran Receiver Trailer.



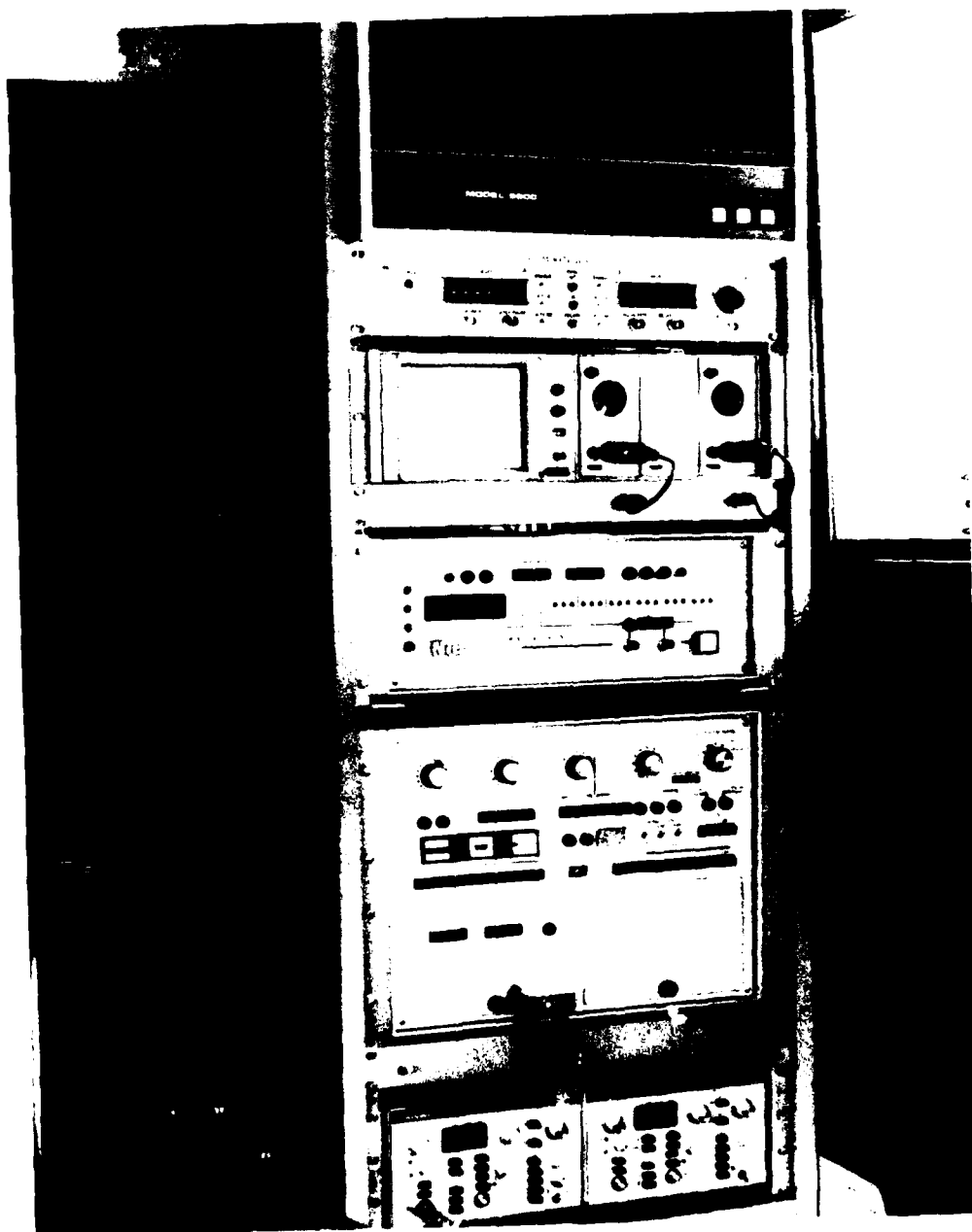


Figure B-3. Inside of Loran Receiver Trailer.

In this operation the first half of the memory was used and 512 waveforms were averaged. Upon completion of the averaging the digital signal was dumped through the Interface onto the Tape Recorder. After this dump is completed a new averaging cycle begins.

The Signal Averager is also used in data analysis. The signal is played back into the memory. A standard signal is selected (refer to Figure B-4(a)) and then transferred to the second half of the memory. This standard signal is then subtracted from all of the other signals to get the value of the sky wave (refer to Figure B-4(c)). The memory address and related word go through digital to analog conversion for X/Y display. The memory addressing also has a slow mode which enables the contents to be put onto a plot (refer to Figure B-4).

The Interface is a Nicolet Model 283. It controls the flow of data to and from the Tape Recorder. It also has switches and a counter for ancillary information.

The Tape Recorder is a Kennedy Model 9800. It is a nine track recorder and uses 1200-foot reels. Each reel is good for just over a thousand records, or seventeen (17) hours for one minute averages.

The Frequency Standard is a Hewlett-Packard Cesium Beam Frequency Standard Model 5060 that has been adjusted to track the Seneca transmitter. It puts out five megahertz to the Pulse Rate Generator and one megahertz to the Time Code Generator.

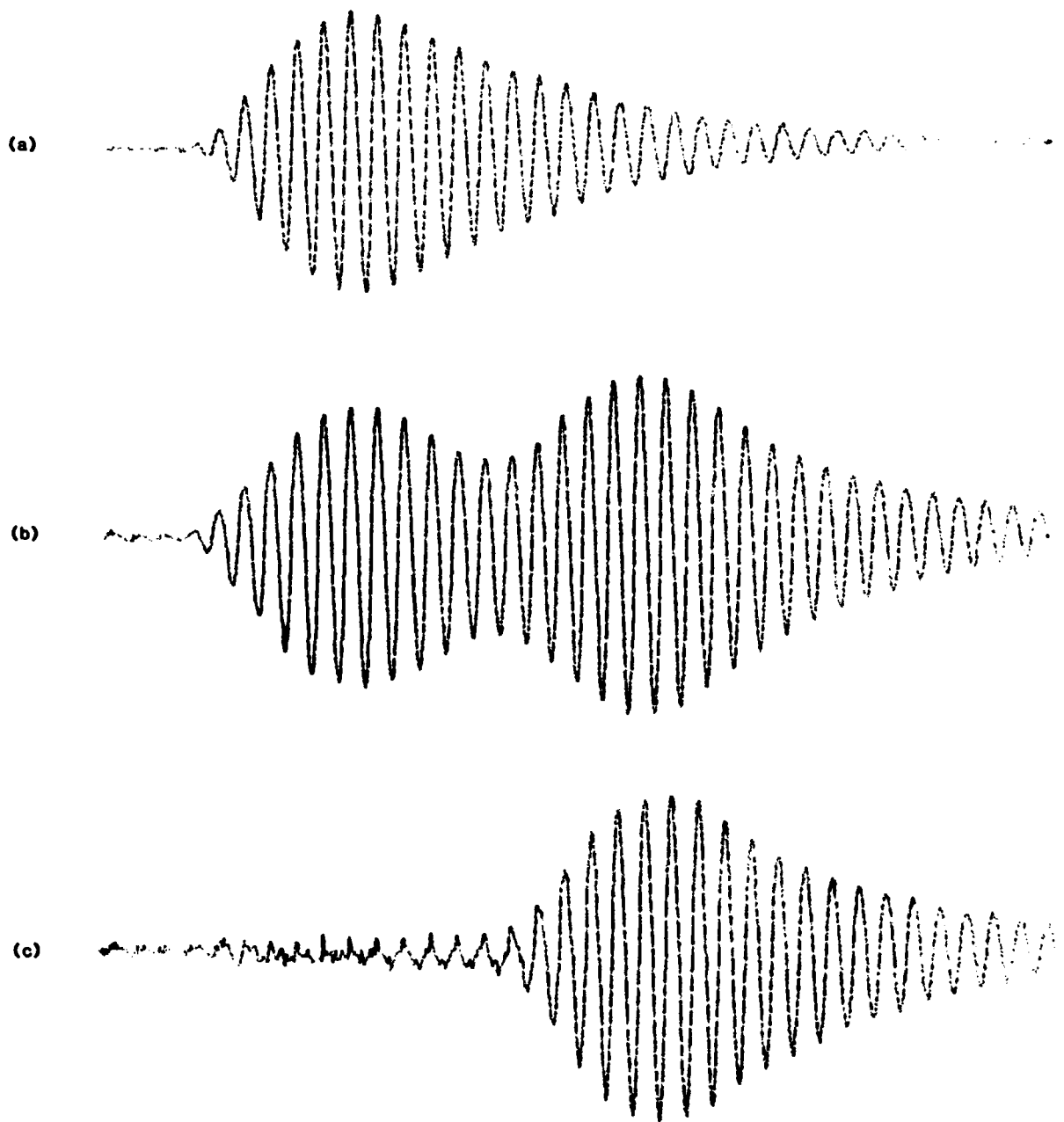


Figure B-4. Loran Signals Received at H.A.F.B. from Seneca on 29 December 1980.  
(a) Ground Wave with no Sky Wave. (b) Ground Wave with Night Time Sky Wave.  
(c) Residual Night Time Sky Wave.

The Pulse Rate Generator was designed by Megapulse, Incorporated. It is a dual unit that can operate on any Loran or other repetition rate with any delay, from one to 999,999 microseconds. The two units can be synchronized or run separately. Section B of the Pulse Rate Generator can also block Section A from putting out a trigger pulse, thereby providing a means to eliminate cross-rate interference.

Section A was set on the Northeast Loran Chain Group Repetition Interval of 99600 microseconds. A suitable delay was dialed in to generate the trigger pulse to start the ground wave pulse from Seneca one quarter of the way through the recorded waveform. Section B was set on the North Atlantic Loran Chain Group Repetition Interval of 5930 microseconds. A suitable delay was dialed in to cut out the Section A trigger when a Loran signal from the North Atlantic Chain transmitter on Nantucket would cause interference.

The Time Code Generator is a Datum Model 9100. It divides down the one megahertz from the Frequency Standard into days, hours, minutes and seconds. It sends a one-minute pulse to the counter in the Interface for generating a count equal to the time of year in two-minute increments.

The Monitor Oscilloscope is used to acquire the proper signal for recording and the proper signal for the cut-out. The X/Y oscilloscope displays the contents from the memory in the Signal Averager.

### B.3 CW Field Measurement

The equipment was set up at the Bonnie Brae Campground in Pittsfield, Massachusetts. The Loran signal from Seneca, New York was tuned in and fed to the averaging equipment. Groups of 512 signals were averaged and then dumped on tape. An average and a dump cycle was performed at the rate of approximately one per minute. This time was selected to show smooth transitions in the amount of reflection. One tape would last fourteen hours, therefore, the tape was changed twice a day. This test started on 2 December 1980 and was run until 5 December 1980, and generated a total of six tapes.

On 10 December 1980, the equipment was set up at Hanscom Air Force Base and again the Loran signal from Seneca, New York was tuned in. The signal from Nantucket (on the North Atlantic Chain at a GRI of 5930 microseconds) was tuned so it could be automatically cut out when it interfered with the Seneca, New York signal. The equipment was run on the 11th, 18th and 29th of December 1980 and also on the 6th of January 1981.

### B.4 Reduction of CW Data

The magnetic tape recordings were analyzed one record at a time to measure ground wave and sky wave amplitudes. A record would be played back from the tape into the memory of the signal averager. It would then be compared to a standard waveform. A standard waveform is one that was selected at local noon with no distortion (no sky wave). This standard waveform was stored in the second half of the memory for reference purposes.

Figure B-4(a) shows a standard Loran ground wave which was used for reference. Figure B-4(b) shows a commonly occurring nighttime sky wave. Figure B-4(c) shows what is the nighttime sky wave component.

Each record was read and tabulated. The records from HAFB were plotted and clearly showed the turbulent nature of the ionosphere. One point of interest is how rapidly the ionosphere can change from nighttime conditions to daytime conditions. A section of the plot for 19 December 1980 (between 0600 and 0700 local time) is shown where the nighttime sky wave is larger than the ground wave and several minutes later there is no sign of a sky wave, see Figure B-5.

This rapid transition of the sky wave amplitude approximately one hour (0609) before local sunrise (0711) is in agreement with other researchers (Bracewell, 1951).

The records for each one hour time period were averaged together for various dB levels and plotted (refer to Figures B-6 and B-8). The plot shows the percent of signals between 0 dB and up, between -3 dB and 0 dB, between -6 dB and -3 dB, between -10 dB and -6 dB and between -20 dB and -10 dB. The percentages were totaled and plotted to show the cumulative value above each dB level (refer to Figures B-7 and B-9).

During the collecting of the data and its analysis, the ionosphere appears to be very unpredictable. Nighttime conditions at HAFB indicate that a strong sky wave will usually be present. Daytime conditions at HAFB indicate, on occasion, that there will be a fairly strong sky wave present.

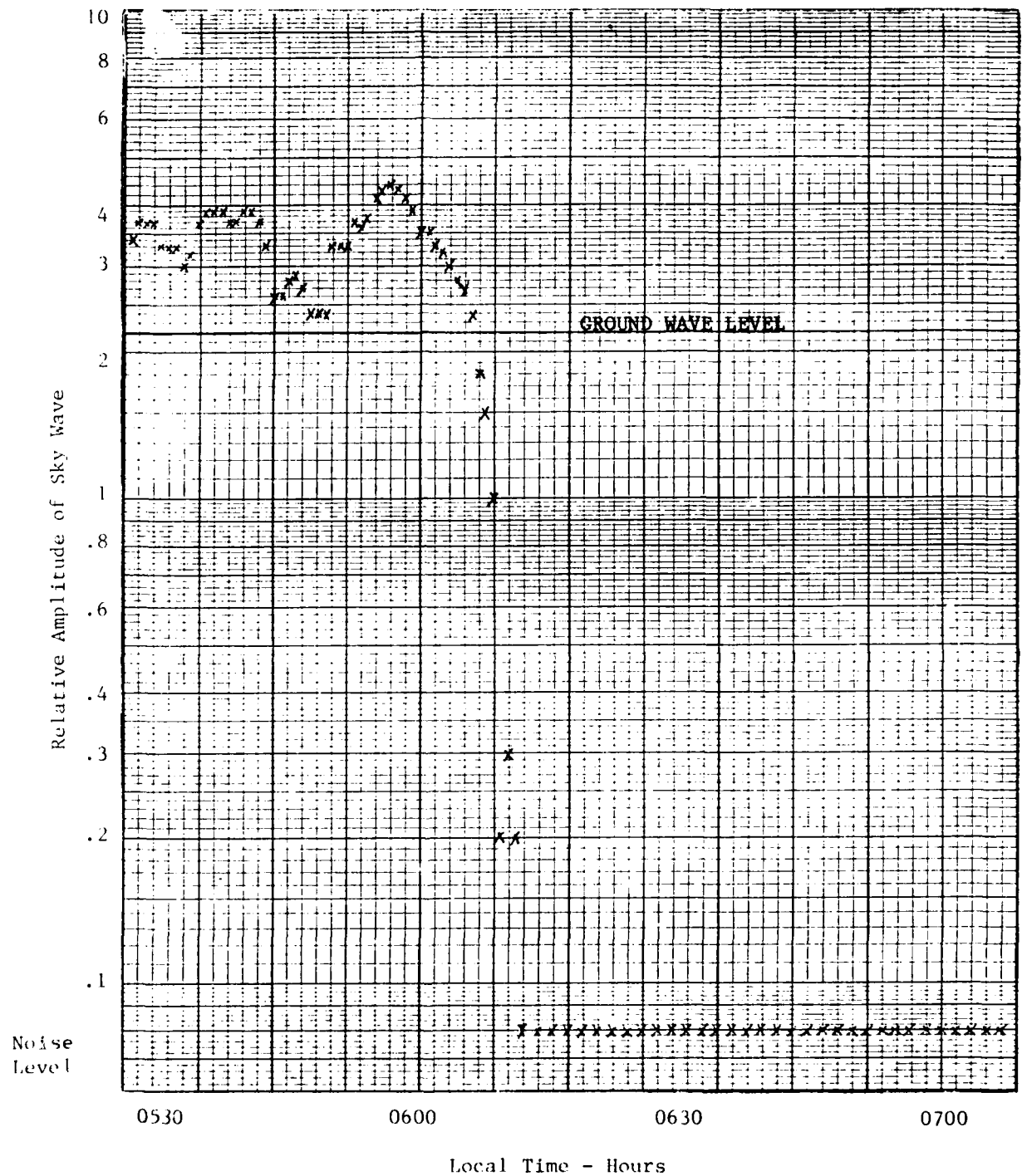


Figure B-5. Plot Showing the Rapid Transition of the Ionosphere at Dawn.

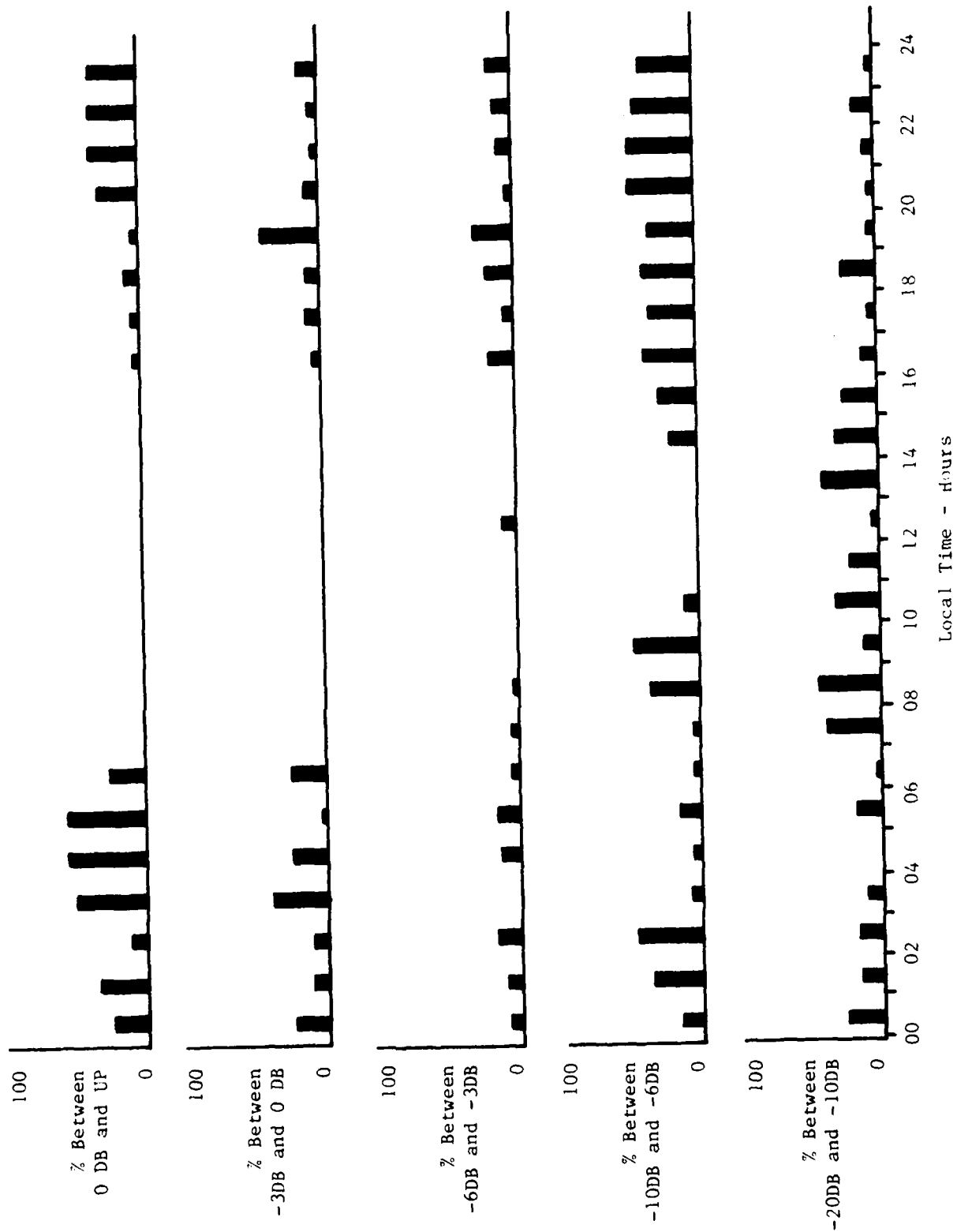


Figure B-6. Averaged Loran Sky Wave Ground Wave Ratios Between Levels, Seneca to H.A.F.B.



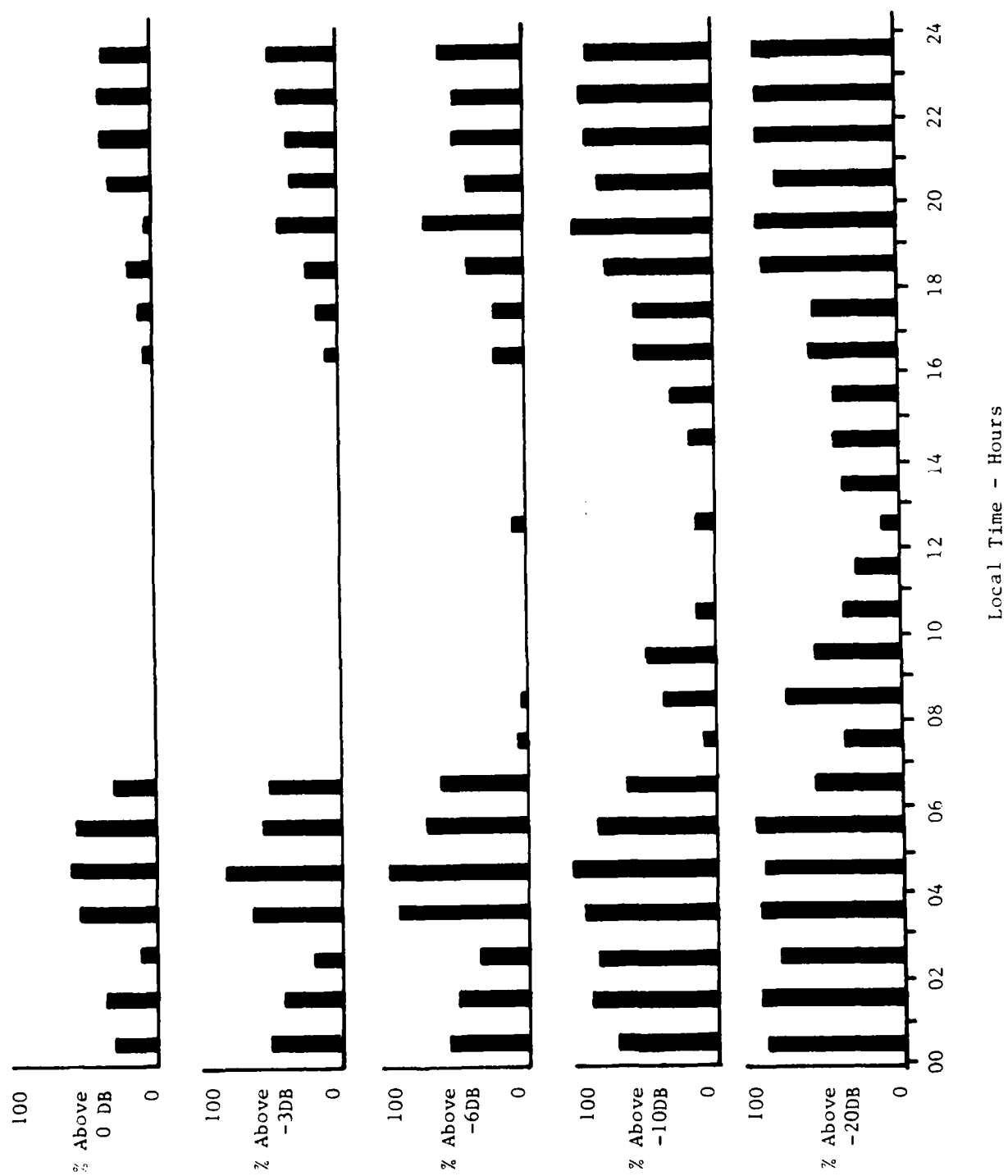


Figure B-7. Averaged Loran Sky Wave Ground Wave Ratios Above Levels Seneca to H.A.F.B.

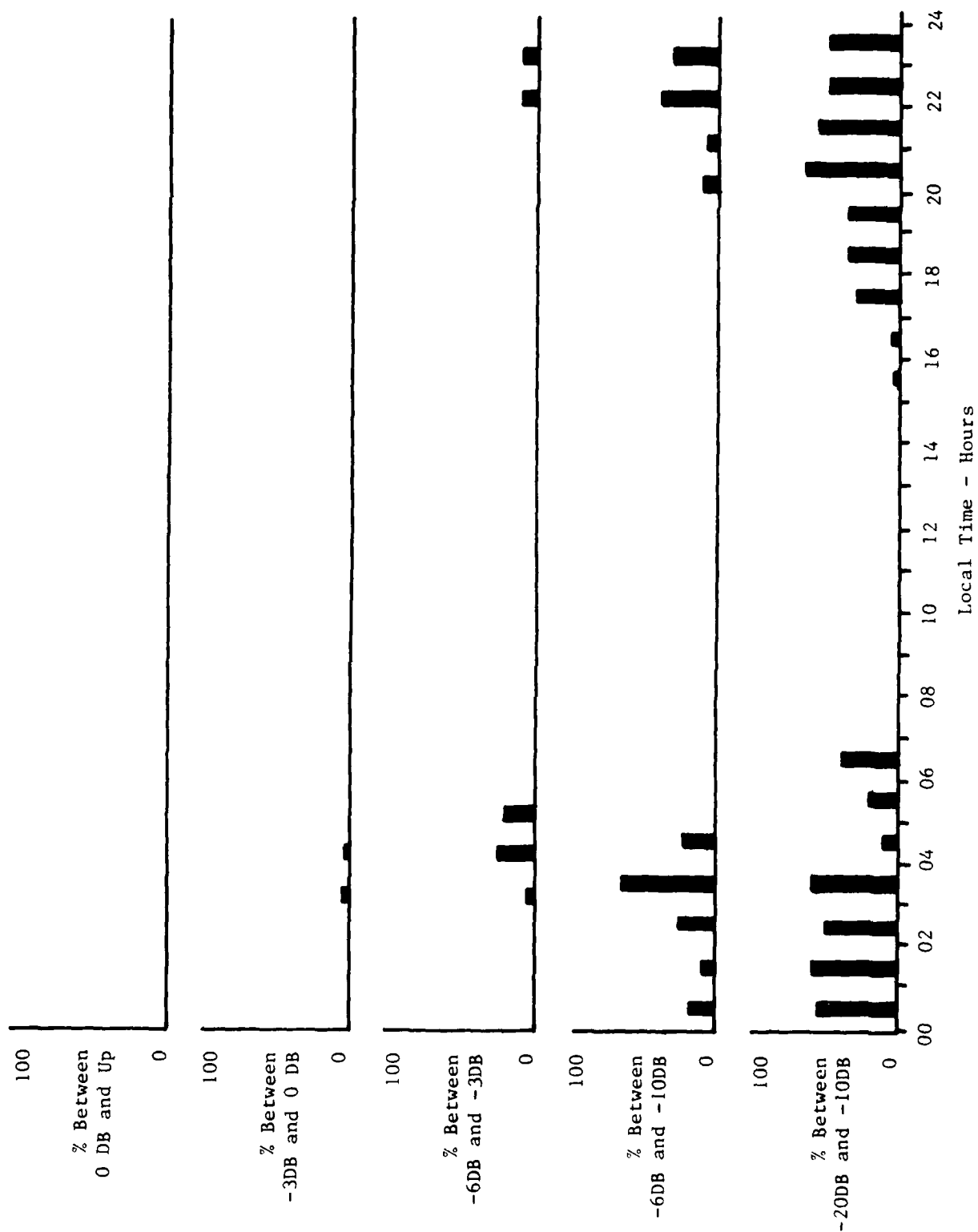


Figure B-8. Averaged Loran Sky Wave Ground Wave Ratios Between Levels, Seneca to Pittsfield, MA.

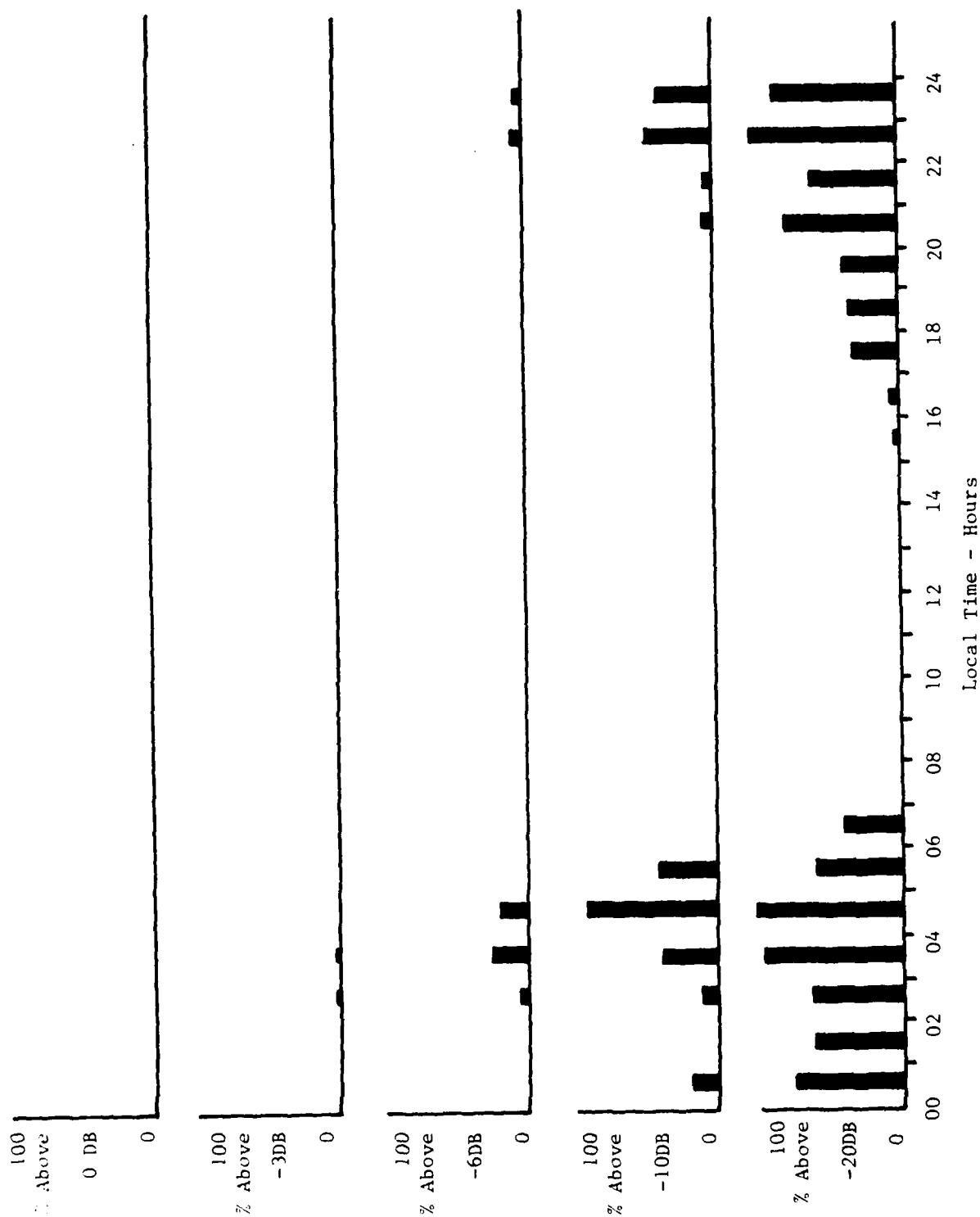


Figure B-9. Averaged Loran Sky Wave Ground Wave Ratios Above Levels, Seneca to Pittsfield, MA.

Nighttime conditions at Pittsfield, MA show that there is sky wave present and on occasion gets up to -3 dB. During the daylight hours at Pittsfield there is no sign of a sky wave.

The variations at both locations seemed to be related to the status of the D-Layer of the ionosphere. Basically, four conditions seemed to prevail.

- 1) Nighttime, no D-Layer, strong reflection from the E-Layer.
- 2) Daytime, D-Layer, no reflection from either layer.
- 3) Daytime, D-Layer, with reflections from the D-Layer.
- 4) Sunrise, sunset reflections from both layers (especially sunset).

#### B.5 Demonstration of Pulse Position Modulation Communication

For a communication system using pulse position modulation, the existing VLF ionosounder (whose transmitter is at Forestport, New York) was used. The receiving trailer was located in Troy, New Hampshire a distance of 230 kilometers from the transmitter.

The description of the VLF ionosounder is covered in Section C of this report.

The transmitted pulse is one cycle long with a period of 33 microseconds. The basic time interval between pulses was a constant 2,244 microseconds. By shifting the pulse transmission time with respect to the reference time generators by discrete amounts, intelligence can be transmitted. In this experiment 260 microseconds of the 2,244 microsecond time interval were subdivided in-

to 16 time blocks, and each block was assigned a letter description (see Table B-1). The full alphabet was not used. The presence of the received pulse in a particular time block indicated which letter was being sent. This demonstration was not performed in real time, the receiver data was recorded on tape and the CDC 6600 computer was used to decode the message, which was an easy task since the computer had already been programmed for the ionosounder experiment. The transmitter was operated for a period of time at a fixed interval. The signal at the receiver trailer was averaged sufficiently long to reduce the noise, while enhancing a good strong reference signal.

For test purposes, a code using eight sample points per character and sixteen characters was generated. This consisted of fifteen letters and a space. The character and space assignment is shown in Table B-1. This assignment was chosen to fit the message:

#### RAS TESTING GROUNDWAVE SYSTEM.

A coding board was designed, built and installed in the transmitter to send this message.

The message was sent from Forestport and received and recorded on tape at the Troy receiving trailer. It was deciphered using the computer and the message recovered. The same message was sent again with reduced power, and received and processed in the same way. The correlation using the computer was poor. Visually the signal was adequate when played back on the reader (a hardwired

TABLE B-1  
CHARACTER AND SPACE ASSIGNMENT

Character Number	Designation	Delay Increment	Total Delay in Microseconds
1	Space	0	20
2	A	1	35
3	E	2	52
4	I	3	68
5	O	4	84
6	U	5	100
7	D	6	116
8	G	7	132
9	M	8	148
10	N	9	164
11	R	10	180
12	S	11	196
13	T	12	212
14	V	13	228
15	W	14	244
16	Y	15	260

computer that reads the tapes into memory and through a digital to analog converter displays the signals on an oscilloscope). Therefore, the method of signal recovery through the computer was suspect. A review of the program showed that the whole record of 256 sample points, which included the turn on transient, was being looked at for the recovery of a signal. The computer program was modified using a forty point window to look at each of the possible signal positions. The tape was reprocessed and the message was recovered. The correlation was good but not perfect. It is believed that with improved detection techniques (such as synchronized time of signal shift and narrower windows), the correlation could be increased.

Also, if only the first character position that has correlation could be recognized, the sky wave could begin to overlap the ground wave and detection still could be achieved. This could increase the possible range of operation.

#### B.6 Conclusions

The conclusion from the CW tests is that a CW ground wave communication system would be practical up to ranges of approximately 250 kilometers throughout a twenty-four hour day and a slightly longer range during daylight hours.

The short pulse system could be practical out to much greater distances since it would be possible to distinguish the contaminating sky wave from the ground wave on the basis of arrival time.

REFERENCES, SECTION B

Bracewell, et al.; "The Ionospheric Propagation of Low- and Very-Low Frequency Radio Waves over Distances Less than 1000 km", Proceedings, Institute of Electrical Engineers, Volume 98, Part III, May 1951.



## SECTION C

### C-LAYER IONOSOUNDING WITH THE FORESTPORT TOWER

#### C.1 Introduction

Back in the time period 1971 to 1973, RADC's new short pulse high resolution ionosounding technique was being tested over a propagation path from Camden, NY to Bethel, VT. In December of 1972, in addition to the classical D region reflections, there were clear indications of a discrete, daytime only, reflection from a still lower (63 km) altitude (Rasmussen, 1980). This reflection appeared quickly around sunrise, remained remarkably steady through the day, and faded quickly around sunset. An ad hoc explanation invoked an essentially constant source of ionization at 63 km, possibly cosmic rays. At night the free electrons produced by this source would quickly become attached to neutral atoms, leaving too few free electrons to produce a noticeable reflected wave. However when the region was illuminated by the sun, the photo-detachment process would greatly increase the population of free electrons whose presence would show up by reflecting the ionosounding pulses. Previous observers working with CW waves had reported a transient VLF reflecting layer (C-Layer) having a brief existence only around sunrise. The question then arises as to whether or not the day-long reflection revealed by the RADC short pulse measurements come from this same C-Layer, or is to be regarded as a different phenomenon. In this report, the RADC

reflections are referred to as C-Layer reflections, although the reader should bear in mind that the identification is not yet positive.

Originally the C-Layer was seen at Bethel for an observational period of only about three weeks. The investigation undertaken by Megapulse was to extend the period of observations, explore different propagation paths, and seek additional clues as to the nature and origin of the phenomenon.

## C.2 Instrumentation

Ideally, Megapulse would have set up a long-term monitoring experiment over the same propagation path where the C-Layer was first noted. Regrettably, as part of an independent cost-reduction measure, RADC/DCCL had in the meantime closed the Camden test site and cut down the three 625-foot towers there, preferring instead to concentrate test operations at the Forestport facility. With active Megapulse participation, negotiations were undertaken among RADC/DCCL, RADC/EEPL and the RADC frequency manager for permission to use the 1200-foot tower in an extended ionosounding program.

It was agreed that EEPL could utilize the tower whenever DCCL was not using it, so long as means were provided for rapid switch-over. Further, the congested helix building was to be kept free of hot parts during EEPL transmissions. The frequency authorization of 36 kHz was on a non-interference basis, so that any complaint about our operations which reached the frequency manager could result in termination of our experiment.

The operating conditions agreed upon were satisfied as follows. The C-Layer transmitter and timer were housed in a semi-trailer and placed just outside the safety fence surrounding the tower base, as shown in Figure C-1. The connection point to the tower inside the helix room was provided with a set of high-power vacuum relays to permit rapid changeover of tower control, and to ground the tower when power failed. A special micrometer/lightning gap was installed at the tower base. Finally, our pulsed transmissions were coded and made to appear random to a conventional CW receiver, so as to minimize their interference potential.

Megapulse delivered a special solid-state, single-cycle VLF/LF ionosounding transmitter for the C-Layer tests to EEPL under Contract F19650-78-C-0031 in April of 1978. The transmitter was designed to operate into the .01 mFd capacitance of the 1200 foot tower, and deliver single 36 kHz r-f current pulses of a precise level at repetition rates of up to 400 pps. The transmitter was made to withstand transients at its output caused by lightning, and to be self-restoring in the event of prime power failure. Special care was taken to control the spurious outputs above the VLF band, where any RFI complaints were sure to originate. The calculated radiation resistance of the tower is 0.76 ohms at 36 kHz, and our peak pulse amplitude about 20 A, for a peak radiated power of 150 W.



Figure C-1. Transmitter Trailer at Base of 1200' Tower.

A standard EEPL pulse-rate generator was adapted to operate with a dithered pulse-repetition format in which the interpulse period jumped around its nominal value of 2500  $\mu$ s in a pseudo-random manner. A similar dithered rate generator was used to gate the receiver in time with the transmitted signal, exact synchronism being obtained by a systematic sliding of the receiver timing with respect to the fixed transmitter.

The C-Layer receiver shown in Figure C-2 was essentially a duplicate of the Qanaq equipment. It was housed in a small camping trailer (Figure C-3) to facilitate moving it about from one trial receiving site to the next. The receiver location survey was carried out during the Fall of 1978. Twenty-four hour-long data segments from the five sites are shown in order of increasing range in Figures C-4 and C-5. It can be seen that the time separation between the ground wave and its sky waves is greater at the closer ranges. On the basis of this short survey Troy, New Hampshire at a range of 245 km from Forestport was chosen as the permanent site, and the trailer set up on the property of Mr. and Mrs. George Dubina. A special electric service was run in and a telephone installed.

### C.3 Data and Conclusions

Data was recorded at Troy, New Hampshire from 24 December 1978 to 29 September 1980, and computer processed into the standard 3-D form using the CDC 6600 Computer at Hanscom Air Force Base. The results were delivered to RADC/EEPL for additional



Figure C-2. Receiving and Recording System.



Figure C-3. Trailer Containing Receiving System.

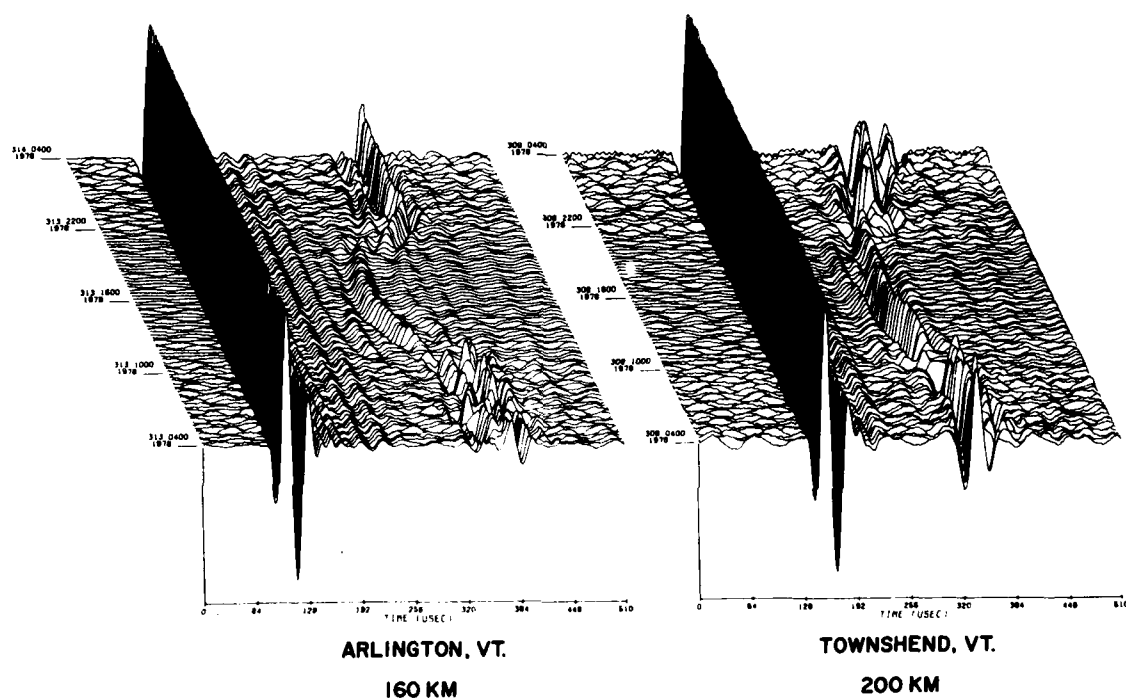


Figure C-4. Data Samples at 160 km and 200 km from Transmitter.



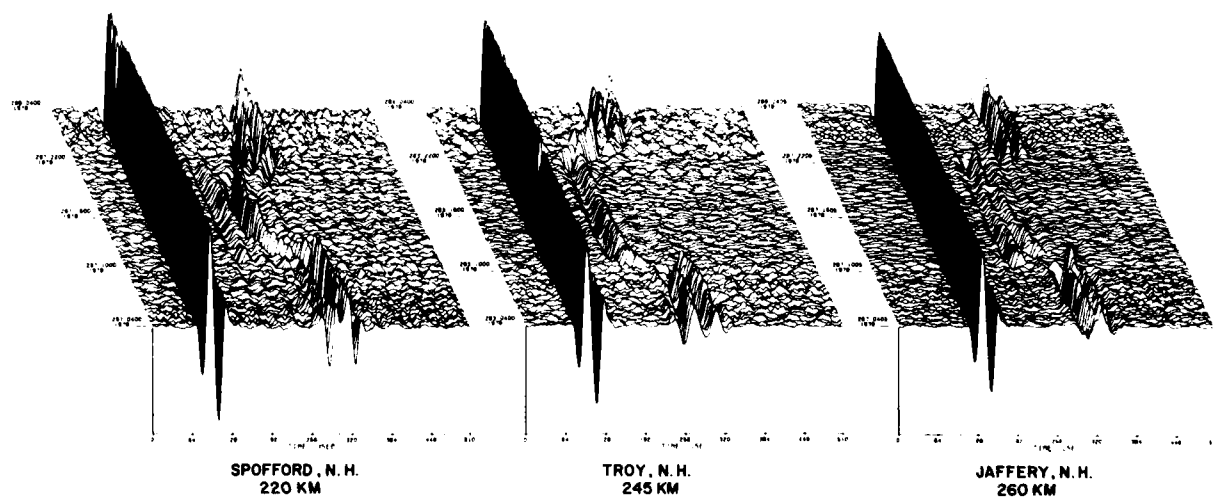


Figure C-5. Data Samples at 220, 245 and 260 km from Transmitter.

analysis and interpretation. A data sample showing one of the interesting phenomena, is shown in Figure C-6. This data continuously covers the period starting on 17 February 1980 and ending on 24 February 1980. A change in the type of daytime sky wave (pulse arriving around 190 usec on the scale in Figure C-6) between the 19th and 20th. Previous to the 20th, the daytime ionospheric reflection heights (actually delay times) were quite constant during the hours of solar illumination on the path. From the 20th onward, the daytime reflection height shows a pronounced curvature, strongly suggestive of the "log secant of zenith angle" variation typical of the well known Chapman Model (Bracewell, 1952). The reason for the dual behavior remains unknown. At no time during the period of these observations were the two types of behavior clearly present during the same day as they were in previous data (Rasmussen, 1980).

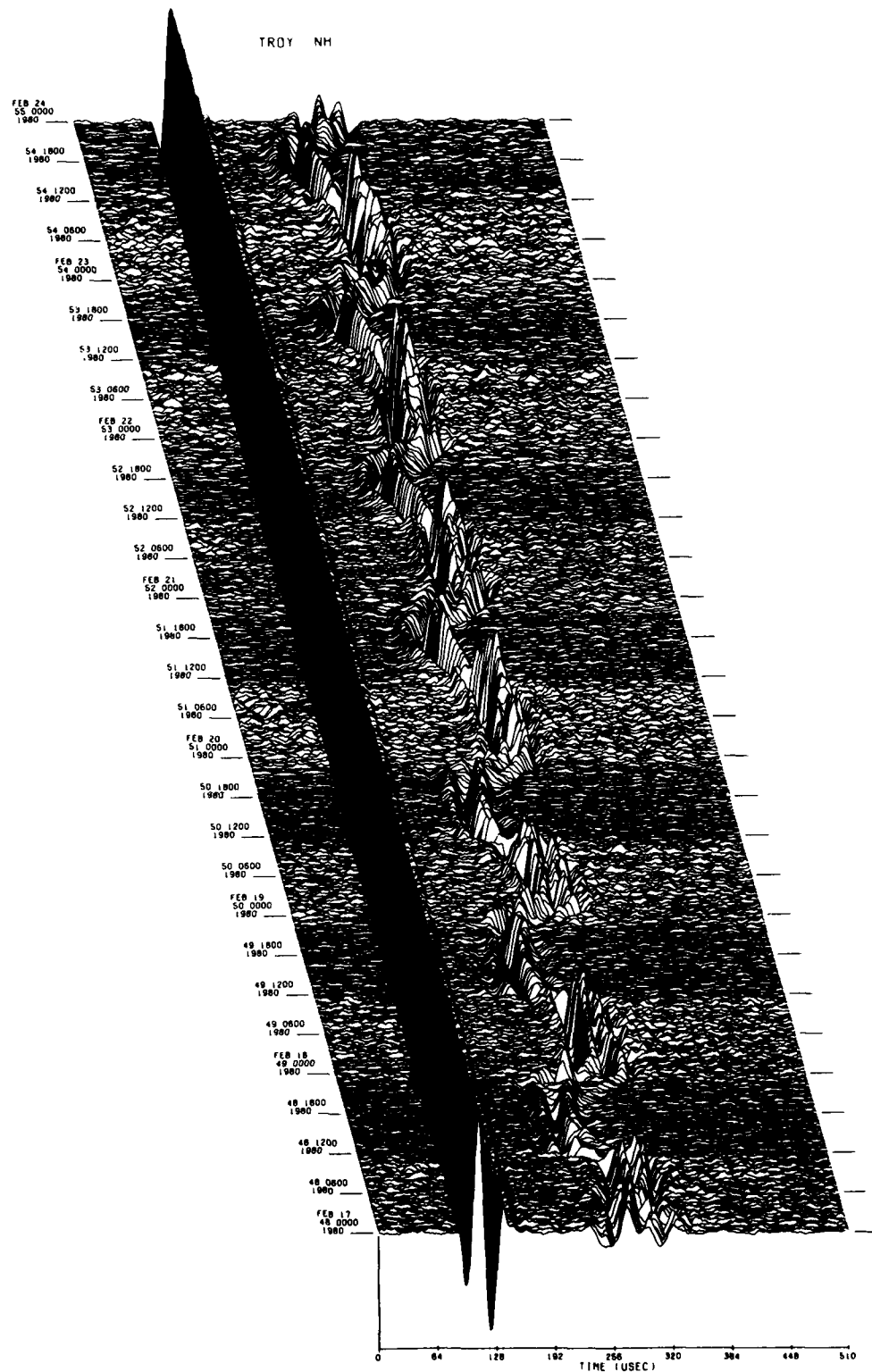


Figure C-6. Data Sample Showing Two Types of Daytime Ionospheric Reflection.

REFERENCES, SECTION C

Bracewell, R.N. and Bain, W.C.; An explanation of radio propagation at 16 kc/sec in terms of two layers below E layer, J. Atmos. Terr. Phys., 2, Pages 216-225; 1952.

Rasmussen, J.E., Kossey, P.A., and Lewis, E.A.; Evidence of an Ionospheric Reflecting Layer Below the Classical D Region, Journal of Geophysical Research, Page 3037; 1980.

SECTION D  
PHASE STABILITY OF GROUND WAVE PROPAGATED  
LORAN-C PULSES

D.1 Introduction

A study was undertaken to measure slight variations in the ground wave propagation time of LORAN-C pulses on a fixed propagation path and to look for any clear connection between such variations and synoptic weather changes which might change the average refractive index along the path. The detection of such changes in time of arrival (TOA) (which would appear as very small phase-changes) requires a source of very time-stable transmissions, a very stable receiving system and a very stable time-reference at the receiver.

The classical theory of ground wave propagation on a smooth, uniform, spherical Earth contains allowances for the refractive index ( $n$ ) of the air, and for an assumed constant rate of change ( $dn/dh$ ) with height ( $h$ ). As expected, an increase in  $n$  reduces the phase velocity, and retards the phase of the wave. The role played by  $dn/dh$  is much more complicated. Numerical computations (Heckscher, 1979, Private Communication) shows that variations in  $dn/dh$  may mask, and in some cases even reverse, the effects of changing  $n$ . Furthermore, the relative sensitivity of the two factors is a function of ground conductivity along the path. The complexity of this relationship in the theory, and the require-

ments of a very high order of equipment stability in order to make reliable measurements (Dean, 1978), have hindered progress in understanding the phenomena. If a unique interpretation of the phase variations could be demonstrated, LORAN-C might be able to provide information on tropospheric conditions affecting radio wave propagation over a large portion of the Earth. With the improved equipment, especially time standards, and improved computerized techniques for massive data handling and interpretation now available, it was decided to take another look at the phase stability problem.

LORAN-C is a pulsed radionavigation aid operating at 100 kHz with precisely controlled pulses (Wild Goose, 1976) (see Figure D-1). The reference zero crossing D has a maximum allowable deviation of the mean of zero nanoseconds. It has a maximum allowable peak to peak jitter of 100 nanoseconds. Therefore by averaging to reduce the jitter the reference zero crossing is a stable reference for making time of arrival measurements.

The TOA (Doherty, 1975) of a groundwave pulse is:

$$\tau = \frac{dn}{c} + t_c$$

$\tau$  = travel time in microseconds

$d$  = distance in kilometers

$c$  = velocity of light in kilometers per microsecond

$n$  = index of refraction

$t_c$  = secondary phase factor.

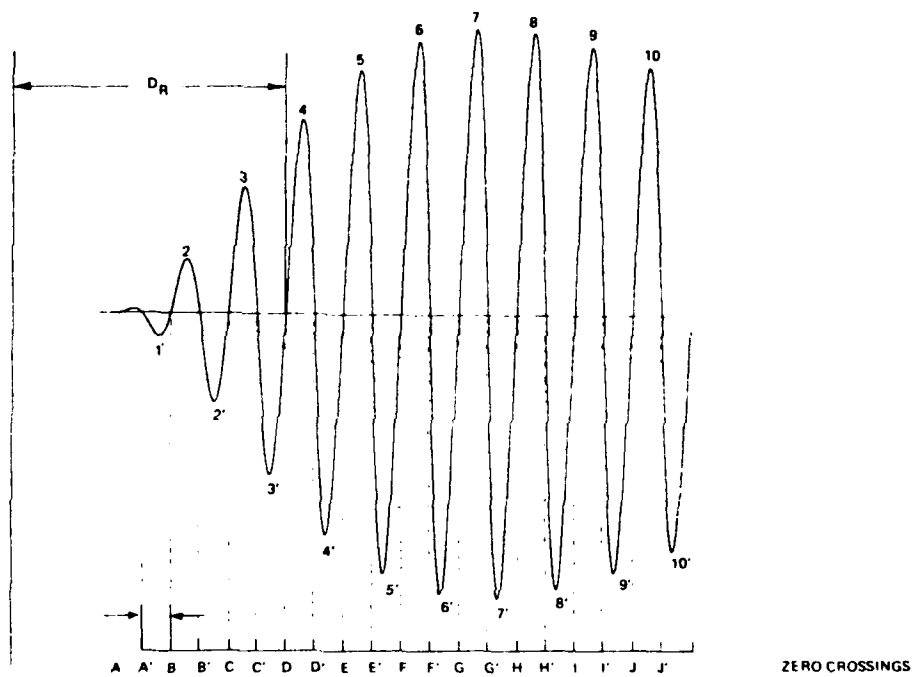


Figure D-1. Loran Pulse Showing Reference Zero Crossing - D.

In the above expression,  $n$  and  $t_c$  are variables with  $n$  being the variable of primary interest. Values of  $t_c$  as a function of earth conductivity, taken from NBS Circular 573 (Johler, 1956), are shown in Figure D-2.

Earth conductivity was measured at several points along the path with a Geonics Conductivity Meter, Model EM31. The average conductivity was 7.5 millimhos per meter, which is a reasonable value for this type of terrain.

Therefore, from the chart secondary phase factor for a distance of 450 kilometers is approximately four microseconds. In this experiment it is treated as fixed.

The nominal value of the index of refraction is:

$$n = 1.000300$$

with changes in parts per million being of significance.

The formula for refractivity is:

$$N = \frac{77.6 P}{T} + \frac{3.76 \times 10^5 e_s RH}{T^2}$$

Where  $N$  = refractivity  $\approx (n-1) 10^6$  = Ground level value

$P$  = atmospheric pressure

$T$  = temperature , °K

$e_s$  = saturation pressure of water

$RH$  = relative humidity.

A parameter  $\alpha \equiv \frac{N}{N_h}$  ,

where  $N_h = N$  at a height of two kilometers, provides a measure of the variation with altitude.



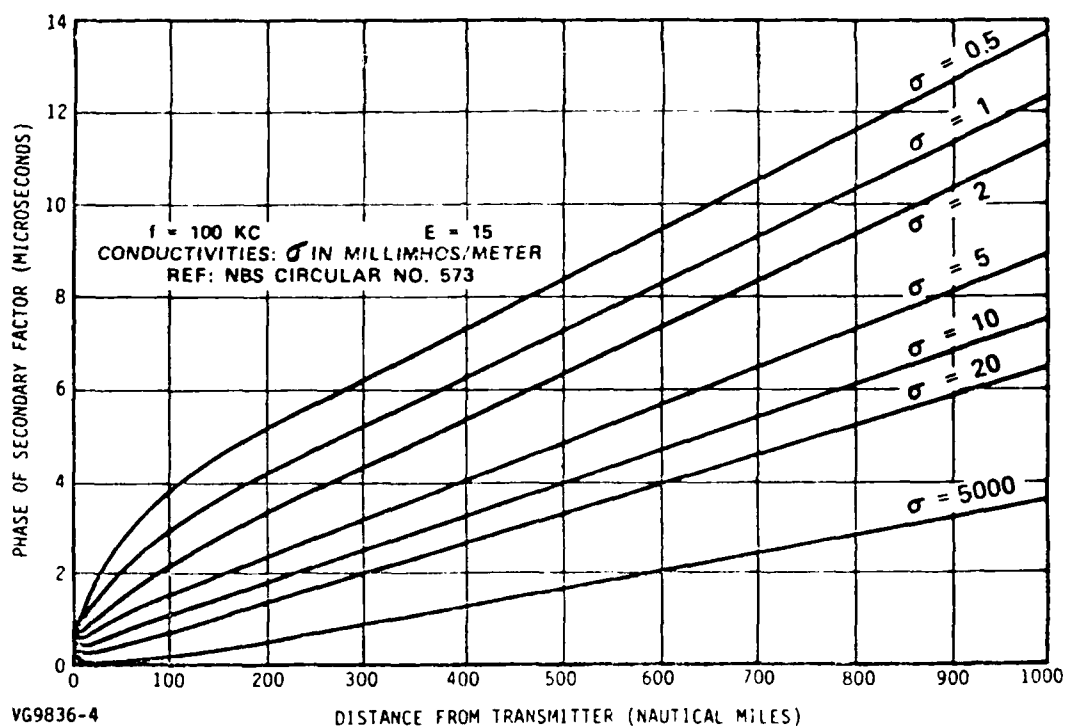


Figure D-2. Variation of Secondary Factor vs. Range for Different Ground Conductivities.

## D.2 Experiment Approach

The experiment consisted of receiving, averaging and recording LORAN-C pulses at Hanscom AFB from a Master Station at Seneca, New York. The propagation path length was about 454 km.

The Loran pulses from Seneca were recorded on digital magnetic tape for computer processing after 4,000 pulses had been averaged, utilizing a sophisticated receiver system designed for this purpose. This receiver, after being perfected under this program, was used on other programs. The description of this equipment is given under the CW portion of Section B, SURVIVABLE GROUND WAVE COMMUNICATIONS.

The weather data along the path was obtained from the National Oceanic and Atmospheric Administration Daily Weather Maps and supplemented by weather instruments at the receiver site. The weather instruments at the receiver site were a recording hygrothermograph for recording temperature and relative humidity and a recording barometer for recording atmospheric pressure.

The values of  $N$  and  $\alpha$  were available from a computer program which computed and plotted them on a weekly scale (see Figure D-3) for convenient comparison to the TOA of the Loran pulse.

Another computer program computed from the digitized received Loran pulse, the TOA of the referenced zero crossing with respect to a local time standard and plotted them on a weekly scale (see Figure D-4).

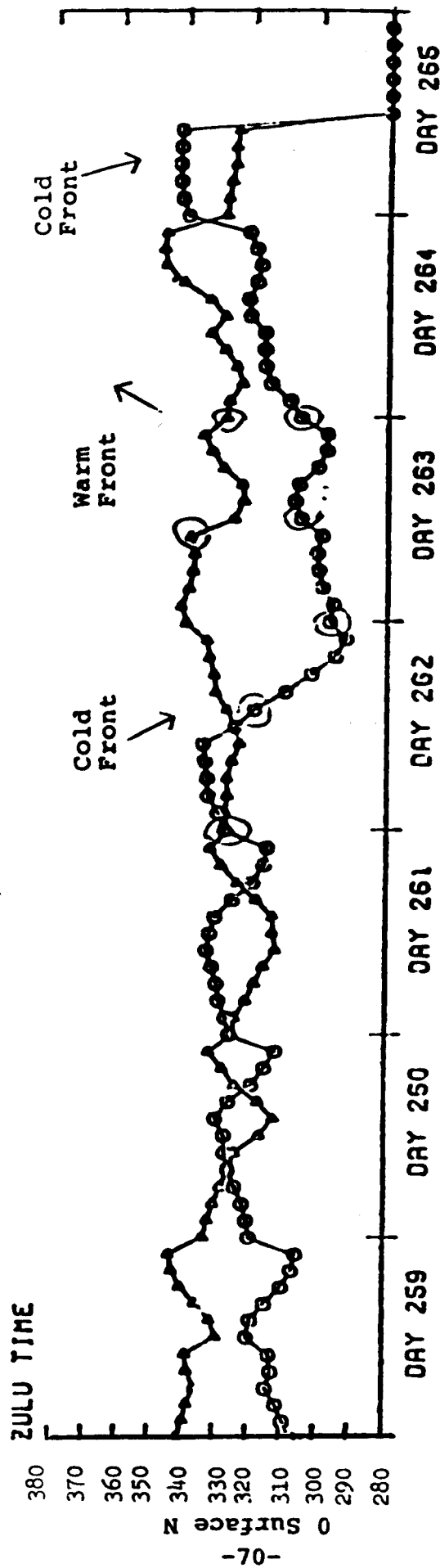


Figure D-3. Plot of Surface N and Alpha for a Week in Mid-September 1979 Between Seneca NY and H.A.F.B.

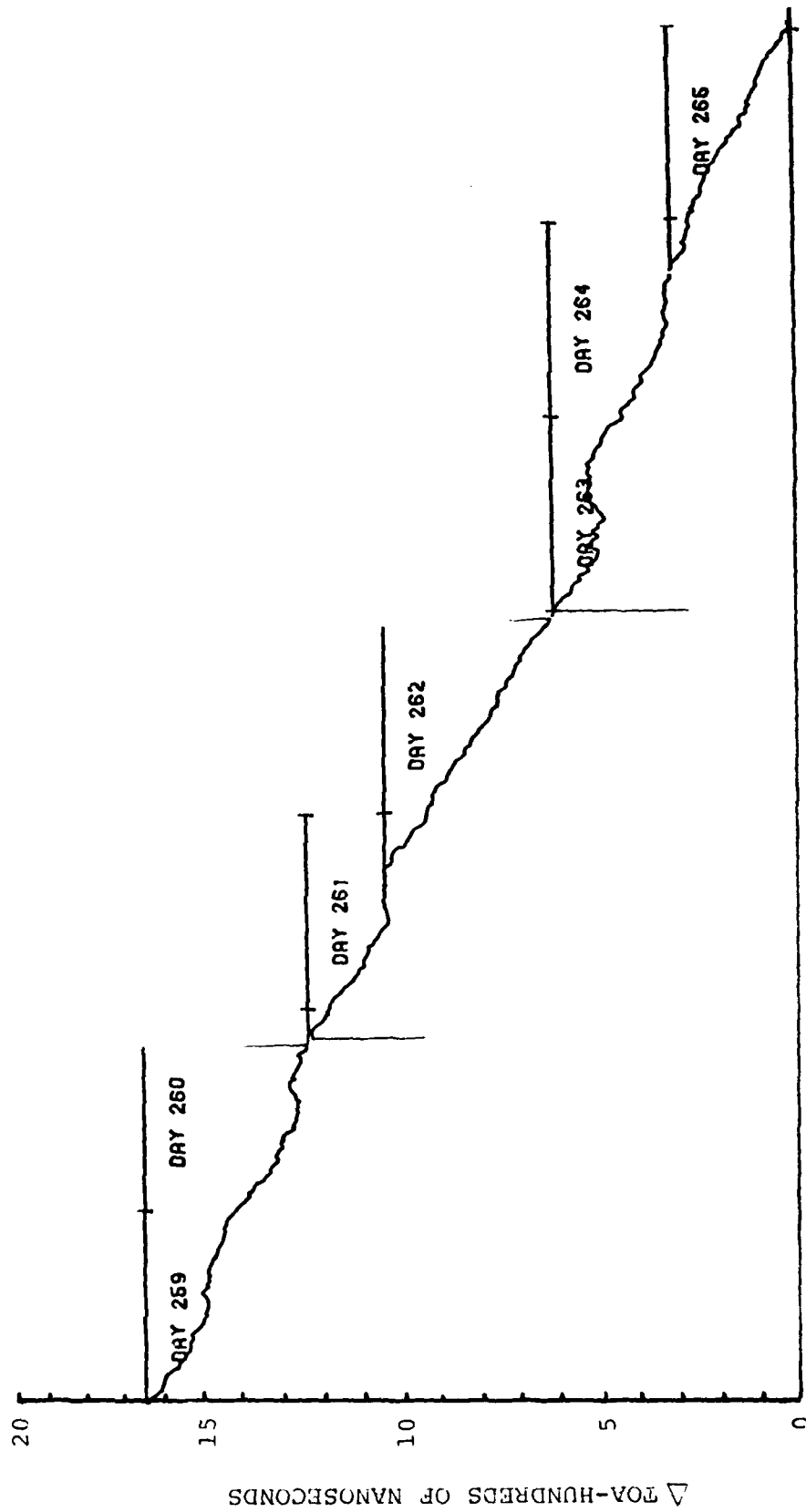


Figure D-4. Plot of Time of Arrival for a Week in Mid-September Between Seneca NY and H.A.F.B.

Figure D-3 is a typical plot of Surface N and Alpha. Notice that on day 262 a cold front came through and clearly showed on the plot of Surface N. On day 263 a warm front came through, and this shows up for both Surface N and Alpha. On day 265 a cold front came through and a change shows on both Surface N and Alpha, but different from the previous cold front of day 262.

Figure D-4 is the corresponding plot for Figure D-3. The variation of slope of the line is the change in TOA. The maximum values are +75 and -125 nanoseconds which is the range expected for changing weather conditions.

On day 262, the day of the greatest Surface N variation, there was a minimum change in TOA. For the change in Surface N on this day of forty units we would have expected a change in TOA of 60 nanoseconds. According to NBS 573, Alpha should have increased to account for this change, but it was fairly steady. Other records were looked at and they lacked any definite correlation.

From the plot of Surface N and Alpha and the plot of TOA, a definite correlation was expected. Instead, more questions came to light.

Since this experiment requires stability approaching one part per billion/per day, many doubtful areas had to be assessed and resolved. These problems are enumerated for future experimenters.

The first question was which pulse of the Loran group was most stable. Opinion was that the third pulse in the group would be most stable, especially in a dual-rated system where there would be variable off time.

The third pulse was locked onto and tests performed. There was an apparent sky wave contamination from the previous pulse. Therefore, the rest of the experiment was done using the first pulse in the Loran group with no apparent sky wave problems.

Another problem was the scatter in successive readings of the TOA. This was actually two problems: (1) a waveform recorder turn on transient, and (2) a noisy base line. Therefore, the signal was recorded well after the turn on transient was over. To establish a base line, the record was averaged after the turn on transient and before the start of the signal.

The stability of the system was still in question, since there were random jumps in the successive records. After a study, it was apparent that the Loran signals from Nantucket on another chain were contaminating our signal. A gating circuit was developed to cut out this interference.

The motor-driven variac in the voltage regulator generated transients that showed in the records; therefore, it was replaced by a saturable reactor type regulator.

It now became apparent that the signal to noise ratio of the records could be improved. Therefore, a narrow band preamp (30 kHz wide) was built and installed, and the records were averaged for a longer period of time.

The records now showed a smooth daily variation. It was a believable diurnal change, but it was the ambient temperature affecting the Biomation 8100 Waveform Recorder. A check with the

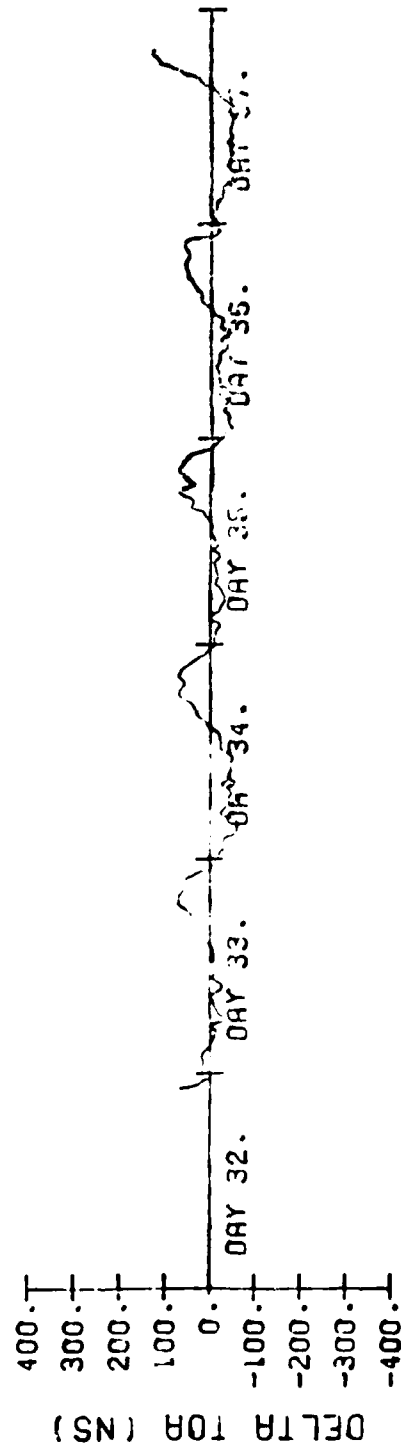


Figure D-5. Time of Arrival with Slope Removed.

manufacturer indicated that there would be no way to get the required stability from this unit. Therefore, a Biomation 805 Waveform Recorder was installed and this had the required stability.

Since the maximum sample rate of the 805 is five megahertz, the sample rate generated was modified to work more directly from the five megahertz from the frequency standard.

Also, the newer more highly stable cesium beam frequency standard appeared to have a temperature problem and also could not be adjusted to track the Loran signal from Seneca. An older model was adjusted and tracked Seneca.

At this point it appears that the trailer can properly record TOA.

To correlate the data of the mobile ground wave Loran receiver trailer, a base station was set up at Hanscom AFB. It was similar to the equipment in the trailer but with a few differences and their attendant problems. The idea was to set up to monitor a Master station and two Secondaries. The Master station selected was Seneca, New York and the two Secondaries were Caribou, Maine and Nantucket, Massachusetts. The system was designed to continuously monitor Seneca and to alternate between Caribou and Nantucket.

The system description (see Figure D-6) will be limited to those modifications that make this system different from the system in the mobile ground wave receiver trailer. For a description of the ground wave receiver trailer see Section B, SURVIVABLE GROUND WAVE



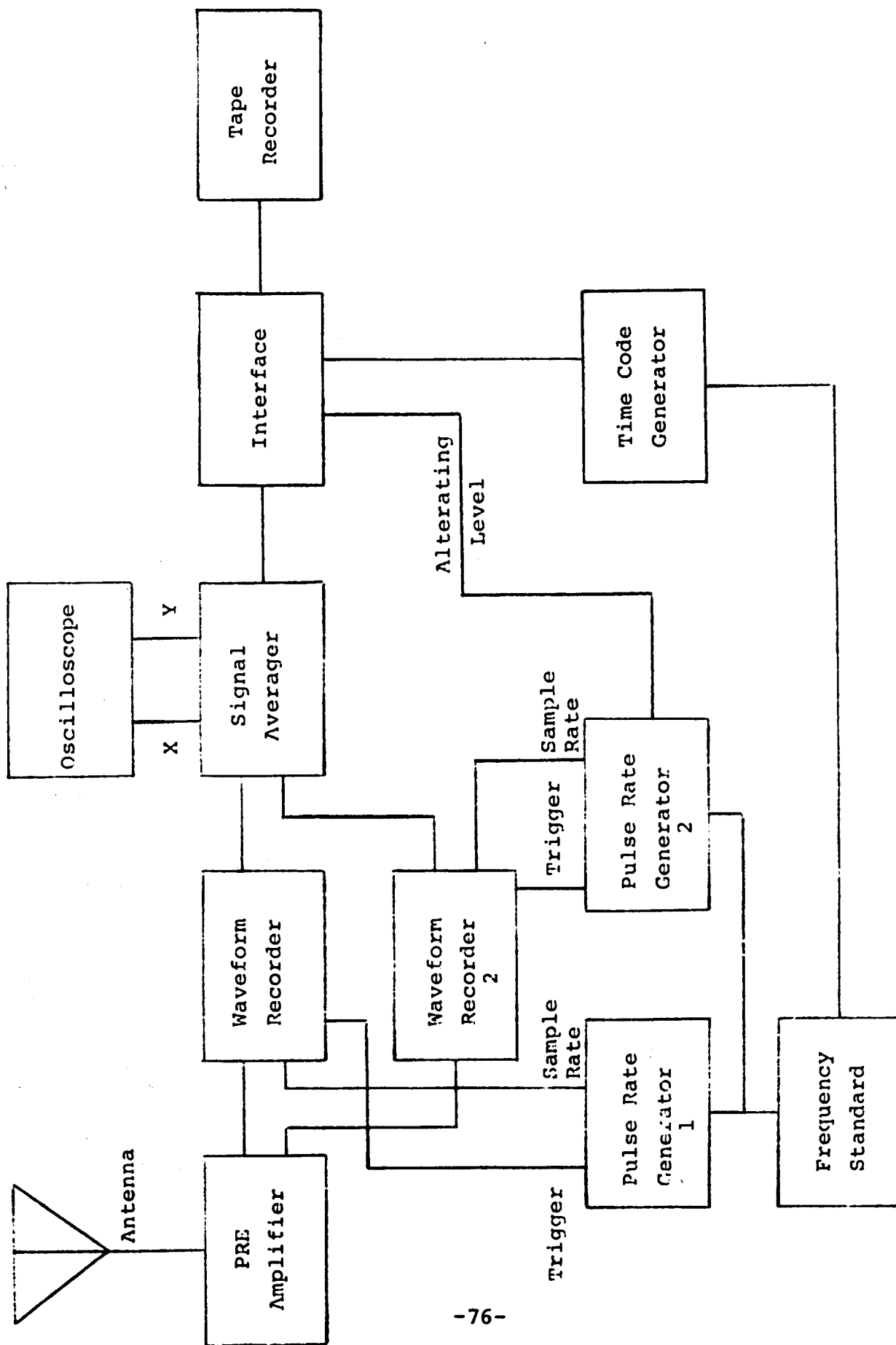


Figure D-6. Block Diagram - Loran Receiver Base Station.

In this system, two Biomation 805 Waveform Recorders are used. Number one is used to capture the Loran pulse from Seneca. Number two is used to alternately capture the Loran pulses from Caribou and Nantucket.

The triggering of these two Waveform Recorders are under the control of two Pulse Rate Generators. Number one controls Waveform Recorder number one. Number two controls Waveform Recorder number two. Number two Pulse Rate Generator was modified to accept a level from the Interface Unit, which would alternate between high and low thus alternately enabling the Caribou and Nantucket trigger pulses.

The Pulse Rate Generators have two identical sections that can be run independently or synchronized. They were set up using Seneca as a reference and the time delay differences could be read from the delay switches.

After each Waveform Recorder had captured a pulse, the pulses were successively transferred to the Signal Averager for averaging, each pulse going to its proper half of the memory. After the pulses had been averaged for 4096 time, they were dumped through the Interface and onto tape.

The Interface had been modified by the addition of a JK flip-flop that was wired to toggle from the record command pulse. The output level of the flip-flop was sent to the Pulse Rate Generator number two to cause the alternating selection of Caribou or Nantucket pulses. The output level of the flip-flop was also sent to the last bit of Tag Word One, which would then put on tape which signal was being received.

A computer program was written to read the tapes and plot the zero crossings of the signals.

Two Loran receivers were also installed in the Base Station for monitoring. They are Internav Model LC 204. After an early failure of one unit, that was repaired under warranty, they both gave satisfactory service. The time differences varied up to 200 nanoseconds, which is the order of magnitude expected. This equates to approximately 200 feet.

### D.3 Conclusions

During the course of this program many equipment problems were resolved and apparent stability was eventually achieved. (See also Section B SURVIVABLE GROUND WAVE COMMUNICATIONS.)

The weather data that had been received and plotted in terms of N and Alpha invariably showed jumps and a lack of correlation with weather fronts, and with the TOA of the Loran pulse. For a continuation of this study weather stations at intervals along the path should be contacted and their values averaged. This would be good for Surface N. The collection of data for  $N_h$  would take additional consideration.

These experiments should continue in order to find what physical parameter or parameters could be measured to account for the change in travel time of the Loran ground wave, whether it is changes in ground conductivity, surface refractivity, lapse rate, or some factor that has not yet been considered.

REFERENCES, SECTION D

W.N. Dean, "Diurnal Variations in Loran-C Groundwave Propagation", Magnavox Government and Industrial Electronics Company, Fort Wayne, Indiana; 1978.

Wild Goose Association, Loran-C System Characterization, WGA Publication Number 1; 1976.

R.H. Doherty and J.R. Johler, "Meteorological Influences of Loran-C Groundwave Propagation", Journal of Atmospheric and Terrestrial Physics, Volume 37, Pergamon Press; 1975.

J.R. Johler, W.J. Kellar, L.C. Walters, "Phase of the Low Radio Frequency Ground Wave", National Bureau of Standards Circular 573; June 1956.

Daily Weather Map, U.S. Department of Commerce, Environmental Science Services Administration, Weather Bureau, available by subscription from U.S. Government Printing Office.

SECTION E  
SPACE ANTENNA STUDY

The possibility of deploying LF/VLF/ELF antennas in space is an intriguing one, because the great lengths of conductor necessary for efficiently exciting electromagnetic waves of low frequency might be achieved in that way. This matter was given little priority in the present contract, but inspired by theories which indicate 100 km long space antennas may be feasible (Colombo, 1974; Dobrowolny, 1976), a few very elementary calculations were made in order to understand some of the basic phenomena. These are different, even surprisingly different, from common experience on the Earth's surface.

A very simple mechanical system is illustrated in Figure E-1. A satellite S (space shuttle?) is supposed to be in a circular orbit of radius  $r + h$ , where  $h$  is the height above the Earth of radius  $r$ . An antenna wire SM of length  $s$  is attached to the satellite, and carries a mass ( $m$ ) at its far end at M. It is instructive to calculate the tension in the wire by elementary mechanics. As a starting point it will be assumed that the satellite is very massive, the antenna wire is light and flexible, and that air drag is negligible. The complexities of a more general treatment at this point would only obscure the basic principles.

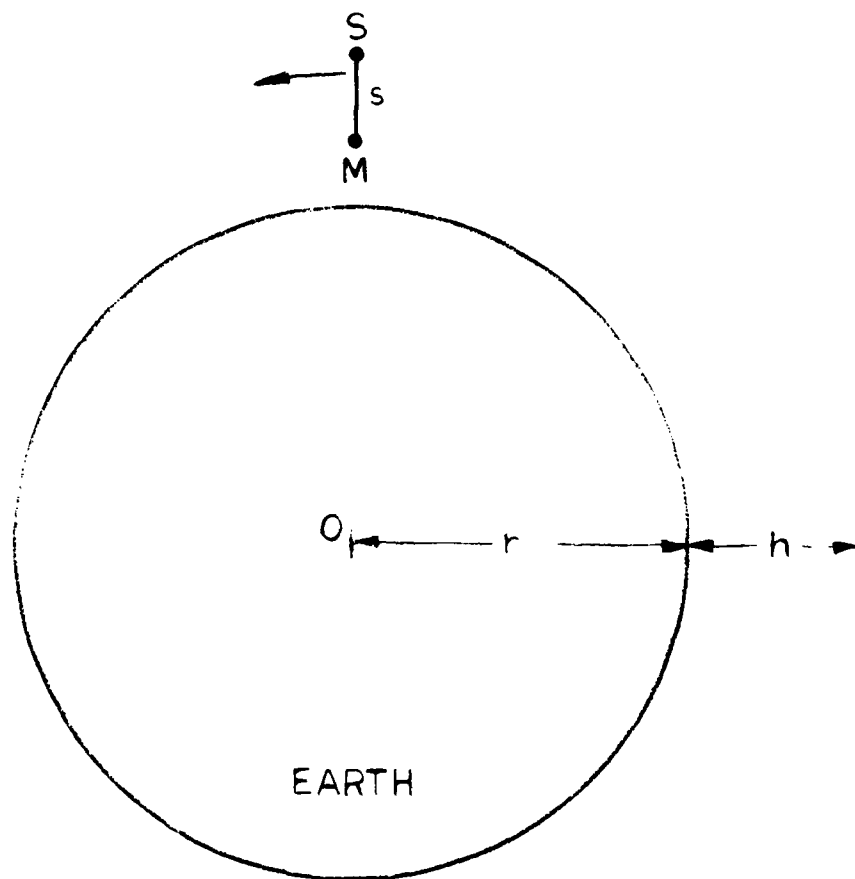


Figure E-1. Monopole Antenna "Suspended" From an Earth Satellite.

If  $g$  is acceleration of gravity at the Earth's surface ( $9.8 \times 10^{-3}$  km/sec<sup>2</sup>) the value at the satellite altitude,

$$g_s = G (r/r+h)^2 \text{ (km/sec}^2\text{)} \quad (1)$$

by Newton's Law of Gravitation. If  $V_s$  is the orbital velocity of the satellite, its centripetal acceleration is simply  $V_s^2/(r+h)$  (km/sec<sup>2</sup>). Since the satellite is in stable orbit, this must equal  $g_s$ :

$$V_s^2/(r+h) = g (r/r+h)^2 \quad (2)$$

so that 
$$V_s = r \sqrt{\frac{g}{r+h}} \quad (3)$$

Assuming that the antenna flies stably in the configuration shown, the velocity  $V_m$  of the mass at point M, is proportional to its orbital radius:

$$V_m = \frac{r+h-s}{r+h} V_s \quad (4)$$

$$= \frac{r(r+h-s)}{(r+h)^{3/2}} \sqrt{g} \text{ km} \quad (5)$$

The centripetal acceleration of point M is  $\frac{V_m^2}{r+h-s}$

or 
$$\frac{g r^2 (r+h-s)}{(r+h)^3} \text{ km/sec}^2 \quad (6)$$

and the acceleration of gravity at M is 
$$\frac{g r^2}{(r+h-s)^2} \text{ km/sec}^2 \quad (7)$$

The net acceleration toward the Earth is then

$$a = \frac{g r^2}{(r+h-s)^2} - \frac{g r^2 (r+h-s)}{(r+h)^3} \frac{\text{km}}{\text{sec}^2} \quad (8)$$

and

$$\frac{a}{g} = \frac{r^2}{(r+h-s)^2} - 1 - \frac{(r+h-s)^3}{(r+h)^3} \quad (9)$$

In those cases when  $s \ll (r + h)$ ,

$$\frac{a}{g} \approx \frac{3r^2}{(r+h)^3} s \quad (10)$$

For a numerical example, take  $r = 6400$  km;  $h = 200$  km.

Then

$$\frac{a}{g} \approx 0.04274 s \quad (11)$$

Thus for a 2 km long antenna ( $s = 2$ ), the net acceleration of the mass is only 8.5% of normal gravity, so that with a 1 kg mass the tension in the antenna wire is only 85 grams! Figure E-2 shows the variation of the mass acceleration as a function of  $s$ . When  $s$  takes on a negative value, the acceleration reverses sign, so that the mass can now "hover" above the satellite! This means that with two wires deployed, a center-fed dipole structure ( $\text{MM}^1$ ) should be possible, see Figure E-3. Center-fed dipoles are relatively easy to drive electrically.



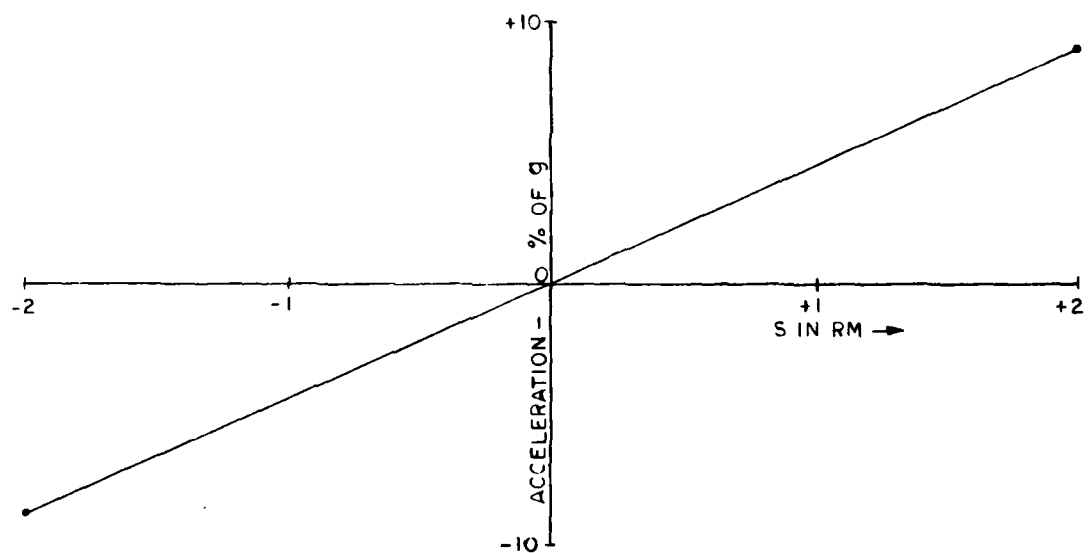


Figure E-2. Acceleration Toward Earth as a Function of S.

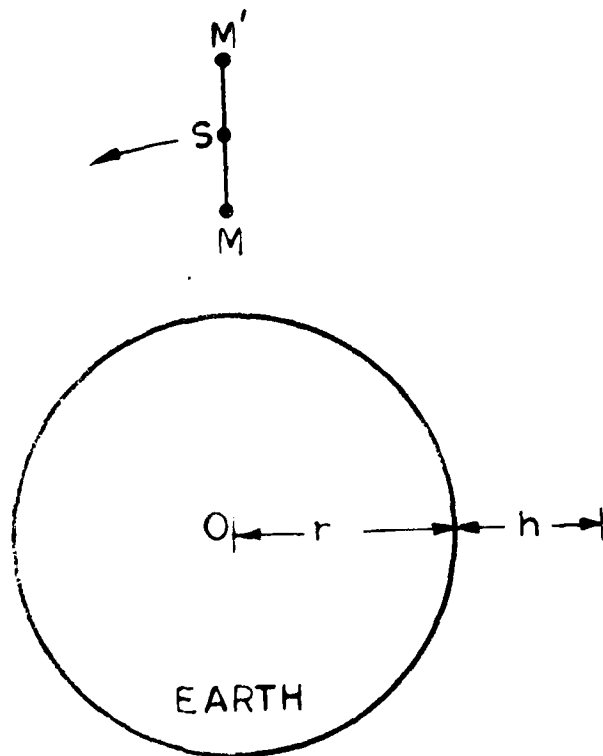


Figure E-3. Satellite with Center-Fed Dipole Antenna.

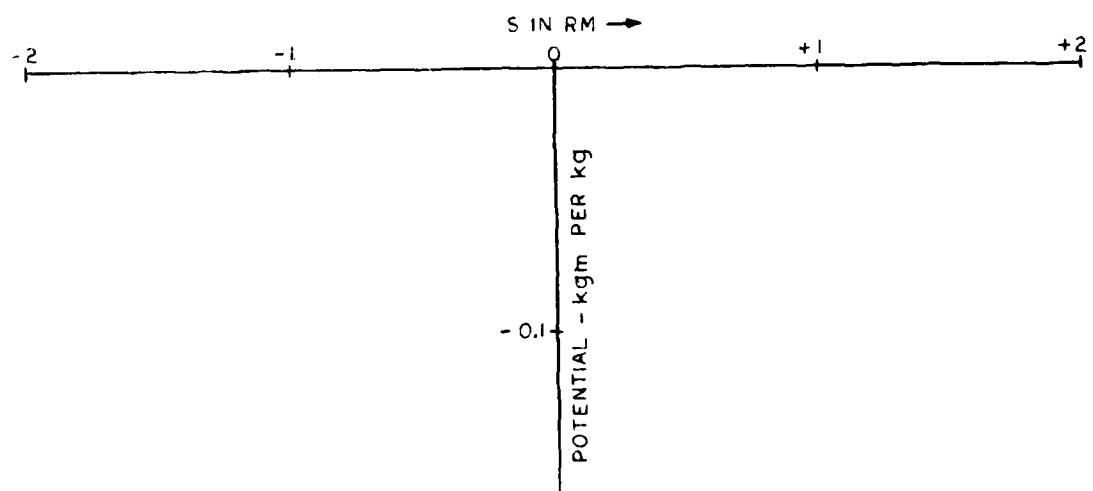


Figure E-4. Potential Function.

The energy necessary to move a 1 kg mass from point M up to the satellite,

$$W(s) = - \int_s^{\infty} \frac{a}{g} ds \quad (\text{kg km per kg}) \quad (12)$$

$$\approx \frac{3r^2}{(r+h)^3} \int_0^s s ds = \frac{r^2}{(r+h)^3} s^2 \quad (13)$$

Continuing the numerical example, the potential function,

$$W(S) = 0.02137 S^2 \quad (\text{kg.km/kg}) \quad (14)$$

The shape of the potential junction is shown in Figure E-4. Evidently a "nudge" will be needed to start the mass moving away from the satellite.

For a 1 kg mass the energy necessary to reel in a mono-pole antenna 2 km long is 0.0855 kg.km, according to Equation (14). Since 1 kg.m is equal to 9.8 joules, the reeling energy is about 838 joules, which is in the order of 2% of the energy in an automobile battery.

When air drag and other forces are considered, the antenna configuration will change, and the above "zero-approximation" values will require revision. However, those matters are beyond the scope of this study.

REFERENCES, SECTION E

G. Colombo, E.M. Gaposchkin, M.D. Grossi, and G.C. Weiffenback, SHUTTLE-BORNE "SKYHOOK": A NEW TOOL FOR LOW-ORBITAL-ALTITUDE RESEARCH, Smithsonian Institution Astrophysical Observatory, Cambridge, Massachusetts, 02138; September 1974.

M. Dobrowolny, G. Colombo, and M.D. Grossi, ELECTRODYNAMICS OF LONG TETHERS IN THE NEAR-EARTH ENVIRONMENT, Smithsonian Institution Astrophysical Observatory, Cambridge, Massachusetts, 02138; October 1976.

SECTION F  
TRANSVERSE ELECTRIC (TE) VLF IONOSOUNDING  
BETWEEN THULE AIR BASE AND QANAQ, GREENLAND

F.1 Introduction

This section discusses the design, implementation, and operation of a pulsed VLF TE ionosounding circuit between Thule and Qanaq, using a horizontal radiator consisting of a three kilometer segment of a former 69 kV power line running approximately East-West between Thule and J-Site (BMEWS). In the discussion of propagating wave patterns in Section A, it was seen that with a highly conducting Earth surface, the excitation of TE waves requires an elevated source, preferably one high in the Earth/ionosphere waveguide. This is not practical for studies intended to continue over a long period in order to observe time varying phenomena. A horizontal antenna above a highly conducting Earth has an out-of-phase image in the Earth which almost completely cancels the radiation field of the antenna if it is near the ground. If the conductivity is poor, the image is no longer as strong, nor as sharply defined, and the cancellation is less exact. This gives rise to the possibility that a low altitude horizontal wire antenna might be driven hard enough to generate a TE signal that would at least be adequate for experimental research purposes.

A current carrying straight, horizontal wire on or near a lossy Earth also generates TM waves which are strongest in the two end-on directions. To see how this happens, consider the currents

which flow in the Earth under the wire. These flow in the opposite direction to the current in the wire, but they also dip down into the Earth to a maximum depth under the center of the wire, and then curve upward toward the surface. The currents in these concave-upward paths, plus that in the wire itself, are equivalent to a current loop in the vertical plane containing the wire. This loop produces TM fields with their nulls in the broadside direction, where the TE fields are strongest. For unambiguous interpretation of TE propagation, the measurements should be made in the broadside direction. It should also be noted that in the broadside plane, the TE fields are weak along the ground, and stronger at more elevated angles. This is the opposite to the behaviour of the TM fields from a vertical antenna, and means that there is relatively little, or no, ground wave with TE waves.

To investigate the possibilities of generating TE radiation for ionosounding purposes, RADC/EEPL converted a three kilometer section of an unused high voltage power line at Thule into an experimental TE CW antenna. This segment with its East-West direction has almost an ideal broadside orientation for transmitting TE waves in the direction of Qanaq, the site already being used for receiving TM ionosounding pulse transmissions from the RADC 130 meter vertical antenna at Thule (Rasmussen, 1975). Preliminary experiments indicated that a detectable TE signal could be received at Qanaq but the interpretation of these signals remained unclear. The objective of the Megapulse effort was to convert the

TE system to pulse operation in a way which would be compatible with the TM system already operating successfully. With both the 130 meter TM ionosounding system and the TE power line system operating, it is possible to probe a common ionospheric volume simultaneously with both polarizations, and for the first time obtain the data needed to develop values for all four elements of the plane wave reflection coefficient matrix. The unique features of our experiment attracted the attention of the editors of Aviation Week and Space Technology (see Figure F-1).

## F.2 Installation

We arranged with the Danish Arctic Contractor (DAC) to disconnect the drive line at Pole 8-13 and tie the ends together, perform a similar operation at Pole 6-14 and divide the line into two 1.5 km pieces by cutting the bridging wires at a strain tower (numbered 7-12) where the power line crossed an old road leading from GLOBECOMM to the Base Waterworks. DAC moved in a small building to house the transmitter, installed prime power and telephone lines, and connected the two power line halves to r-f feed-through insulators in the roof of the structure. Figure F-2 is a view of the transmitter shelter, and a portion of the power line.

Under a separate contract (F19650-78-C-0067), Megapulse delivered a solid-state, single-cycle VLF transmitter designed to excite the antenna as if it were a balanced, center-fed pair of transmitter lines. Equal but oppositely-signed current pulses



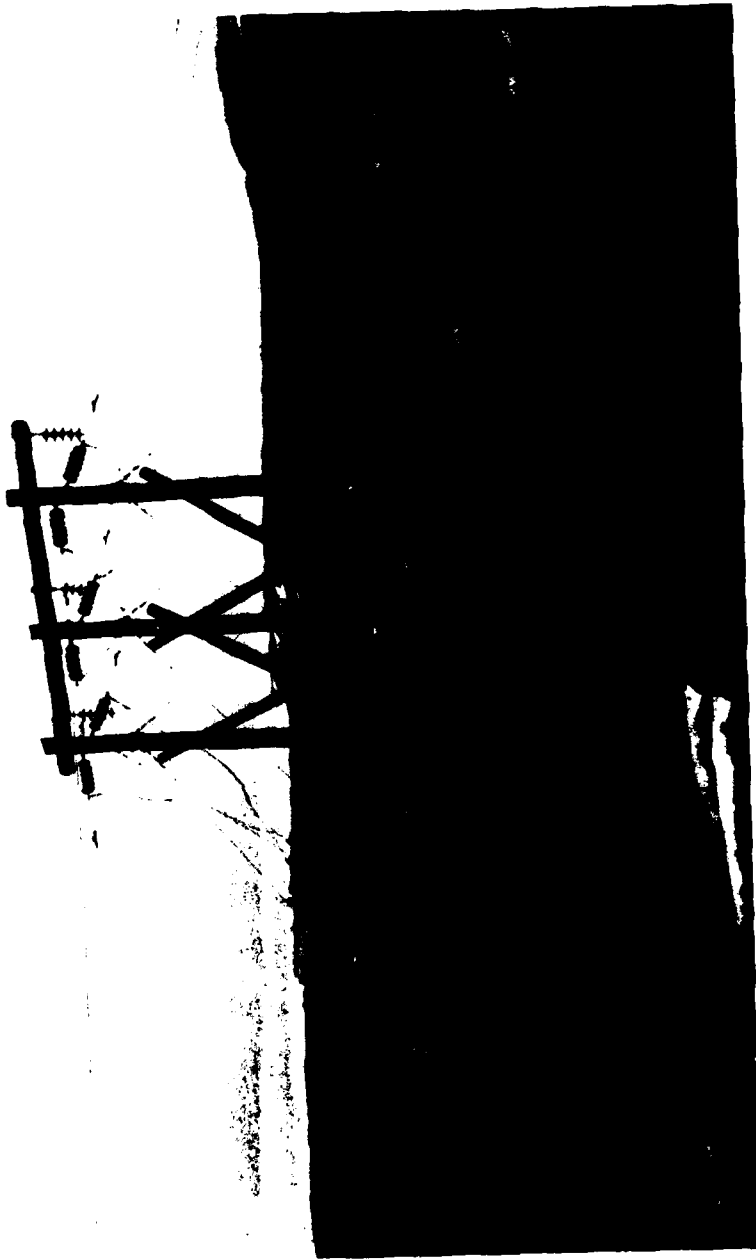


Figure F-2. Transmitter Shelter and Powerline Antenna.

were to be applied simultaneously to the two line segments from a center-tapped output transformer, the center being grounded to the building and the Base ground system. Early in the transmitter development it was realized that our power line experiment could be a potent source of radio frequency interference to LF users on the Base, particularly (1) the 167 kHz receiving site on South Mountain and (2) the two entertainment radio stations. An earlier Navy ionosounding experiment had caused all the telephones on the Base to ring, and the North Mountain TM ionosounder could be heard on the 167 kHz receivers and between stations in the broadcast band. Special high-Q traps were built into the transmitter to eliminate spectral lines near 167 kHz, and shunt RC networks to ground from each side of the antenna to ground bypassed higher frequencies.

### F.3 Verification Tests

Installation of the power line transmitter was accomplished during the March 1979 equinox period as part of an ambitious experimental series during which a portable receiver was taken by chartered aircraft to Grise Fiord, Canada and later to Qanaq. In accord with theoretical predictions, the power line radiated a vertically-polarized TM signal off its end pointed toward Grise Fiord, and horizontal, TE waves in the perpendicular direction toward Qanaq. As anticipated, no appreciable TE ground wave reached the receiver 70 miles to the North, but a whole series of sky wave reflections could be seen.

Our preparations to combat RFI from the transmitter were completely successful, so that no public notice was taken of the new ionosounder. The VLF pulse width was set so that 167 kHz was in a spectral null area, as observed on a spectrum analyzer viewing the antenna current. We were delighted to find that the antenna current due to the two Base radio stations exceeded our own emissions on the same frequencies by more than 10 dB!

A puzzling result of the first power line experiments was that the received signal did not look like the antenna current at all. The former was a series of violent, high-Q oscillations in the area of 50 to 70 kHz, while the latter was a smooth, single cycle at the design frequency of 16 kHz. Apparently the radiation efficiency of the power line antenna rises rapidly with frequency up to the first parallel self-resonance around 50 kHz, where the three kilometer structure is one-half a wavelength long. The observed radiation under single-cycle VLF excitation results from a high-pass filtering of the terminal current, which greatly emphasizes the slope discontinuities at the two ends of the VLF pulse.

Having successfully proved the technical feasibility of TE ionosounding from the power line to Qanaq, the next step was to go fully operational on a year-round basis. Because of the remoteness of the transmitter building from the plowed roads, special effort had to be made to insure that the transmitter would operate with minimal attention from DAC. The building needed a thermostatic control for its heating system. A calibration technique

was desired to determine the excitation applied to the ionosphere by the power line. Owing to the lack of ground wave at Qanaq, there is no "reference" radiated signal with which to compare the received waveforms. This situation contrasts to the TM experiment, where the radiated wave can be accurately calculated from the antenna current and the calculation verified by comparison with the received ground wave. The TM experiment is self-calibrating, since each received record has the ground wave available as a time- and frequency-spectrum reference. Knowing the ground wave propagation as a function of frequency over the band of interest, corrections can be applied, but these are small.

Conversion of the power line transmitter to operational status was accomplished in September 1979 with installation of a thermostatically controlled exhaust fan and heaters, two windows, a roof-mounted warning light and a complement of equipment spares, tools and hardware. A calibration experiment was attempted, and finally a portable receiver was integrated into the Qanaq facility to provide continuous monitoring of the TE signals.

#### F.4 Calibration Experiment

The calibration was to be based on the well-known principle of reciprocity between an antenna's properties as a receiver and a transmitter. A TE wave polarized in the East-West direction was to be radiated from the North Mountain site, bounced off the ionosphere and picked up off the power line used as a receiving antenna. The ratio of down-coming incident wave amplitude to the power

line antenna current produced could be found by two measurements with the portable receiver. By reciprocity, the same ratio should apply to radiated waves generated when the power line was excited by the current from the pulsed transmitter. The latter current was to be digitized using the portable receiver.

A special antenna structure separate from the power line was needed to produce a vertically directed TE wave to bounce off the ionosphere. The 130 meter North Mountain tower could not be used by itself, since its radiation pattern would have a null in the desired vertical direction. After some study, it was decided to use the abandoned Navy antenna leg running near the 130 meter tower as a TE radiator. One wire of the antenna was grounded at its former termination point near Dundas. The loop resistance was measured between the antenna wire and the Base ground at North Mountain, and found to be only 70 ohms. The Navy antenna was excited with the thyatron transmitter by setting up a .01 mFd capacitor as a dummy antenna in place of the 130 meter tower, and "grounding" the low end of the capacitor via the 6 kilometers of wire running to Dundas. When first operated into the long wire, the transmitter output current was violently oscillatory, apparently due to traveling waves bouncing back and forth. These were damped out by shunting the sending end of the wire to local ground through a bank of resistors. Only the sum of the resistor current and line current could be monitored with the existing

Pearson transformer. The sum current was a smooth but heavily damped VLF cycle, with a long tail-off to zero which we later observed in the radiated field.

The next step in the calibration of the power line was to observe the anticipated down-coming reflected wave from the ionosphere, and the current produced in the power line therefrom. We were surprised to discover that the field near the power line was badly contaminated by scattered radiation which exhibited the same oscillatory behavior seen in the receiver data from Qanaq and Grise Fiord. It was impossible to separate the ground wave from the sky wave owing to the long persistence of the former. We moved the receiver to South Mountain in an attempt to see the exciting wave in the absence of the local scattering by the power line. There we found that the sky wave reflection was almost nonexistent, and greatly overshadowed by the long exponential tail of the ground wave. It was subsequently learned that a Polar Cap absorption event was in progress at the time of the test.

The calibration exercise brought home several important points for future investigation. The Navy antenna proved to be a good VLF radiator, but needed to be terminated differently to get a sharp pulse. Effectively we had created a giant R-L single-pole network, with the inductive energy stored in the antenna being dumped through the terminating resistor long after the transmitter current had gone to zero. Secondly, we found how small the sought-after ionospheric reflection was in relation to the local

ground wave and scattered fields. Finally, we saw how much better it would have been to use two smaller pulse receivers for simultaneous measurements of the ionospheric reflected field and the corresponding power line current.

The closing phase of the September 1979 trip was to integrate the portable power line receiver into the Qanaq receiving station so that simultaneous continuous monitoring of TE and TM signals could begin. Figure F-3 shows the final Qanaq equipment configuration.

Figure F-4 is a typical sample of TE data, recorded at Qanaq in the period 28 February 1980 to 6 March 1980. A trace of attenuated ground wave is visible at the left hand edge of the figure, followed in 300 us by the large first-hop sky wave, and at 800 us by the weaker second-hop sky wave. A diurnal variation of about 50 us is evident in the first-hop sky wave, and roughly twice as much in the second-hop wave. The vestigial ground wave is absolutely steady in time as expected. Figure F-5 is a comparison of TE data with TM data taken at the same time, during a polar-cap absorption event (PCA) which commenced on 4 April 1980. The PCA virtually wipes out the TE first-hop sky wave, as the group mirror height declines rapidly from 85 km before the event down to a minimum of 55 km. The TM sky wave is apparent throughout the disturbed period, but the TE reflection remains very small for a full 48 hours. Nearly four full days elapses before the normal diurnal behavior is reestablished.

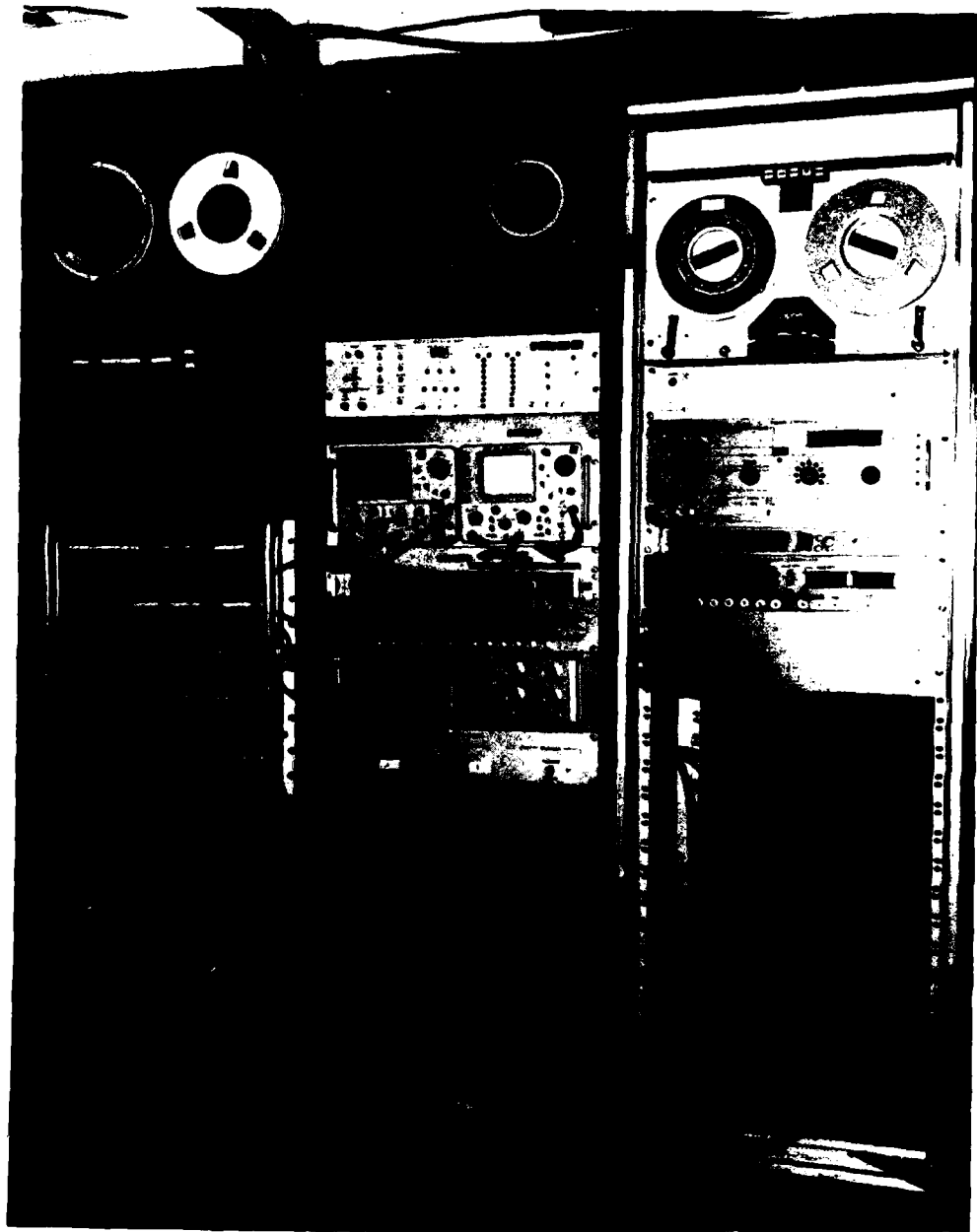


Figure F-3. TE Receiving Equipment at Qanaq.



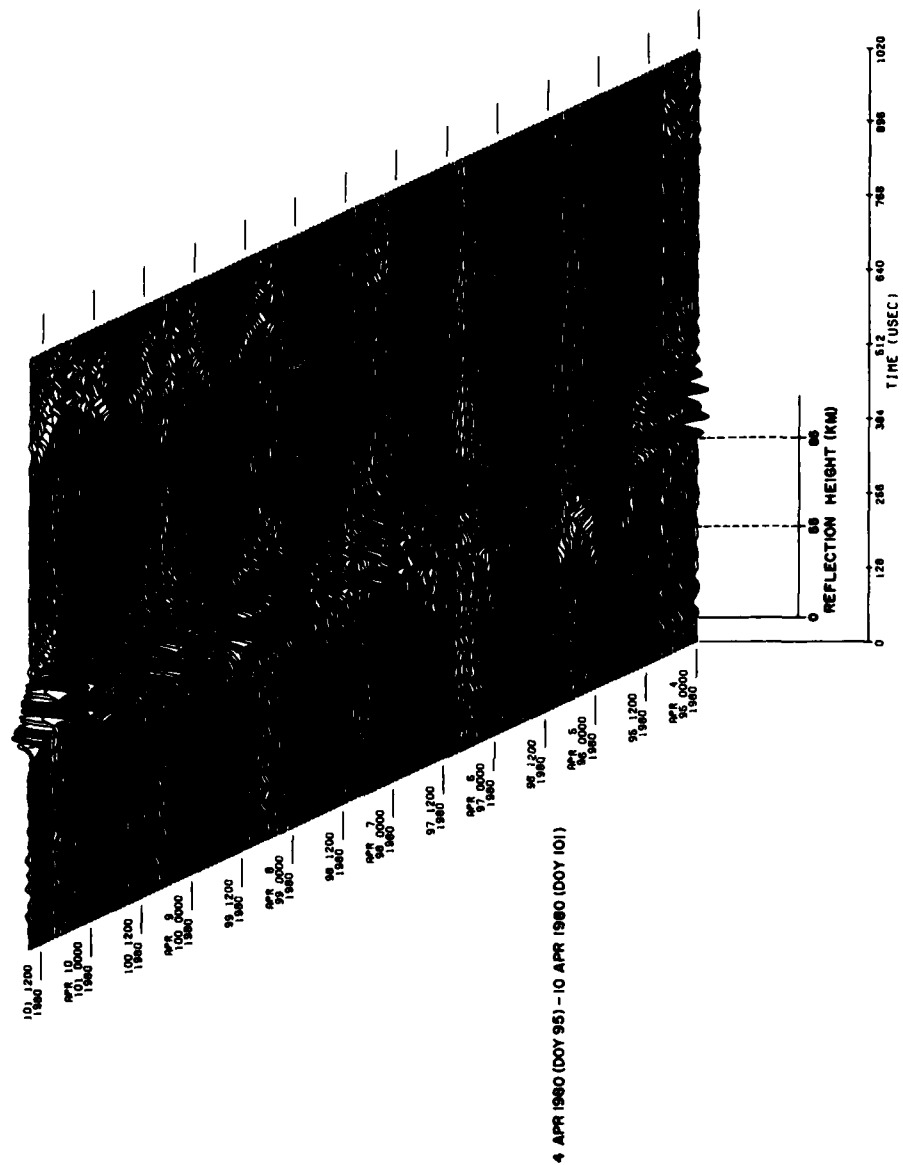


Figure F-4. PCA Effects on TE Reflectivity.

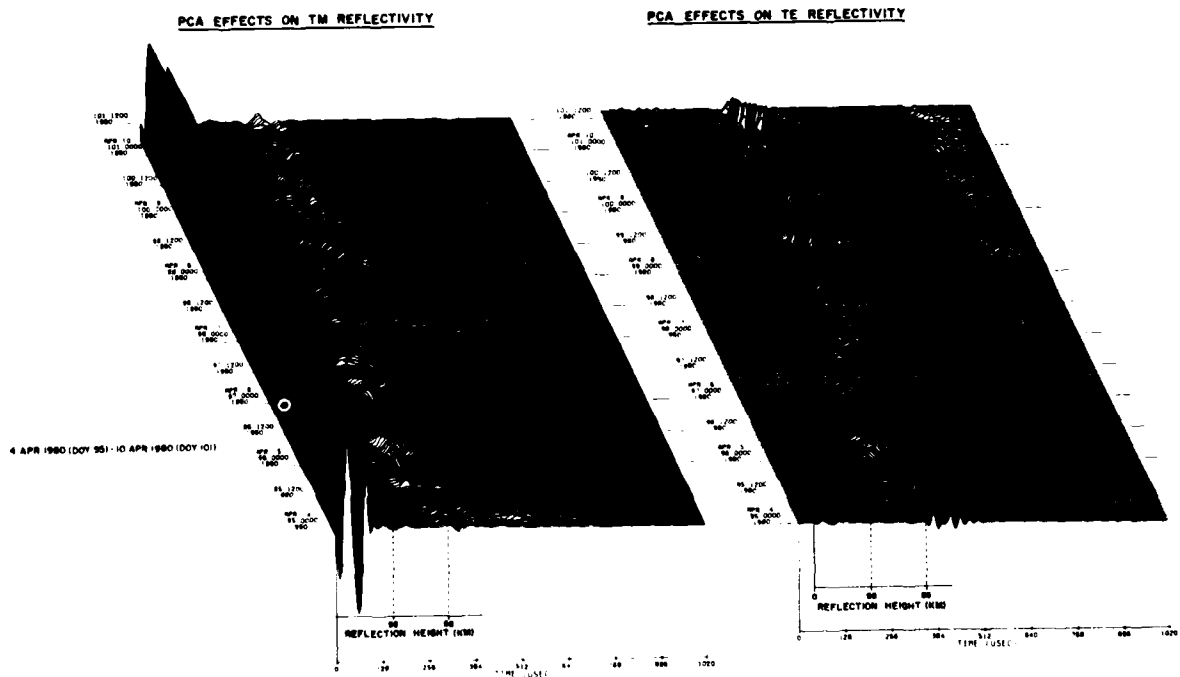


Figure F-5. Comparison of TE and TM Data from a PCA.

The effectiveness of the Megapulse Thule to Qanaq TE pulse ionosounding system has been well demonstrated. The system performs as expected during normal ionospheric conditions, it has sufficient signal-to-noise ratio to show two hops at night, and resolution clarity to show absorption events. The system is in operation and the data are being supplied to RADC/EEPL.

#### F.5 Waveform Improvement

Early in the TE experiments we recognized that the waveform radiated from the power line was far from ideal for ionosounding. The energy was concentrated in a fairly narrow band of frequencies near 60 kHz, and the pulse was long and poorly damped. First it appeared that by introducing a frequency-dependent resistance across the two halves of the line we could damp the half-wave resonance and shorten the pulse. Experiments with several filter forms failed to produce the desired result, however. Meanwhile, the test of the grounded Navy long-wire antenna had shown that a well-behaved VLF pulse could be radiated from a grounded structure. The obvious next step was to try grounding the ends of the power line, converting it from an open-circuited, half-wave dipole into a giant center-fed loop.

The big unknown in grounding the power line was the magnitude of the RF resistance which could be achieved with a ground system of reasonable cost. It appeared that the single-cycle transmitter would operate reasonably into a load resistance of at most a few hundred ohms. Published maps showed the ground conductivity in

Greenland to be only about  $10^{-5}$  mho/meter, far too low for a conventional wire-star ground system to be effective. Conversations with S.A. Arcone and Paul Feldman of the U.S. Army Cold Regions Research and Engineering Laboratory revealed to us that (1) Arctic ground conductivities showed wide variations with location, time of year, water content, etc. and (2) commercial equipment for measuring ground conductivity was available from Geonics, Ltd. of Mississauga, Ontario. We were encouraged to measure the local conductivity in the area where we wanted to install the ground system, and proceed with our design from there.

Megapulse purchased a Geonics EM-16R instrument, which measures the local surface impedance at VLF by comparing the tangential magnetic field from a remote station with the voltage drop along 10 meters of the propagation path. A direct readout of ground resistivity in ohm-meters is obtained, along with the relative phase of E and H. Armed with this instrument and a Trackmaster vehicle provided by the USAF, on 10 May 1980 Megapulse surveyed the ground resistivity at several locations along the power line, and found it to be remarkably low, ranging from 500 ohm-m near the Base end and transmitter shack up to 1500 ohm-m at the BMEWS end. Resistivities were checked also on the Ice Road to Dundas and on the surface of the pond where the Navy ground had been placed. At both locations the resistivities were too low to measure, but consistent with the accepted value of 4 mhos/meter for sea water.

An interesting collateral piece of information on Arctic grounding was obtained by digging through the records of the GLOBECOMM radio station in Building 1696 on North Mountain. Measured data taken on the 400 meter tower in November and December of 1952 by W.W. Brown and H. Adams showed very good radiation efficiency even as low as 50 kHz, implying excellent ground system performance. The ground system employs 120 radials of #6 AWG copper, each 400 meters long, buried ~~at~~ 1 foot deep. The measured total resistance at 50 kHz was 2.0 ~~ohms~~, and the calculated radiation resistance is 1.47 ohms. Thus the mid-winter ground system resistance is only 0.53 ohm.

On the basis of our resistivity measurements and the 1200 foot tower data, we abandoned our earlier plan to dig artificial lakes for grounding in favor of much simpler radial-wire systems. Two systems of twelve, 100-meter wires each were installed by DAC during the brief 1980 construction season, and the star centers connected to the power line ends. The d.c. loop resistance was measured on 22 September 1980 and found to be an acceptable 200 ohms. Megapulse expected the transmitter to operate until the equivalent series resistance rose to around 600 ohms, at which point the energy returning from the antenna would not be sufficient to commutate the main SCR. Surprisingly, the resistance has risen steadily to more than 5,000 ohms at this writing (10 February 1981) and the transmitter is still running. Initially, the resistance of the star in the wet area at the Base end of the

line (73 ohms) was lower than that at the rocky BMEWS end (125 ohms). By 5 December, the BMEWS end was up to 652 ohms, and the Base end had risen to 750 ohms. The substantial difference in the behavior of the two resistances is probably due to the higher water content of the ground at the Base end. The CRREL reports show that the resistivity of wet ground rises rapidly as the temperature falls below the freezing point.

REFERENCES, SECTION F

Rasmussen, J.E., McLain, R.J., Turtle, J.P., Klemetti, W.I.;  
VLF/LF Reflectivity of the Polar Ionosphere 20 July - 20 September  
1975, USAF Rome Air Development Center Report, RADC-TR-76-327;  
October 1976.

## SECTION G

### C-LAYER STUDIES IN BRAZIL

#### G.1 Introduction

The so-called C-Layer revealed by high resolution, short pulse ionosounding technique is described in Section C (see also list of references). The proposed explanation of this thin reflecting layer at 63 km altitude requires three essential elements: (1) a fairly constant source of primary ionization in the ionosphere, (2) neutral atoms to which free electrons (created by the source) can become attached, and (3) solar photons which can keep a significant population of electrons detached, and hence capable of interacting with the VLF wave. Now if, as suspected, cosmic rays are the source of the ionization, the C-Layer might prove to be weak (or non-existent) at the geomagnetic equator, because it is known that at least some components of the cosmic radiation cannot penetrate the screening effect of the geomagnetic field. This line of thought is difficult to quantify, but it adds interest to exploring the latitude distribution of the C-Layer, especially at low latitudes. Accordingly, some experiments were undertaken in Brazil, where a short pulse ionosounding facility already exists.

#### G.2 Description of Experiment

During a period from 6 May 1980 through 4 June 1980, a series of VLF Test Measurements were performed by a team of USAF and Megapulse scientists in the Southern section of Brazil primarily to study the C-Layer. These measurements were carried through in



cooperation with the Air Force of Brazil, using the Brazilian VLF Transmitter located near the city of Pôrto União in south central Brazil, at south magnetic latitude of approximately  $23^{\circ}$ . The measurements were made using a newly developed modular portable receiving system (see Figures G-1, G-2 and G-3) designed and constructed by Megapulse, Incorporated with an eye toward portability and ease of maintenance. Throughout the entire test period, this receiver operated in remote locations without any major failures, and collected quantities of valuable data. These receivers were transported between the various test sites by two or three people using a VW bus or other such vehicle. It had been planned to use two systems in the field and have spare modules in case of problems, but the reliability of the systems allowed the spare modules to be combined into a third system. This allowed the use of three sites simultaneously during the program, so that approximately 33% more data was gathered. In any case, this receiving system is designed to allow easy replacement of modules (see Figure G-4) to permit quick repair of problems in the field. It is a tribute to the reliability of these systems that all three systems remained in operation during the whole test series without the need for exchanging a single module.

These measurements were made at nine different receiving sites (see Figure G-5) within 280 km of the Brazilian transmitter at Porto Uniao. At some locations, the Brazilian Air Force arranged for suitable buildings to house the receiver systems. A

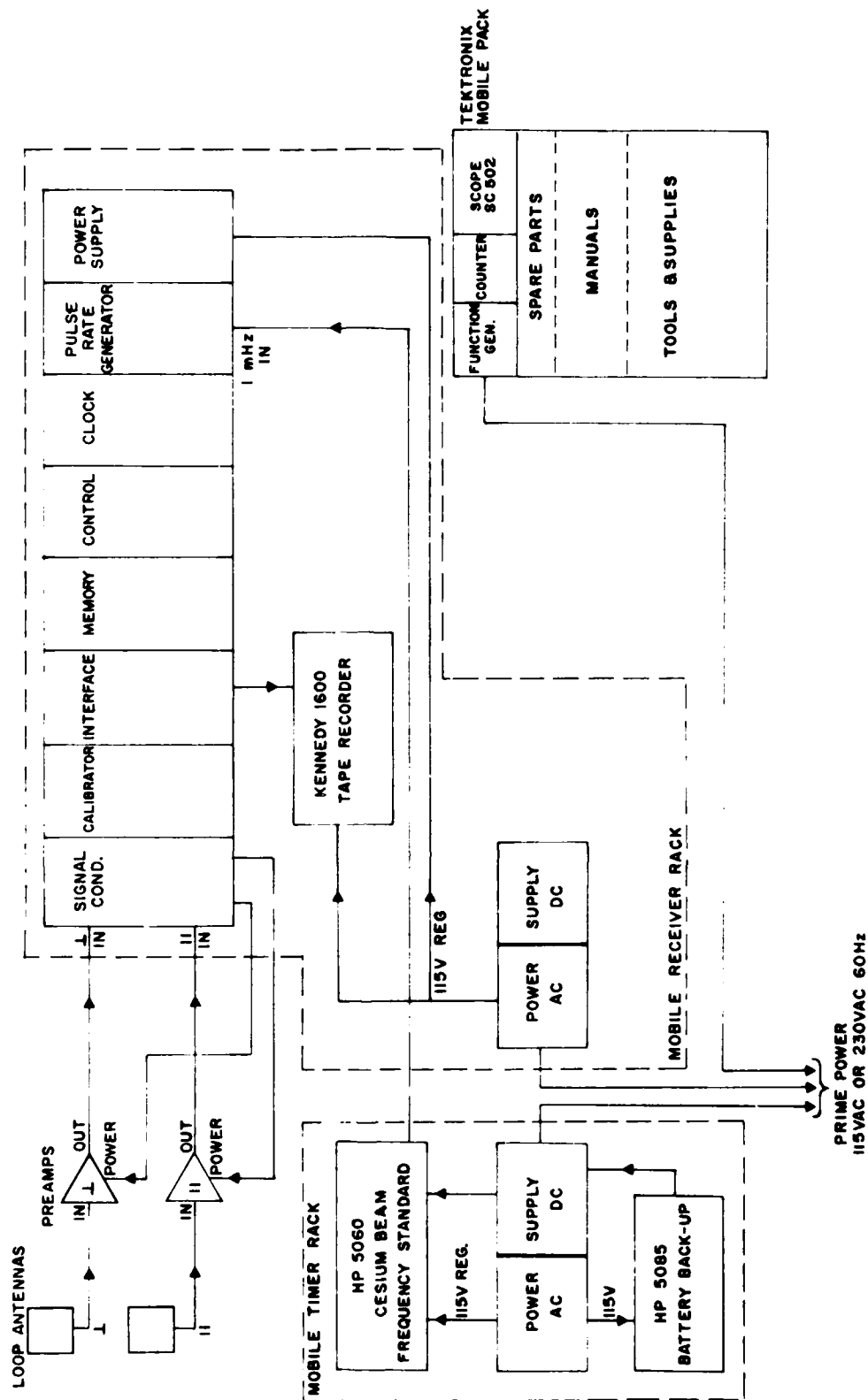


Figure G-1. Block Diagram - Portable Ionosounder Receiver System.

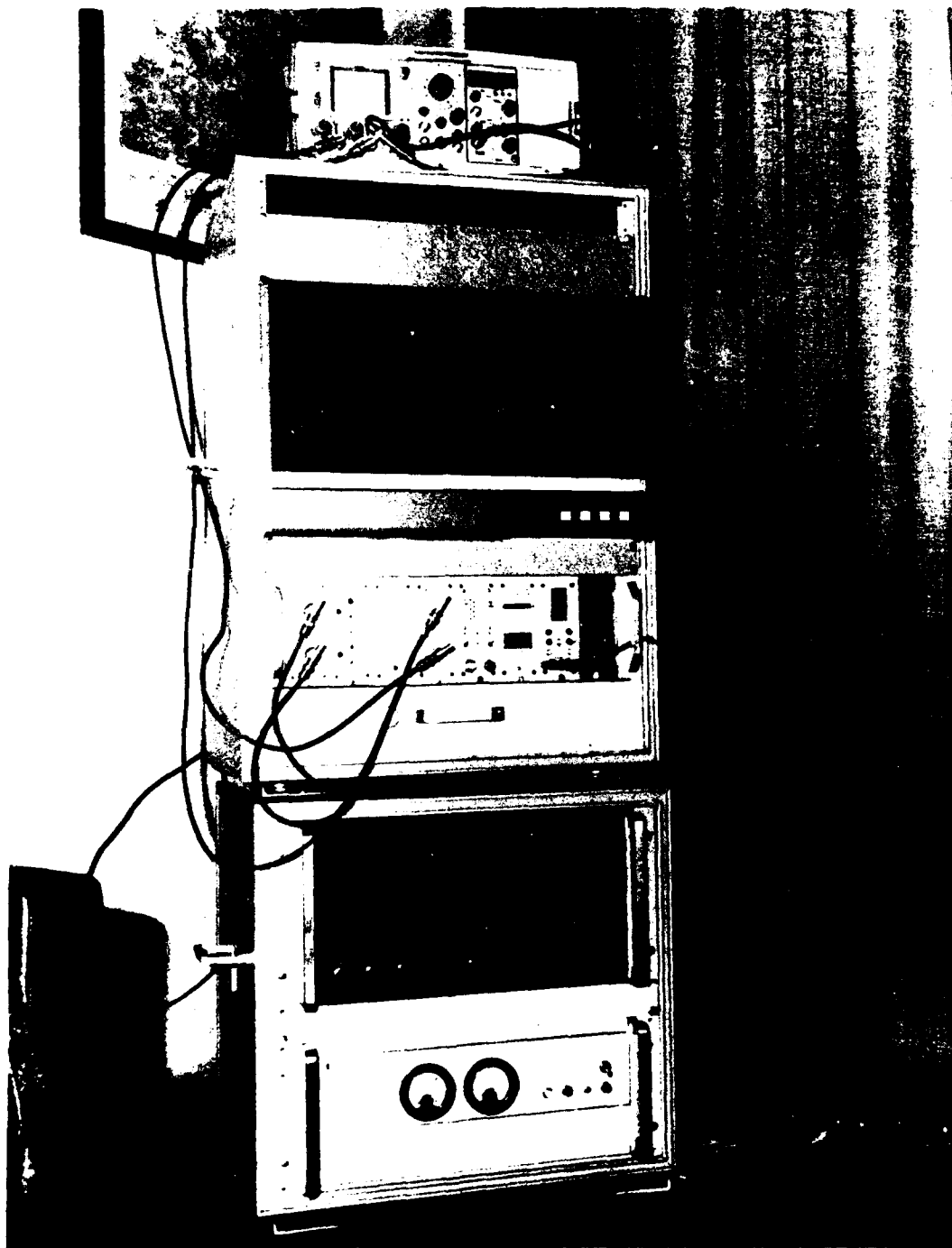


Figure G-2. Portable Ionosounder Receiver.

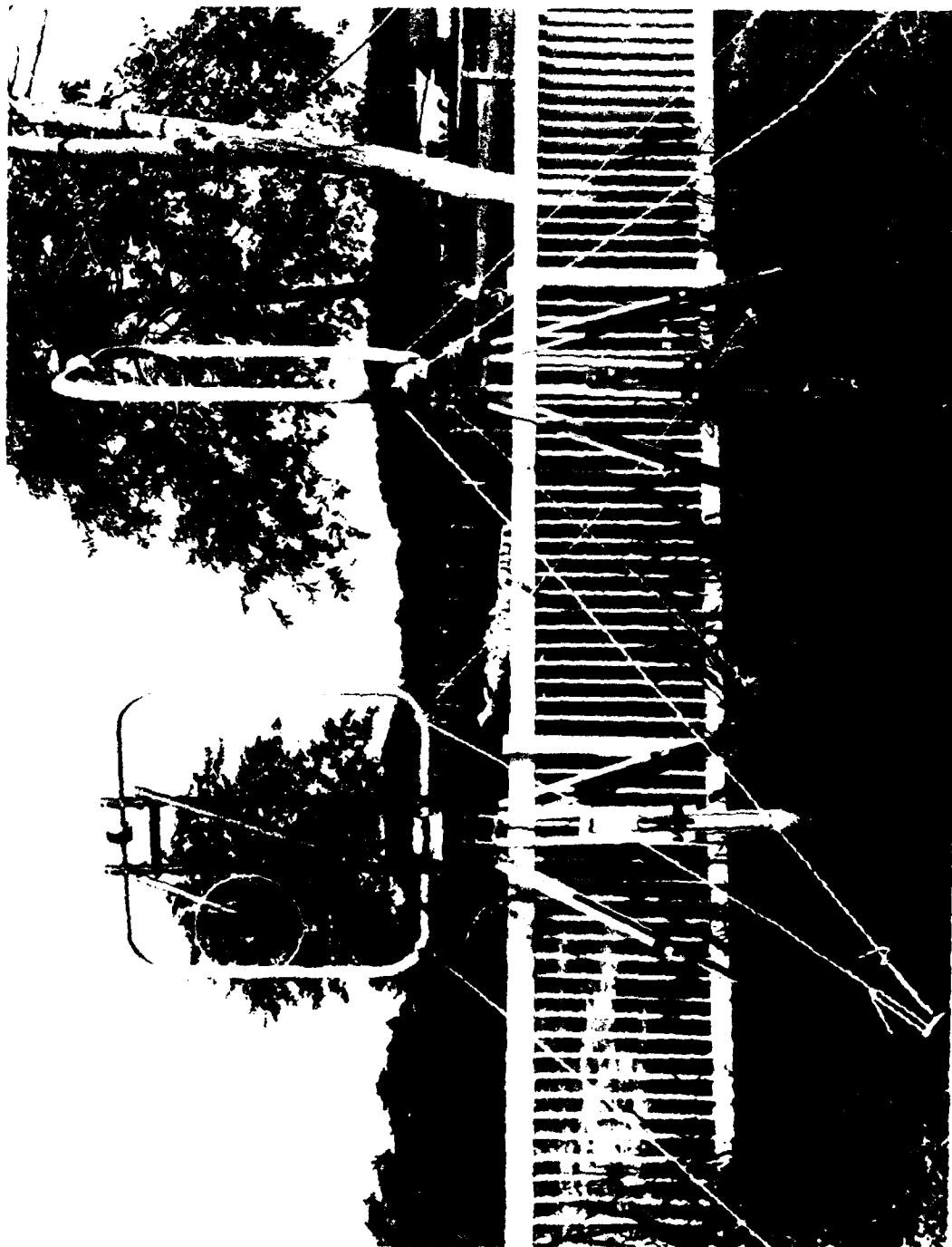


Figure G-3. Receiving Antennas Set-Up at Blumenau.

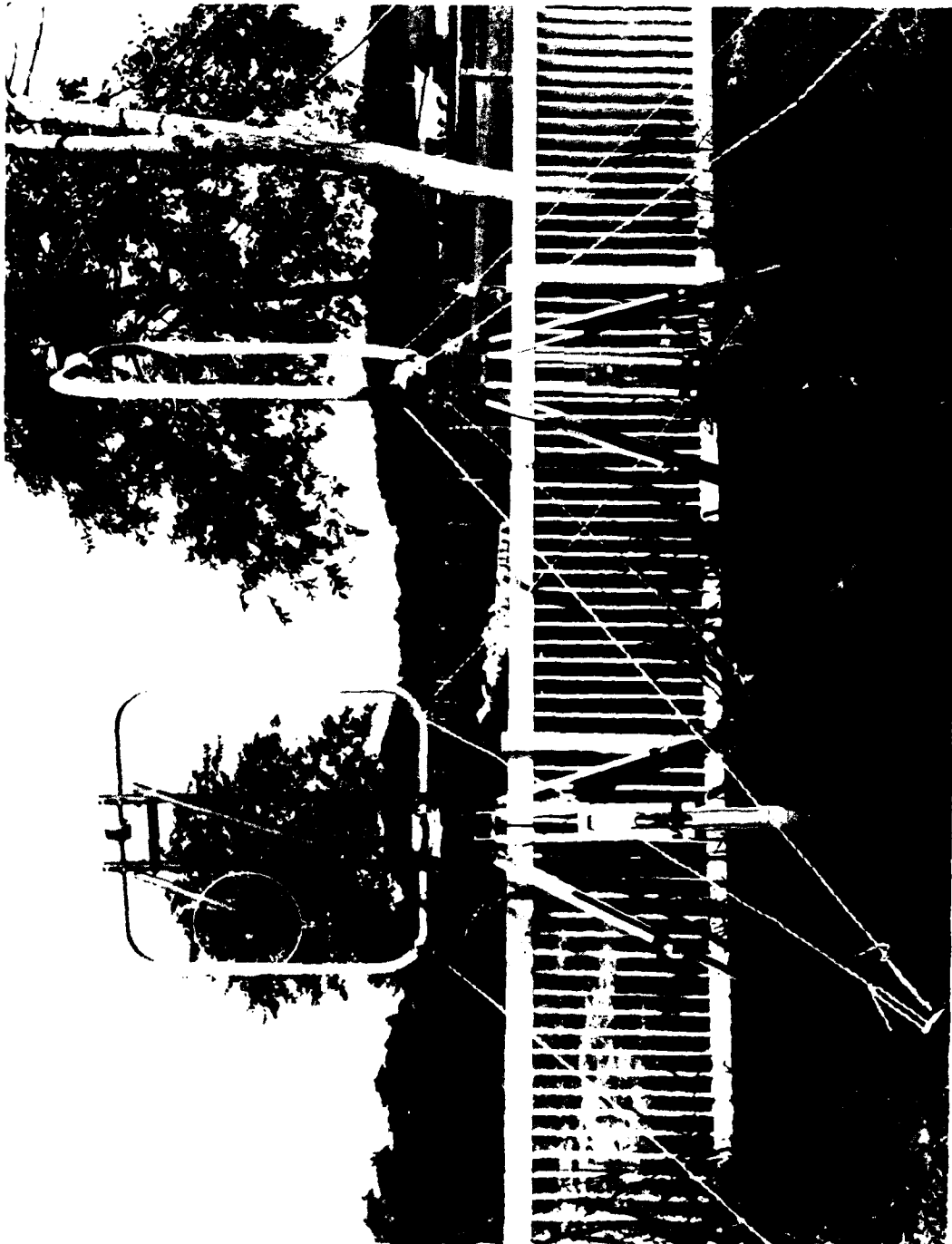


Figure G-3. Receiving Antennas Set-Up at Blumenau.

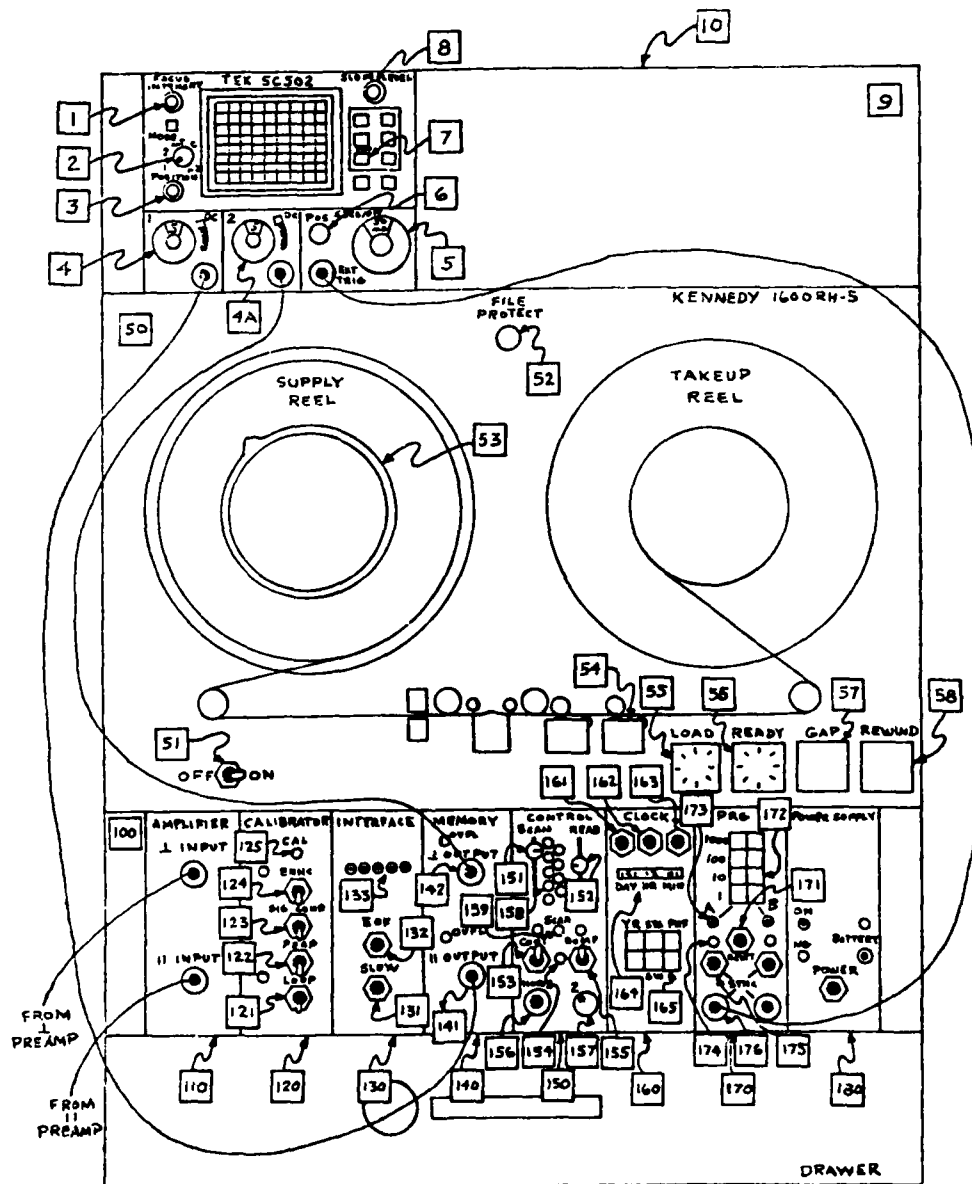


Figure G-4. Receiver Unit.

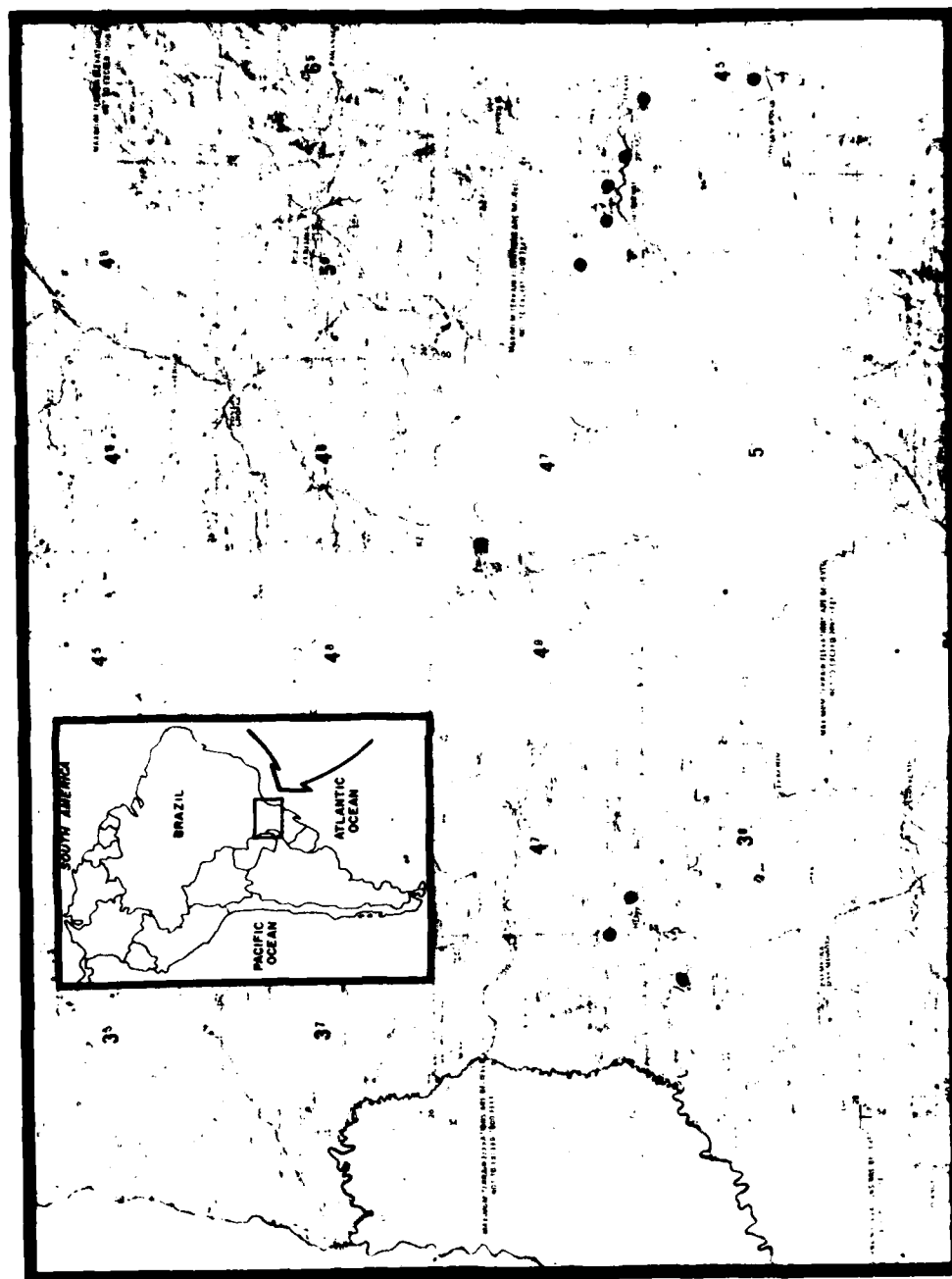


Figure G-5. Map - Transmitter and Receiver Sites.

typical example is shown in Figure G-6. Other measurements were made with the receivers housed in a small trailer or in a van, both provided by the Brazilian Air Force (see Figure G-7). A base of operations was established at the Brazilian Air Force fixed-receiver site near the town of Gaspar. At this location, the receivers were unpacked and tested in advance of being sent to the various sites. This base of operations was also used as a central location to check the data tapes being produced in the field. The tapes were all scanned on an oscilloscope and interesting segments were then automatically plotted on an X/Y recorder, controlled by Megapulse designed and built equipment.

The initial series of measurements was made at locations of different ranges with the same bearing as the receiver site at Gaspar. This was done to allow a range to be chosen that might best provide the most desirable data. Two sites were then chosen toward the east of the transmitter, and the third system was installed in the trailer and transported to the west of the transmitter. The trailer was then moved to three different locations of approximately the same ranges as used in the east. This allowed for a comparison of data between the east and the west with regard to propagation differences with geomagnetic azimuth from the transmitter. Aside from some minor problems with local power, these receivers provided a nearly continuous record of VLF transmissions for the period of operation. Because of the ease of operation and maintenance, it was possible to leave the systems



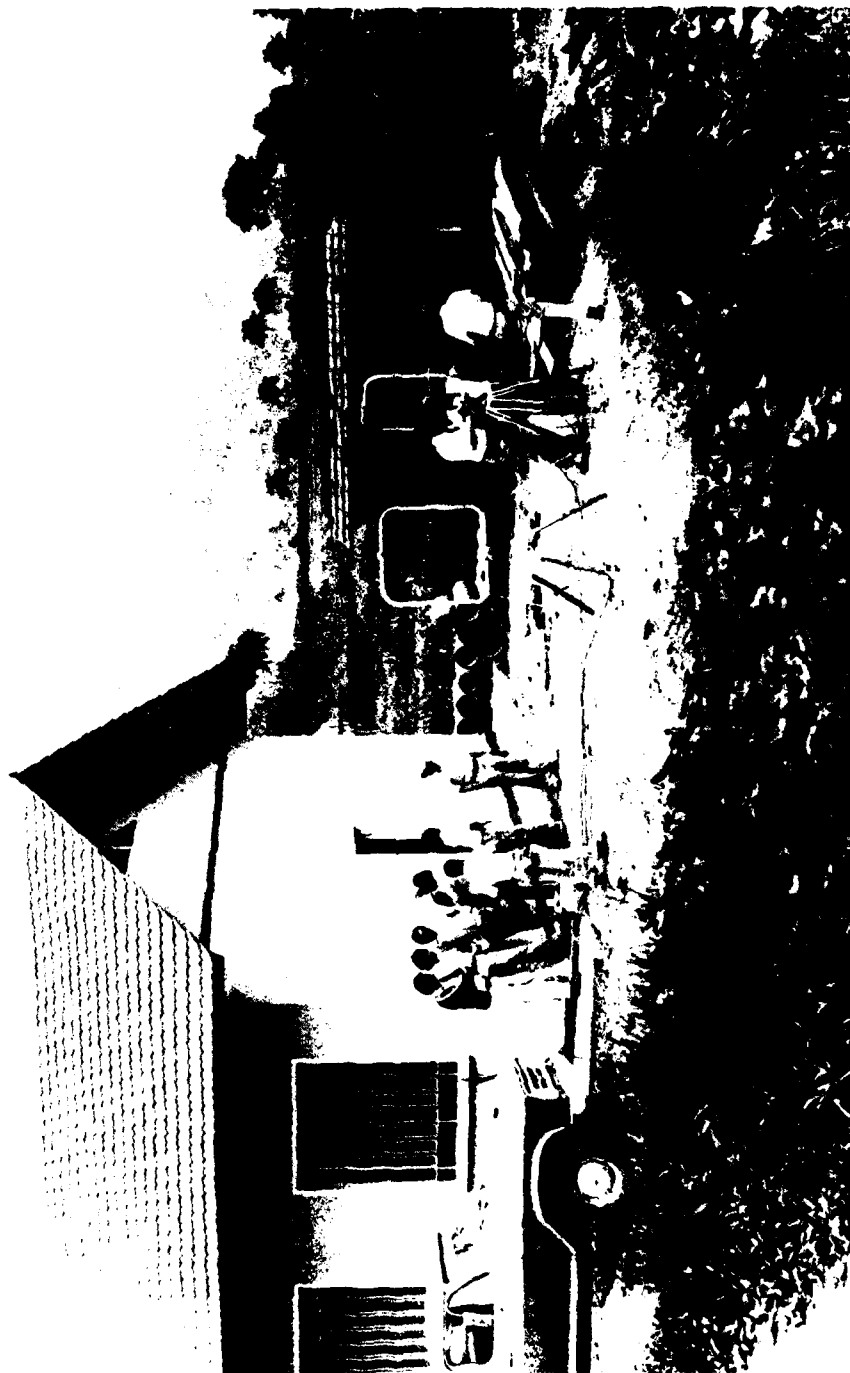


Figure G-6. Receiver Site at Timbo.



Figure G-7. Trailer and Van Containing Receiver Systems.

operational for some additional time with the Brazilian technicians to record the data. Two systems continued operation for one additional month and were then shipped back to the USAF. The third system remains with the Brazilian Air Force to continue measurements for an unspecified period of time. The ease of operation and dependability of the receivers was demonstrated again by their being left in Brazil for an extended period of operation.

### G.3 Data and Conclusions

During the period of this contract, only very preliminary analysis of the data has been performed, but even this seems to indicate some interesting phenomena. On some days, during the periods of sunrise and sunset, a low level reflection (possible C-Layer) was observed at a number of sites. This layer was not always present, but seemed to fade and increase, being considerably stronger on some days than others. The sunrise and sunset low level reflections observed at Camboriu are shown in "three dimensional" form in Figure G-8. This site showed the clearest C-Layer reflections, but more distinct separations from the usual D-Layer reflections appear in records produced at sites somewhat closer to the transmitter, particularly Gaspar and Blumenau Airport. Further analysis of this data should provide interesting information about this layer.

Figure G-9 shows a 24-hour period as recorded at five receiver sites all operating during this time period. It can be noted that each shows a similar series of disturbances possibly caused

# CAMBORIU, BRASIL

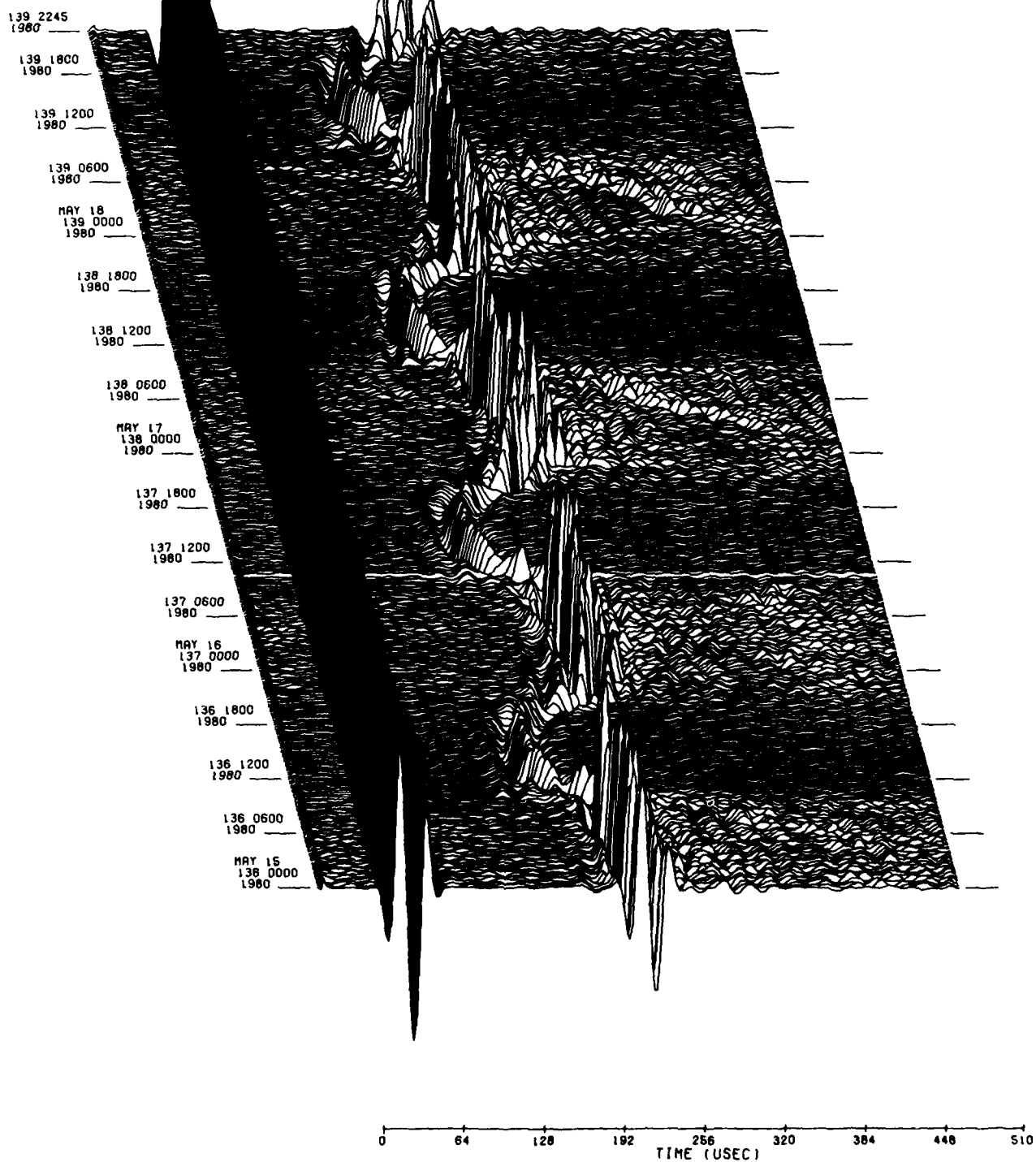


Figure G-8. Received Ionosounder Waveforms at Camboriu for a Four-Day Period.

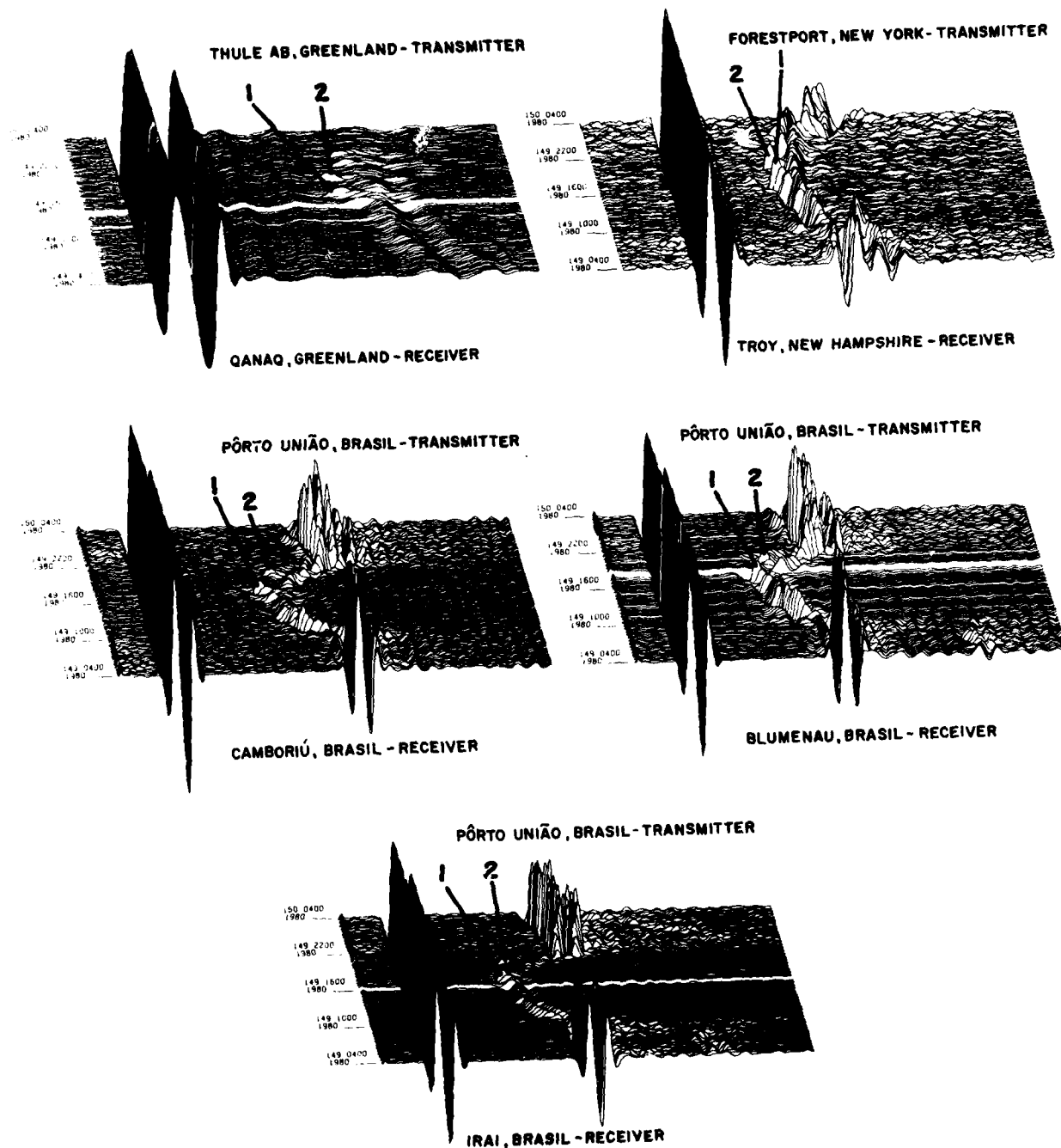


Figure G-9. 3-D Plots for 28 & 29 May 1980 at Five Sites Showing Possible Solar Flare Disturbances.

by solar flares. Two of these events appeared at all five sites. These events are indicated (1) and (2) in Figure G-9. On Julian Day 149 (20 May) between 1705 and 1753 UT (1 in Figure G-4) a M3 flare was reported. Also on the same day between 1924 and 2053 UT (2 in Figure G-9) an X1 flare was reported. These seem to coincide quite accurately with times of the disturbances (1 and 2) visible on all five plots. Two other disturbances (M2 between 2153 and 2236 UT and an M6 between 2332 and 0045 UT) are visible on the Greenland and New Hampshire plots because of the extended period of solar illumination in these areas at this time of year.

An inspection of the nighttime portions of these records show that irregular reflections occur on some nights, as for example the night of 16/17 May in Figure G-8. These irregularities may possibly be due to particle precipitation. In this connection it is noted that this area of Brazil is not far removed from the South Atlantic Magnetic Anomaly, where the locally weak geomagnetic field is specially favorable for particle precipitation.

The data tapes have been reproduced and averaged. For each site, a three dimensional plot of the received waveforms has been produced. Also, a tape for each site has been produced that has the residual groundwave and off-path reflections removed in order to be able to better visualize the actions of the ionospheric layers.

The above items have been delivered to RADC. It is believed that there is a good deal more to be learned from further analysis of the data.

#### REFERENCES, SECTION G

Enge, P.; "The C-Layer," unpublished paper, 1979.

Hargeaues, J. K.; "The Behaviour of the Lower Ionosphere Near Sunrise," Journal of Atmospheric and Terrestrial Physics, 1962, Vol. 24, Pages 1 - 7.

Peterson, J. R.; "Sunlight Photodestruction of  $\text{CO}_3^-$ ,  $\text{CO}_3^- \cdot \text{H}_2\text{O}$ , and  $\text{O}_3^-$ : The Importance of Photodissociation to the D Region Electron Densities at Sunrise," Journal of Geophysical Research, March 1, 1976.

Abdu, M. A.; Ananthakrishnan, S.; Krishnan, B. A.; Massambani, O.; "Cosmic Ray Ionization in the D Region at Sunrise: Evidence from VLF Phase Measurements," Radio Science, Volume 8, Nos. 8, 9, Pages 733-737, August - September 1973.

Sechrist, C. F., Jr.; "Comparisons of Techniques for Measurement of D-Region Electron Densities," Radio Science, Volume 9, No. 2, Pages 137 - 149, February 1974.

SECTION H  
POSSIBILITIES FOR CONTINUOUS WAVE OPERATION OF  
THE 120-METER (400-FOOT) TOWER AT THULE AFB

H.1 Introduction

For ionosounding purposes, both the 120-meter (400-foot) vertical monopole antenna, and the horizontal dipole ("powerline") antenna at Thule AFB transmit short pulses. However, for certain future experiments involving propagation paths too long for time-resolution of ground waves and sky waves, the use of continuous waves (CW) may be desirable. Accordingly some characteristics of the two antennas, which would be of interest in converting to CW transmissions, were examined as described below.

H.2 120-Meter (400-Foot) Tower

In the present TM ionosounder, the 120-meter (400-foot) tower is charged to a predetermined DC voltage of about 40 kV prior to each pulse, then discharged to ground through an inductor. The resulting single cycle of 16 kHz antenna current is the result of resonance between the .009 mFd antenna capacitance and the 11 mH tuning inductor. Peak antenna current is given simply by the quotient of DC voltage and the 16 kHz reactance, about  $40 \text{ kV} / 1100 \Omega = 36 \text{ A}$  under present operating conditions. The proportion of the total energy radiated is miniscule, being about  $I_a^2 R_a = 1/2 (36)^2 (.0167) = 10.8 \text{ W}$ . Since the antenna's 1100 ohm reactance at 16 kHz far exceeds its series resistance of about 17 ohms, the present rudimentary ground screen is adequate for pulsed operation.



It is the total system resistance which determines how much CW power can be radiated with a given transmitter, since the series reactance is tuned out and acts only as a restriction on operating voltage and bandwidth. For example, the new 8,000 W. ENI amplifier can deliver a maximum of  $\sqrt{8000/17} = 21.7$  A to the 120-meter (400-foot) tower with its present ground screen, corresponding to a radiated power of 7.86 W at 16 kHz. The -3 dB operating bandwidth would be:

$$\frac{1}{2\pi} \left( \frac{R}{L} \right)^2 = 492 \text{ Hz}$$

the final factor of 2 arising because the total resistance in a matched system is twice the resistance of the antenna alone.

It is difficult to estimate how low a ground resistance might be achieved with reasonable effort and expense. We were able to find data taken in December 1952 on the neighboring 360-meter (1200-foot) tower indicating a resistance for that antenna at 50 kHz of only 2 ohms, of which 1.47 ohms can be attributed to radiation resistance. The ground screen is a standard radial design, consisting of 120 equally-spaced copper #6 AWG wires 360-meters (1200-feet) long buried 12 inches below the surface. Megapulse estimates that a ground system resistance of 2 ohms might be achievable at the 120-meter (400-foot) tower with 36 buried radials 120-meters (400-feet) long. The literature on ground systems emphasizes that with low ground conductivity, the best strategy for reduction of resistance with a given screen is to use longer radials rather than more of a given length. Thus, if wires longer than 120-meters (400-feet) are practical in all directions, the longer the better.

Tuning coil resistance is another important factor for CW operation. A Q of 1,000 is generally easy to achieve using litz wire in a multi-layer coil design, which implies a series resistance of  $1100/1,000 = 1.1$  ohms for the 11 mH coil needed for 16 kHz. Assuming that the tuning coil plus ground resistance was an optimistic 3 ohms, the 8000 watt amplifier could deliver 51.6 A to the 120-meter (400-foot) tower, for an average radiated power of 44.5 watts. The tower voltage developed would be a hefty 56.7 kilovolts rms, double the peak voltage now employed.

Operation of the 120-meter (400-foot) tower at a higher frequency would be much more advantageous, as the following calculations for 50 kHz will demonstrate. The radiation resistance would increase to  $.0167 \times (50/16)^2 = .163$  ohms, and the capacitive reactance would drop to 352 ohms. The tuning coil resistance for a Q of 1,000 would drop to 0.35 ohms. If the same 2 ohm ground resistance were assumed, the 8,000 watt transmitter could deliver about 56.5 A to the tower, for an average radiated power of 521 watts, nearly 12 times that possible at 16 kHz. Tower voltage would be only 27.8 kV peak.

In summary, the major factors involved in converting the 120-meter (400-foot) tower for CW operation in order of difficulty are (1) improving the ground screen, (2) building a high Q tuning coil to handle the 50 A rms current at the selected frequency and (3) matching the resulting total antenna system resistance to the 50 ohms required by the ENI amplifier.

### H.3 TE Power-Line Antenna

The same antenna reactance and resistance considerations outlined for CW operation of the 120-meter (400-foot) vertical tower apply also to the TE power-line antenna. Unfortunately, we do not have a simple circuit model upon which to base voltage and current calculations, nor do we know how much power is radiated per ampere of power-line current. We do have a limited amount of measured impedance data taken on 10 May 1980 when the lines were still open circuited at the ends, plus dc resistance data taken over the winter of 1980-81 on the grounded structure.

Figure H-1 is a plot of the series resistance and reactance between the J-site segment of line and ground, taken with a GR916-AL bridge while the GLOBECOMM 69 kHz transmitter was off the air. The impedance of the Thule line segment, shown in Figure H-2, is very similar except for a small shift upward in frequency apparently due to a difference in the two line lengths.

For CW operation, the equivalent series resistance of the power line antenna is its important feature. When open circuited, the two lines will have a combined resistance of over 400 ohms throughout the VLF band when driven in the usual push-pull mode of operation. When matched to the 8,000 watt ENI amplifier, the resulting rms line current will be only 4.5 A, compared to the 15 or 20 peak amperes now achieved with the Power Line Pulser.

It was hoped that by grounding the far ends of the two line segments the antenna impedance could be greatly reduced, and the troublesome self-resonance near 70 kHz damped out. Two ground

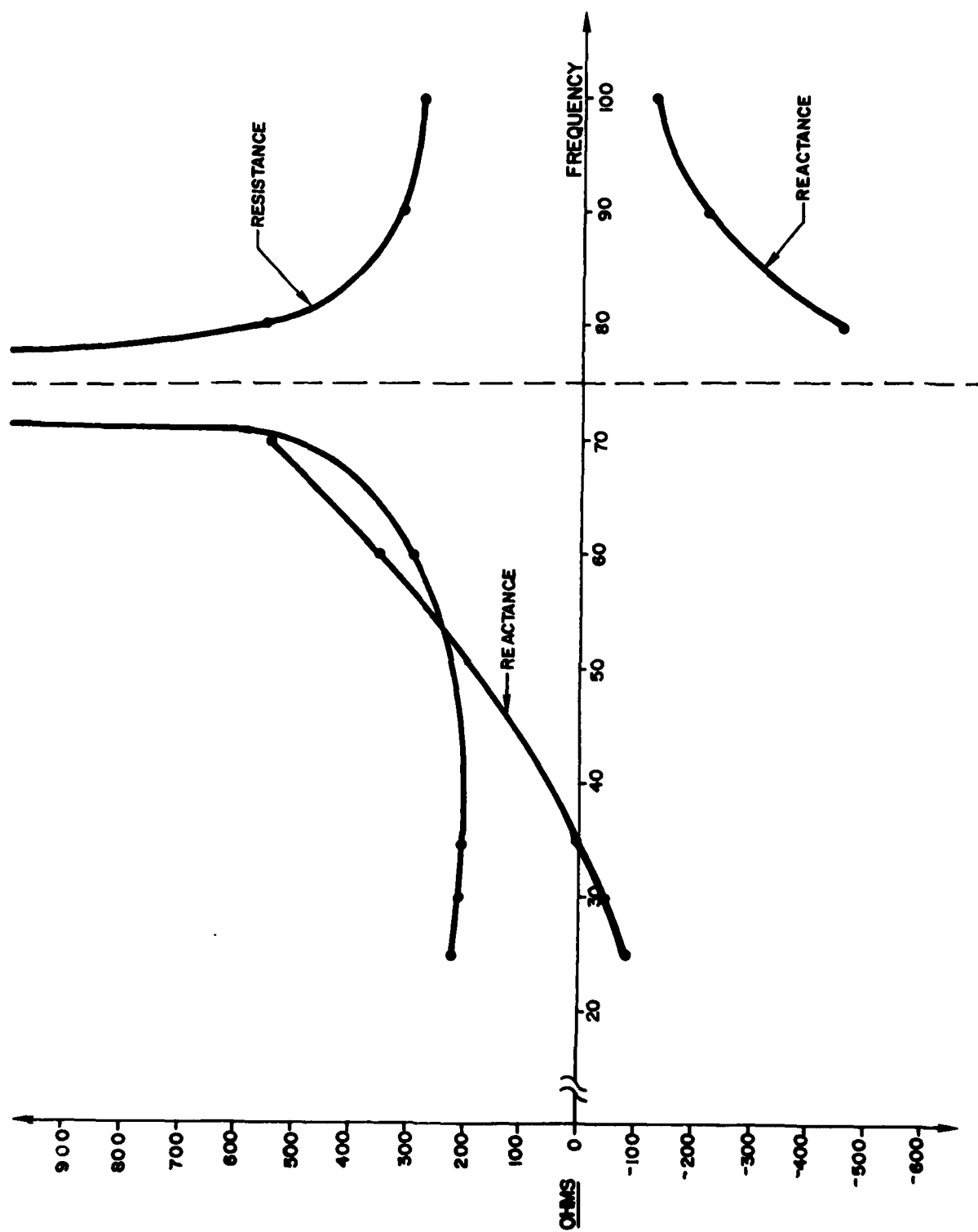


Figure H-1. Impedance Between Ground and J-Site Side of Powerline Antenna.

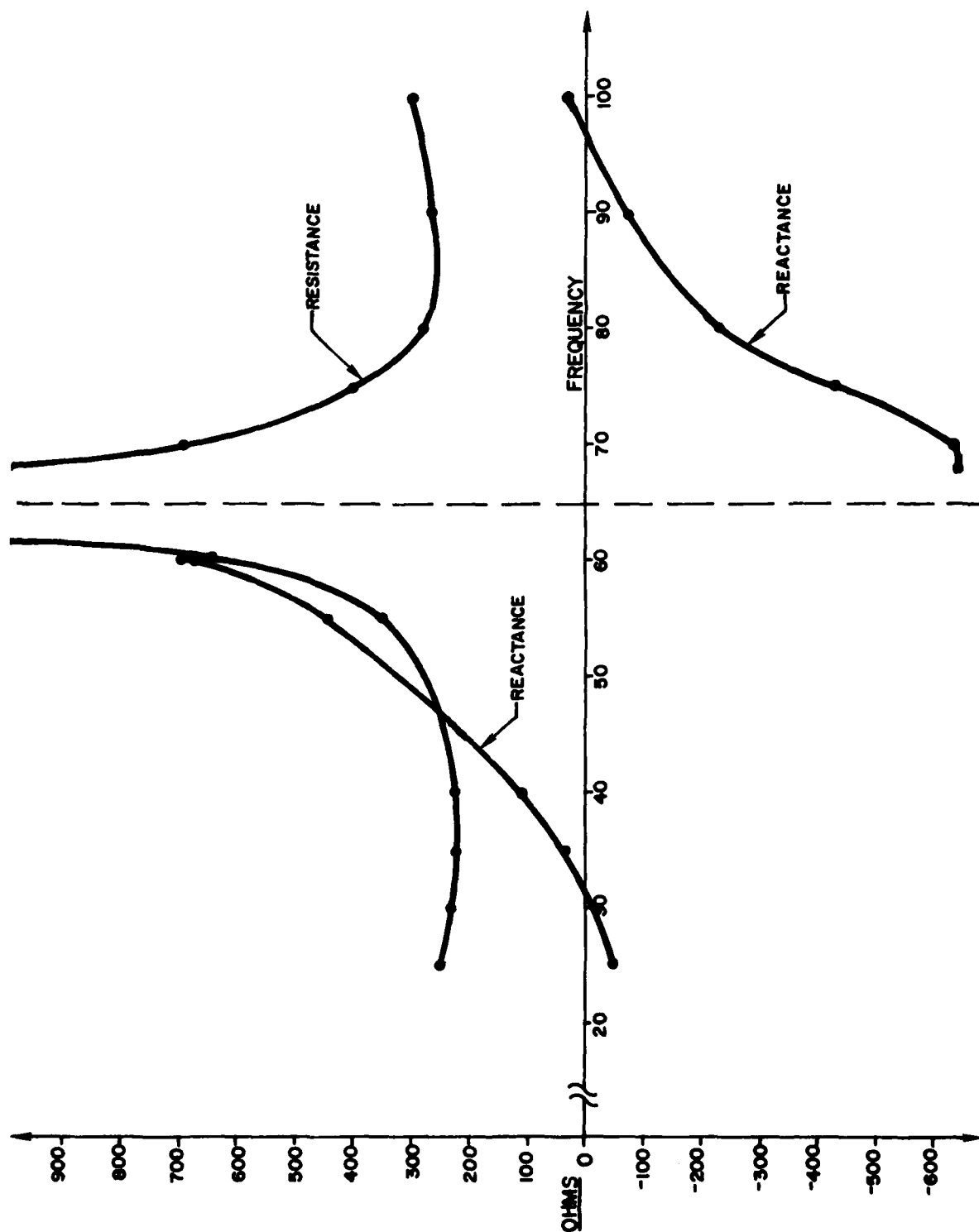


Figure H-2. Impedance Between Ground and Thule Side of Powerline Antenna.

systems consisting of ten #10 AWG 300-foot buried radial wires were laid in September 1980 by DAC. The dc loop resistance measured immediately after installation was about 90 ohms. The Power Line Pulser operated successfully into the new antenna through the winter months, and periodic loop resistance measurements were taken by DAC. The highest resistance was reported at 6000 ohms in the February 1981 measurement.

The high series resistance values obtained with both power-line configurations will seriously limit the line current which can be developed with a CW source. With the best loop resistance of 90 ohms, the line current will be under 9.5 A rms. There is a good possibility that the ground-screen terminations can be improved, but it is difficult to estimate by how much. The seasonal variation of resistance is very substantial, probably caused by water freezing in the upper layers of soil.

U S GOVERNMENT PRINTING OFFICE : 1981-500-000/42